ISSN 1000-9620

Marine Science Bulletin

Volume 4 · Number 2 2002

ISSN 1000-9620
02>
9 771000 962001

NATIONAL MARINE DATA AND
INFORMATION SERVICE OF CHINA

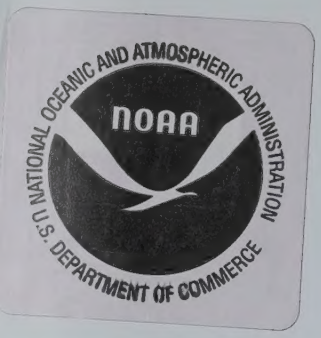

LIBRARY
Pacific Islands Fisheries Scien
NOAA Fisheries
Honolulu, Hawai'i

LIBRARY
MAR 13 2003
National Oceanic & Atmospheric Administration
U.S. Dept. of Commerce
WITHDRAWN

MARINE SCIENCE BULLETIN

Vol.4 No.2 Oct., 2002

CONTENTS

Experimental Investigation of Lift Forces on Horizontal Cylinder near Bottom in Oscillating Flow ..... *Gui Jinsong* (桂劲松) *et al.* (1)

Advances in the Study of Geochemistry and Paleo-oceanography of the Co-rich Crust ..... *Cai Yihua* (蔡毅华) *et al.* (8)

Analysis of Interannual Variations of Inorganic Nitrogen in the Bohai Sea..... *Shi Qiang* (石 强) *et al.* (15)

Biogeochemical Character of Dissolved Inorganic Nitrogen and Phosphate at Plume Front in the Changjiang River..... *Fu Ruibiao* (傅瑞彪) *et al.* (25)

Distribution and Changes of Specification of Phosphorus in the Yellow Sea ..... *Chen Hongtao* (陈洪涛) *et al.* (32)

Surficial Sedimentary Diatoms in Okinawa Trough and Its Response to Kuroshio Current ..... *Lan Dongzhao* (蓝东兆) *et al.* (39)

The Functions of China Marginal Sea Sediments in the Cycle of Biogenic Elements..... *Sun Yunming* (孙云明) *et al.* (46)

Fractal Determination of Coastal Types Based on GIS ——A Case Study of China..... *Zu Xiaohua* (朱晓华) *et al.* (61)

Induction Effect and Genetic Analysis of NG to Conchospores of *Porphyra* ..... *Xu Pu* (许 璞) *et al.* (68)

Induction Effect and Genetic Analysis of NG to Thallus of *Porphyra* ..... *Xu Pu* (许 璞) *et al.* (76)

Cloning and Structural Analysis of Calmodulin Gene from the Mangrove Plant *Sonneratia Paracaseolaris*..... *Xiong Lingyuan* (熊玲媛) *et al.* (83)

Mechanism of Gonadal Precocity in Cultured Large Yellow Croaker, *Pseudosciaena Crocea* : A Study of Microstructure and Submicrostructure of Leydig Cell and Sertoli Cell in Testis ··· *Fang Yongqiang* (方永强) *et al.* (90)

U.S. Dept. of Commerce
National Oceanic &
Atmospheric Administration
MAR 1 2 2002
LIBRARY

Experimental Investigation of Lift Forces on Horizontal Cylinder near Bottom in Oscillating Flow*

Gui Jinsong (桂劲松)[1,2], Liu Hong (刘 红)[3], Zhou Yanhui (周岩辉)[4], Kang Haigui (康海贵)[1]

1 *Dalian University of Technology, Dalian* 116024

2 *Dalian Fisheries University, Dalian* 116024

3 *Zhejiang Institute of Hydraulics and Estuary, hangzhou* 310020

4 *Dalian KangTai Construction Technique Consultation & Development Co., LTD., Dalian* 116011

Abstract The lift forces on horizontal cylinder near bottom is experimentally investigated at Reynolds numbers (*Re*) in the range of 2 500~10 000 and Keulegan~Carpenter numbers (*Kc*) in the interval of 5~20, and gap ratio (*e/D*) is from 0.2 to 1.0. Lift force coefficient (C_L) and the deviation value of lift force (a_0) are analyzed by using the Fourier analysis method. It is found that both C_L & a_0 are the functions of the *Kc* number.

Keywords oscillating flow, horizontal cylinder, lift forces, Fourier analysis

1 Introduction

With the exploretion and utilization of offshore oil and gas fields in recent decades, oil and gas pipeline engineering is developing rapidly. Pipeline on the sea bottom is affected by a relatively heavy wave force (include in-line force and lift force). Usually the lift force has higher frequency, normally twice, 3 or 4 times that of wave frequency. Under certain conditions, it can cause sympathetic vibration of the structure, and the structure may be damaged due to fatigue. Therefore, how to calculate the wave force, especially the lift force on pipeline, is very important from the viewpoint of engineering. The lift force on horizontal cylinder near bottom can be expressed as:[1,2]

$$F_L / \frac{1}{2}\rho D U_m{}^2 = a_0 + \sum_{k=1}^{n} C_L(k)\cos(k\omega t + \varphi(k)) \qquad (1)$$

Where F_L is lift force, ρ is water density, D is cylinder diameter, Um is cylinder velocity, a_0 is a constant distance to the axis X, $C_L(k)$ is lift force coefficients of order k, $\varphi(k)$ is phase angle.

2 Physical model experiment

2.1 Equipment for the experiment

The physical model test of lift force on horizontal cylinder near bottom in oscillating flow was performed by the author in Edinburgh University during his visit to UK. An oscillating pile was used to simulate the oscillating flow (oscillating a cylinder in static water). The tank is 6m long, 1m wide and 0.5m deep. There was a trolley on the tank, and a cylinder is fixed under the trolley. The trolley is

Received on May 13, 2002

* This research is financially supported by Natural Science Fund of Liaoning province.

controlled by the computer and oscillating harmonically. The physical model configuration is shown in Fig.1.

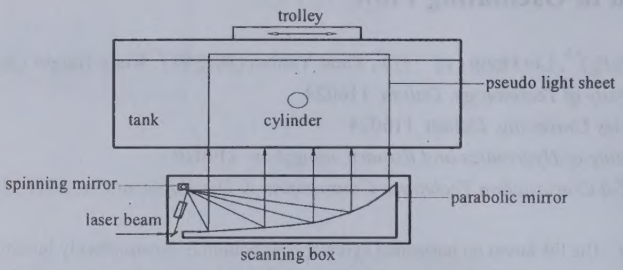

Fig. 1 Physical model configuration

The cylinder model is made of an organic glass, with a diameter of 50mm.The total length of the model is 840mm with the fixed part being 107mm, and the stressed length of cylinder is 620mm. A force sensor is fixed on one end of the cylinder, and the in-line force and lift force can be measured simultaneously.[3,4]

2.2 Test arrangement

The lift forces on horizontal cylinder near bottom in oscillating flow are mainly investigated. The non-dimensional coefficients *e/D* are chosen as 0.1, 0.2, 0.5 and 1.0 respectively, in which *e* is the clearance between cylinder and bottom, and *D* is the diameter of cylinder.

Tab. 1 Experimental parameters

Kc	*T* (s)	*U* max(m/s)	*Re*
5	5	0.05	2 500
8	5	0.08	4 000
10	5	0.10	5 000
13	5	0.13	6 500
20	5	0.20	10 000

2.3 Experimental range of *Kc*, *Re* numbers

In this experiment, the diameter of cylinder is 50mm; the maximum oscillating period is 5s; the maximum oscillating speeds are 0.05 m/s, 0.08 m/s, 0.1 m/s, 0.13 m/s and 0.2 m/s respectively. So, the corresponding *Kc* numbers are 5, 8, 10, 13 and 20 respectively. Under the room temperature, $\nu = 10\sim6$ m/s. The *Re* numbers are 2 500, 4 000, 5 000, 6 500 and 10 000.

3 Analysis methods of the experimental data

3.1 Statistical analysis of lift force

First we select 10 oscillating periods within the lift force time history continuously, and then choose the biggest amplitude of the lift force in each period to form a random sample for the further statistical

analysis. To avoid unstable lift forces at the beginning and the end of the tests, the middle part of test records of lift forces is usually selected as the sample for analysis. The statistically characteristic values of lift force $A_{1/10}$, $A_{1/3}$, $\overline{A}$ are shown in Table 2.

Tab. 2 Statistical analysis of the biggest amplitude of lift force

Kc	*e/D* = 0.1			*e/D* = 0.2			*e/D* = 0.5			*e/D* = 1.0		
	$A_{1/10}$	$A_{1/3}$	$\overline{A}$	$A_{1/10}$	$A_{1/3}$	$\overline{A}$	$A_{1/10}$	$A_{1/3}$	$\overline{A}$	$A_{1/10}$	$A_{1/3}$	$\overline{A}$
5	2.018	1.949	1.824									
8	0.708	0.700	0.650	0.482	0.480	0.452	0.694	0.675	0.631	0.471	0.454	0.414
10	0.599	0.588	0.543	0.352	0.341	0.306	0.595	0.565	0.534	0.405	0.403	0.377
13	0.385	0.383	0.366	0.235	0.229	0.210	0.313	0.301	0.274	0.284	0.277	0.260
20	0.235	0.223	0.208	0.173	0.171	0.163	0.165	0.158	0.134			

3.2 Data processing

Through the experiment, it can be found that the lift forces change periodically and regularly, and the frequency of lift force is always the multiple of oscillating flow frequency (the frequency of oscillating flow is 0.2Hz in this experiment). To make the research convenient, a time history of lift force is intercepted within 2 periods of representational oscillating flow and the time is non-dimensionalized by dividing the period T. The point of the biggest value of the lift force is selected as the origin of time, as shown in Fig.2. According to the lift force intercepted, the average values of the biggest amplitude of each period are calculated, as shown in Table 3. Compared with the statistical characteristics of the lift force from 10 periods, the average value of the lift force intercepted is between $A_{1/3}$ and $\overline{A}$. Therefore, it can be seen that the intercepted parts have representativeness.

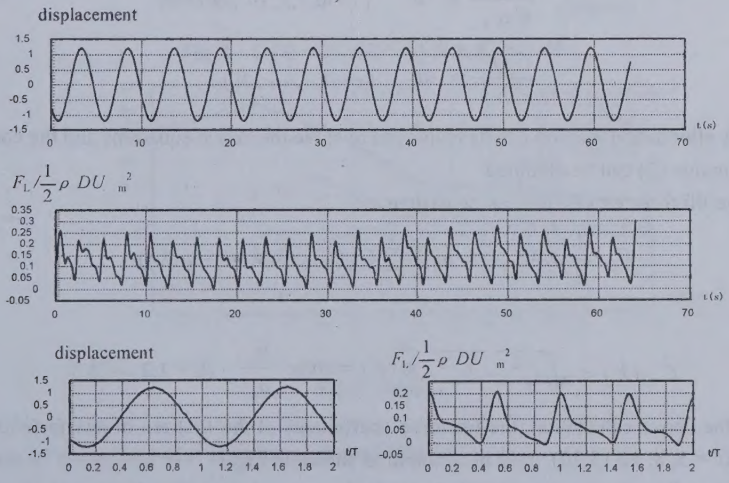

Fig. 2 *Kc* = 20, *e/D* = 0.1, the displacement and lift force process line after experiment and interception

Tab. 3 Average values of the biggest amplitude of the lift force on each intercepted part

Kc	*e/D* = 0.1	*e/D* = 0.2	*e/D* = 0.5	*e/D* = 1.0
5	1.840			
8	0.700	0.478	0.640	0.421
10	0.520	0.340	0.535	0.386
13	0.375	0.217	0.281	0.275
20	0.216	0.162	0.136	

4 Obtaining the parameters of Fourier series

The lift force can be expressed by Fourier series as follows:

$$y = a_0 + \sum_{k=1}^{N} a_k \cos(k\omega x) + \sum_{k=1}^{N} b_k \sin(k\omega x) \tag{2}$$

According to the principle of laest square method, the coefficients of the above Fourier series a_0, a_1, b_1, a_2, b_2,..., a_N, b_N can be obtained by the following procedure:

If (x_i, y_i) denotes the lift force by test and y_i^* denotes the lift force by Fourier series, the difference d_i between y_i and y_i^* can be expressed as:

$$d_i = y_i - y_i^* \tag{3}$$

The sum of square of difference d_i can be written as:

$$Q = \sum_{i=1}^{M} d_i^{\,2} = \sum_{i=1}^{M} \left\{ y_i - \left[a_0 + \sum_{k=1}^{N} a_k \cos(k\omega x_i) + \sum_{k=1}^{N} b_k \sin(k\omega x_i) \right] \right\}^2 \tag{4}$$

By solving the following equations, the coefficients of Fourier series can be obtained .

$$\frac{\partial Q}{\partial a_i} = 0 \qquad (i = 0,1,2, \cdots, N) \tag{5}$$

$$\frac{\partial Q}{\partial b_i} = 0 \qquad (i = 1,2, \cdots, N) \tag{6}$$

The Gauss elimination method can be employed to solve the above equations and the coefficients of $2N+1$ in the equation (2) can be obtained.

Alternative lift force expression can be written as:

$$F_L / \frac{1}{2} \rho D U_m^{\,2} = a_0 + \sum_{k=1}^{n} C_L(k) \cos(k\omega t + \varphi(k)) \tag{7}$$

In which

$$C_L(k) = \sqrt{a_k^{\,2} + b_k^{\,2}}\,, \quad \varphi(k) = \operatorname{arctg} \frac{b_k}{a_k} \quad (k = 1,2,\cdots,N)$$

Through the above calculation, the lift force coefficients of the first ten orders for(e/D = 0.1, 0.2, 0.5, 1.0, and Kc = 5, 8, 10,13,20) have been found as shown in Fig.3.

If the distance from the horizontal cylinder to the bottom is large($e/D > 1$), it can be considered that the lift forces on the cylinder are not affected by the sidewall. In this case, the central axis of lift forces is the X axis, and a_0 is zero. If the cylinder is close to the bottom, then the central axis of lift forces would

deviate a certain distance from the X axis, and this value is a_0 . The reason for this is the influence of sidewall. Therefore, for the near bottom cylinder, a_0 is a very important parameter. The value of a_0 can be got by calculation, as shown in Fig.4.

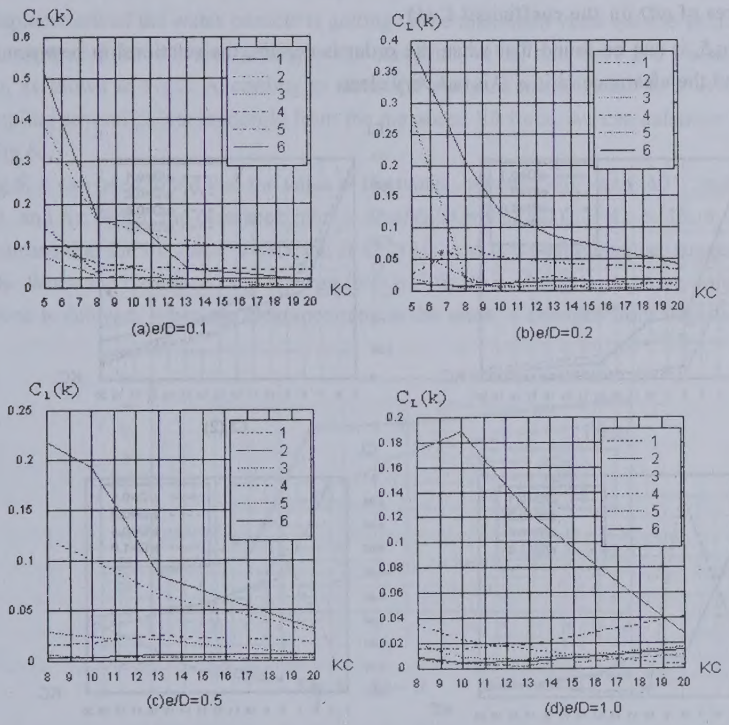

Fig. 3 $C_L(k)$ ~Kc (e/D = 0.1~1.0, Kc = 5~10)

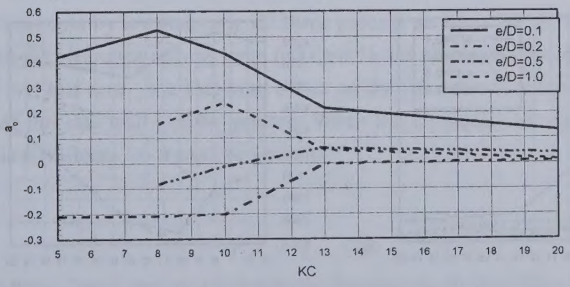

Fig.4 Value a_0

5 Analysis of experimental results and conclusions

5.1 Influences of *Kc* number on the coefficient $C_L(k)$

From Fig.3, it can be seen that when *e/D* is constant, coefficients of the first and second orders are

getting smaller with the increase of the *Kc* number, and the coefficients above the second order is getting gentle. When *Kc* is relatively small ($Kc \leqslant 10$), high order items (higher than order 5) can be ignored. When *Kc* is relatively large, high order items can't be ignored.

5.2 Influences of *e/D* on the coefficient $C_L(k)$

From Fig.5, it can be found that when the order is certain, the relationship between the lift force coefficient and the clearance ratio *e/D* is not very clear.

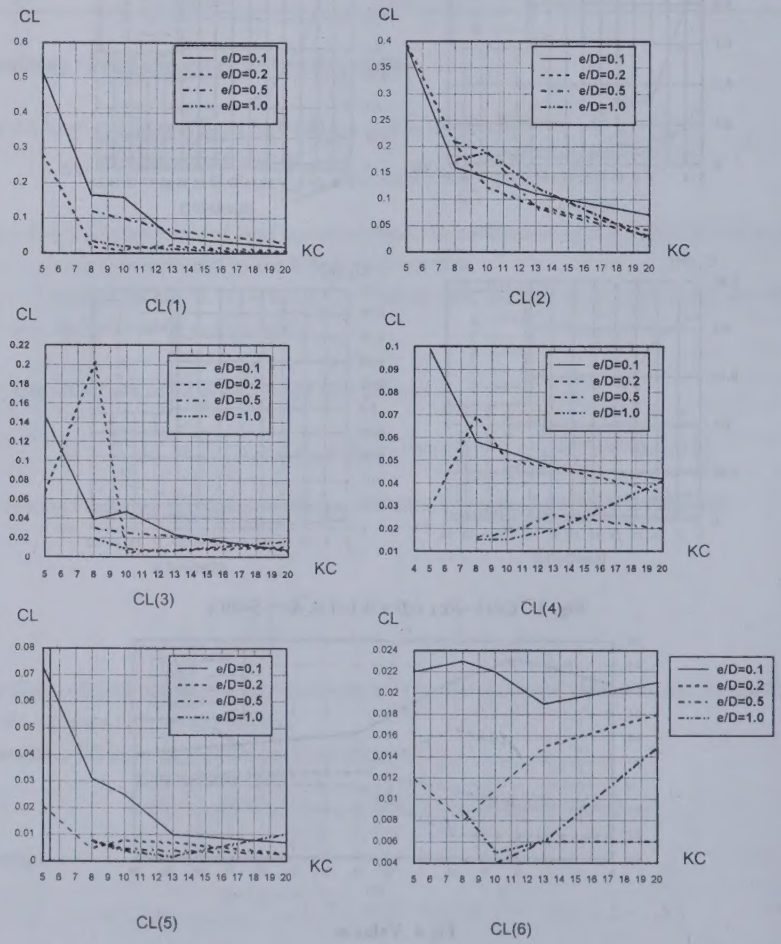

Fig. 5 $C_L(k) \sim e/D$ **curve**

5.3 Influences of *Kc* and *e/D* on a_0

From Fig.4, it can be known that when the clearance ratio *e/D* and *Kc* are both large (*e/D* >= 0.2, *Kc* >= 13), the central axis of lift force heads for the coordinate axis; when the clearance ratio *e/D* is

small and*Kc* is large, the central axis of lift force deviates from the coordinate axis clearly, and a_0 can't be ignored.

5.4 The phase difference between lift force and displacement (or velocity) of water particles

When displacement of the water particle is getting to the maximum value (or the velocity is getting to the minimum), the lift force is also getting to the maximum value, but, there is a phase difference θ between them, as shown in Fig.2. According to statistical analysis, the selection of θ is related to *Kc* and *e/D*. Sampling several points randomly from the measured lift force, we can calculate the value θ, as shown in Fig.6.

From Fig.6, it can been found that the value θ fluctuates between -30° and -40° , and the value is related to *e/D* and *Kc*. When the clearance ratio is small(e/D = 0.1, 0.2) , if $Kc < 10$, θ is a negative value, which means that the lift force is delayed; if $Kc \geq 10$, θ is a positive value, suggesting that the lift force leads. When the clearance ratio is large ($e/D \geq 1.0$), θ is always a negative value, indicating that the lift force is delayed. When the clearance ratio is the same, θ changes from negative to positive gradually.

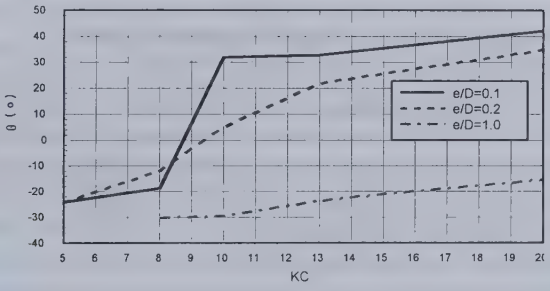

Fig. 6 $Kc \sim \theta$

5.5 The influences of side wall

From the lift force process by test (the only lift force process at Kc = 20, e/D= 0.1 is listed here), it can be seen that when the clearance ratio is large ($e/D \geq 0.5$), the lift force process line is symmetrical to the coordinate axis . At this time , the side wall effect on the lift force is relatively small; and when $e/D \geq 1.0$, influences of the side wall can be ignored. When the clearance ratio is small, the side wall effect on the lift force is significant, so it can't be ignored.

References

[1] Qiu Dahong (1985) Wave Theory and its Application on Engineering. Beijing: High Educational Publishing House, 274~290.

[2] Li Yucheng (1990) Wave Action on Marine Structures. Dalian: Dalian Univ. of Tech. Press, 141~199.

[3] Kang Haigui (1994) The Hydrodynamics Characteristics of Horizontal Cylinder under Different *Re* Number. *Journal of Hydrodynamics*, **9**(4): 388~394.

[4] Wang J. H., Kang H. G. and Greated C. A. (1997) A Study of Lift Force and Instantaneous Velocity Field Around an Oscillating Circular Cylinder. *China Ocean Engineering*, **11**(4): 419~430.

Advances in the Study of Geochemistry and Paleo-oceanography of the Co-rich Crust

Cai Yihua (蔡毅华), Huang Yipu (黄奕普)
Department of Oceanography, Xiamen University, Xiamen 361005

Abstract The current advances in the study of geochemistry and paleo-oceanography of the Co-rich crust are reviewed in this paper. We summarize the study of geochemistry of the Co-rich crust, discuss the diffusion of elements in the Co-rich crust and the exchange with ambient seawater. Besides, we discuss the effect of phosphatization and substrate rocks on the composition of the Co-rich crust. We also introduce the application of stable isotopes (including the stable isotopes of Pb, Nd, and Hf), radioactive isotopes (including the radioactive isotopes of Be, U and Th), and elements (including the major elements, minor elements and rare earth elements) to the study of paleo-oceanography of the Co-rich crust.

Keywords Co-rich crust, geochemistry, paleo-oceanography, advance

Previous studies on paleo-oceanography were often focused on the sediment core. However, the sediment core doesn't offer a long time scale because it deposites quickly, usually thousands of times quicker than the ferromanganese crust. Comparing with the long sediment core, ferromanganese crust is easier to get and the costs of sampling are lower. Besides, based on the geochemical studies, the Co-rich crust is less disturbed by the ambient environment and the interaction between crusts and seawater can almost be ignored. It acts as a closed system once it is formed. That's why Co-rich crust has become another focus of paleo-oceanography and marine scientists have paid more attention to it in recent years.

1 Summaries on the geochemical studies of Co-rich crusts

The Co-rich crust grows slowly on the substrate rock at a rate of several mm per Ma. It is a long-term record of mineralization environment, marine enviroment and global changes, for example, the changes of provenance, paleocirculation, paleo-redox potential of bottom seawater, paleoproductivity and paleoclimate, *etc.* These are often saved in the elemental and isotopic composition and other characteristics of the geochemistry of Co-rich crusts. Therefore, the elemental and isotopic composition in the Co-rich crust and the related geochemical characteristics should be known first before dating the crust and studying the history of paleo-oceanography. Besides, the geochemical behaviors of elements and isotopes in the crust also determine whether they can be used or not. Accordingly, the important precondition of the paleo-oceanographical study is to understand the geochemical behavior of the Co-rich crust and find the reliable tracer.

In recent years, studies on the source, composition and distribution of the elements in the Co-rich crust and the factors affecting these geochemical characteristics have been carried out. Most of these were concentrated on the material exchange with the ambient seawater and substrate, elemental diffusion

Received on May 26, 2002

and phosphatization effects during crusts' accretion. These studies establish the foundation for the application of stable and radioactive isotopes and elements to the paleo-oceanographical studies of Co-rich crusts.

1.1 Elemental diffusion in the Co-rich crust and exchange with ambient seawater

Henderson and Burton[1] calculated the effective elemental diffusion rates of U, Th, Li, Os, Sr, Be, Nd, Pb and Hf in the Co-rich crust (Table 1). The diffusion of Li, Os and Sr is too quick for us to record the composition of paleo-seawater accurately. Based on the chemical leach experiment, VonderHarr *et al.*[2] also proved that Sr in the Co-rich crust does exchange with the seawater. Diffusion of U is also quick, resulting in the growth rates induced by the depth profile of $^{234}U/^{238}U$ faster than those induced by ^{10}Be, $^{230}Th_{ex}$ dating. This is identical with Neff's results[3] that the exchange coefficient of U between the Co-rich crust and the ambient seawater is 5×10^{-6} a^{-1} obtained from the discrepancy of the growth rates. As Th, Nd, Pb and Be are quite steady in the Co-rich crust, it is reliable to apply these elements to the dating and paleo-oceanographical studies of the Co-rich crust. Hf also diffuses to a certain extent, but David[4] thought the diffusion rate of Hf is much higher than actual since the used concentration of seawater was not correct[5]. If the correct concentration[6] is used, the diffusion rate will be at the same level as Be, which means Hf is also quite steady in the crust. The discussion above shows that many elements, especially particle-active elements, are pretty steady in the Co-rich crust and the diffusion can be ignored, which means the substance exchange with ambient seawater can be ignored.

Tab. 1 Effective diffusivities of some elements in the Co-rich crust[1]

Elements	Th	Nd	Pb	Be	Hf	U	Sr	Os	Li
Diffusion rate (cm^2/a)	2×10^{-12}	2×10^{-11}	3×10^{-11}	1×10^{-10}	3×10^{-8}	1×10^{-6}	2×10^{-5}	3×10^{-5}	2×10^{-4}

1.2 Influence of substrate rocks on the Co-rich crust composition

The Co-rich crust contacts not only with the ambient seawater but also with the substrate rocks at the bottom. This is different from the ferromanganese nodule, which contacts with sediment at the bottom. It is known that the pore water markedly affects the composition of ferromanganese nodule. However, since the early 1980s, studies on the Co-rich crust have always supposed that the substrate rocks don't influence the Co-rich crust composition[7]. This hypothesis wasn't validated until Hein and Morgan[8] approved it based on the studies on the chemical and mineral composition of both the Co-rich crust and the underlying substrate rocks and some other statistical analysis results. This is the only direct and detailed evaluation on the interaction between substrate rocks and the Co-rich crust so far.

1.3 Influence of phosphatization on the Co-rich crust composition

When the climate is steady and the circulation sluggish, the dissolved phosphorus derived from the intense chemical weathering accumulates in large quantities in the deep sea. When the Antarctic glaciation expands and the ocean circulation intensifies, the phosphorus-rich deep seawater would upwell because of the benthal topographhy and stay in the oxygen minimum zone (OMZ) temporarily. As OMZ expands, the O_2-poor and phosphorus-rich seawater would get to the slopes of seamounts where the crust is growing. That will further restrain the precipitate of the crust and the carbonate fluorapatite (CFA) will impregnate. From the late Eocene through Miocene, two major and possibly three minor

episodes of phosphogenesis resulted in the phosphorite formation on equatorial Pacific seamounts. According to the crust age, the major event at 27-21Ma and the minor event at about 15Ma would result in the phosphatization of the crust.

Phosphatization distinctly affects the chemical and mineral composition of the Co-rich crust including major and minor elements and rare earth elements composition, *etc.*[8~10]. Under the influence of phosphatization, CFA impregnates the Co-rich crust and diagenetic remobilization and reorganization in the crust take place. There are controversies on whether phosphatization changes the composition of the steady isotope in the crust. Frank *et al.*[11] thought phosphatization has no effect on the composition of the steady isotopes of Pb and Nd in the Co-rich crust. Christensen *et al.*[12] also thought that phosphatization doesn't change the compostion of the steady isotope of Pb in the Co-rich crust. However, Ling *et al.*[13] thought phosphatization probably has some effect on the composition of the steady isotope of Pb in the Co-rich crust, but has no effect on the steady isotope of Nd. Lee *et al.*[14] thought that phosphatization doesn't alter the history of Hf isotopic composition. Therefore, more attention must be paid to the application of a variety of geochemical characteristics of the old part phosphatization crust to the studies of paleo-oceanography.

2 Progresses in paleo-oceanography studies of the Co-rich crust

Based on the geochemical characteristics of the crust, environmental characteristics of mineralization such as the chemical composition of the ambient seawater can be got directly. A series of studies have been made to get the distribution pictures and time series of the isotopes of Pb, Nd, Os, Hf, Be, U and Th in the Pacific, Indian and Atlantic Oceans. Besides, other studies also show the redox status of the ambient seawater and sediment. The provenance and the movement of water mass may be reflected from the chemical compositions and characteristics of the ambient seawater during the crust growth. The changes of the mineralization environment, paleo-ocean environment, the pattern of ocean circulation, and the interaction between these changes with the changes of paleogeography and paleoclimate can be further studied, thereby, linking the growth of the crust with the global change.

2.1 Application of stable isotopes in the Co-rich crusts to paleo-oceanography

The distribution of isotopes of Pb and Nd in deep seawater in the past 60Ma was controlled by: (a) variations in the oceanic mixing patterns and flow paths of water masses with distinct isotopic signatures related to major paleogeographic changes and (b) variability of supply rates or provenance of detrital material delivered to the ocean, which was linked to the climate change (glaciations) or major tectonic uplift[11]. The major paleogeographic change was closure of the Panama isthmus in 3~5Ma BP, the climate change was the start of the Northern Hemisphere glaciation (NHG), and the major tectonic uplift refers to the uplift of the Himalayas. Consequently, correlative information can be got from the studies of isotopes of Pb and Nd in the crust. These studies show that the closure of Panama isthmus and the start of NHG established the modern pattern of the ocean circulation[13, 15~17]. Further, the changes of the pattern of ocean circulation lead to the distinct changes of the composition of isotopes of Pb and Nd[18~20] and the source of material[19, 21~23] in the deep water. The studies on crusts in Southwest and Central Indian Ocean indicate that the Himalayan erosion contributes little to the composition of the deep seawater of the Indian Ocean in the past 20 Ma[18], while the input of Himalayan errosion can be distinguished from the crust located in North Indian Ocean, and maybe the input was only limited to a

small scale. However, other events like the outcrop of the Greenland-Scotland ridge may probably affect the input of Pb and Nd to the ocean[21].

The isotope of Hf can also be used in the studies on variations of prevenance of material, paleo-climate, paleo-ocean circulation and paleo-georgraphy. Godfrey *et al.*[25] thought that the isotope of Hf in the crusts could be used to determine the source of Hf, probably Fe and Mn. The shifts in the composition of Hf isotope in North Atlantic crust may have been caused by change of the erosion intensity as glaciation progressed in the northern hemisphere, while those shifts of Hf isotopic composition in the crust of Indian Ocean may have been caused by a short-term increase in Himalayan erosion and alternatively by the expanding influence of NADW into the Mid-Indian Basin via circum-Antarctic deep water (CDW) or a reduction of Pacific flow through the Indonesian gateway[26]. Lee *et al.*[14] found that the Hf isotopic composition in the Central Pacific deep water relates closely to the changes in paleo-geography and paleo-ocean circulation. David *et al.*[4] have also proved that the Hf isotope could be used as the tracer of source of elements and water masses.

2.2 Application of radioactive isotopes in the Co-rich crusts to paleo-oceanography

Ratio of $^{10}Be/^{9}Be$ is a good tracer of water mass movement and paleo-flux[27]. Von Blankenburg and O'Nions[28] used the ratio to trace the change in the intensity of NADW and the source of stable isotopes of Nd and Pb. Chabaux[29] thought that the ratio of Th/U and the initial activity ratio of Th related to the changes of ocean circulation in the past 150ka. Eisenhauer *et al.*[30] found the interaction between the growth of crust and the changes of climate in the late Quaternary climate change through the elements input in the water column based on the study of the depth profiles of ^{230}Th in crusts. Huh and Ku[31] studied the change in the intensity of aeolian dust related to the paleo-climate such as NHG through the distribution of ^{232}Th in crusts and nodules.

2.3 Application of elements in the Co-rich crusts to paleo-oceanography

Changes in the elemental compositions of the crusts also reflect the variation of paleo-climate and paleo-ocean environment. Segl *et al.*[32] found that the changes of the chemical composition of the crust happened at the same time as the paleo-climate events from the late Tertiary to the Quaternary. Halbach and Puteanus[33] found that the changes in the composition of the crust reflect the variation of the paleo-ocean environment, including dissolution rate of carbonate, the bottom current and the biological productivity etc. Based on the studies of the chemical composition of seamount crust in the Central Indian Ocean, Banakar and Hein[34] drew the conclusion that the growth of crusts was affected by the changes of carbonate compensation depth (CCD), depth of crust formation, early Eocene productivity, instability of substrate rock, parttern of ocean circulation and oxygenation of Indian Ocean deep water. Hein *et al.*[35] found that changes in the chemical composition of the crust was related to the changes of the paleo-ocean circulation and development of icecap at the poles in the study of the crusts of the Central Pacific Ocean. Besides, the climate change forced by the Earth motion has also affected the composition of crusts.

2.4 Progresses in the paleo-oceanographic study of the Co-rich crusts

Paleo-oceanographic studies of the Co-rich crust have also been carried out in China. Xu Dong Yu[36] summarized the variations of paleo-oceanographic environment of Central Pacific Seamount areas where crusts were growing. Liang Hongfeng *et al.*[37] thought that the growth of the crust located at Jianfeng Seamount in the South China Sea was controlled by the particular marine environment in the

South China Sea and maybe was influenced by the hydrothermal activity from the benthal volcanoes. He also drew the conclusion that the growth of crusts was influenced by the input of material and paleo-oceanographic condition based on the comparison study on the geochemical behaviors of elements in the crust of Central Pacific Ocean Seamount, the Philippine sea basin and the South China Sea[38]. The relation of the geochemical characteristics of major elements to the paleao-oceanographic environment in Western Pacific has also been discussed by Pan Jiahua and Liu Shuqin[39]. The result of Xu Dongyu[40] showed that the paleo-oceanographic environment and events such as Antarctic Bottom Water, upwelling, biological productivity, deposit discontinuity influenced and controlled the formation and distribution of polymetallic nodule, the Co-rich crust and seamount apatite. Further studies should be focused on the complete and accurate explanation of the record of mineralization environment in the crusts, so as to uncover the mechanism of mineralization and establish the pattern of mineralization.

3 Conclusions

Studies on the geochemistry in the Co-rich crusts are reviewed in our article. We focus on the exchange between the crust and seawater and substrate rock, the elemental diffusion in the crust and the effect of phosphatization on the crust, and so on. At the same time, the progresses in paleo-oceanographic studies of the Co-rich crust, including the use of isotopes, elements, are introduced.

Presently, there is still not a whole picture of the geochemical behavior of the isotopes and elements in the Co-rich crust. This limits the application of these isotopes and elements in the paleocaeagraphic studies and counteracts the development of paleo-oceanographic study. More and more will be known about the geochemical behavior and distribution characteristics of the elements and isotopes in the Co-rich crust following the improvement of the analysis methods. This will then promote the further development of paleo-oceanographic studies.

Acknowlegements

This work is supported by grants from China Ocean Mineral Resources R&D Association (COMRA), No.: DY105-01-04-11.

References

[1] Henderson G. M., Burton K. W. (1999) Using $^{234}U/^{238}U$ to assess diffusion rates of isotope tracers in ferromanganese crusts. *Earth Planet. Sci. Lett.*, 170: 169~179.

[2] VonderHaar D. L., Mahoney J. J., McMurtry G. M. (1995) An evaluation of stronium isotopic dating of ferromanganese oxides in a marine hydrogenous ferromanganese crust. *Geochim. Cosmochim. Acta*, 59: 4 267~4 277.

[3] Neff U., Bollhofer A., Frank N., *et al* (1999) Explaining discrepant depth profiles of $^{234}U/^{238}U$ and ^{230}Th in Mn-crusts. *Geochim. Cosmochim. Acta*, 63: 2 211~2 218.

[4] David K., Frank M., O'Nions R. K., *et al* (2001) The Hf isotope composition of global seawater and the evolution of Hf isotopes in the deep Pacific Ocean from Fe-Mn crusts. *Chem. Geol.*, 178: 23~42.

[5] Boswell S. M., Elderfield H. (1988) The determination of Zr and Hf in natural waters using isotope dilution mass spectrometry. *Mar. Chem.*, 25: 197~210.

[6] Godfrey L. V., White W. M., Salters V. J. M. (1996) Dissolved zirconium and hafnium distributions across a shelf break in the northeastern Atlantic Ocean. *Geochim. Cosmochim. Acta*, 60: 3 995~4 006.

[7] Hein J. R., Manheim F. T., Schwab W. C., *et al.* (1985) Ferromanganese crusts from Necker Ridge, Horizon Guyot, S. P. Lee Guyot: Geological considerations. *Mar. Geol.*, 69: 25~54.

[8] Hein J. R., Morgan C. L. (1999) Influence of substrate rocks on Fe-Mn crust composition. *Deep-Sea Res.*, I , 46: 855~875.

[9] Koschinsky A., Stascheit A., Bau M., *et al.* (1997) Effects of phosphatization on the geochemical and mineralogical composition of marine ferromanganese crusts. *Geochim. Cosmochim. Acta*, 61: 4 079~4 094.

[10] Jeong K. S., Jung H. S., Kang J. K., *et al.* (2000) Formation of ferromanganese crusts on northwest intertropical Pacific seamounts: electron photomicrography and microprobe chemistry. *Mar. Geol.*, 162: 541~549.

[11] Frank M., O'Nions R. K., Hein J. R., *et al.* (1999) 60 Myr records of major elements and Pb-Nd isotopes from hydrogenous ferromanganese crusts: Reconstruction of seawater paleochemistry. *Geochim. Cosmochim. Acta*, 63: 1 689~1 708.

[12] Christensen J. N., Halliday A. N., Godfley L. V., *et al.* (1997) Climate and Ocean Dynamics and the lead isotopic records in Pacific ferromanganese crusts. *Science*, 277: 913~918.

[13] Ling H-F., Burton K. W., O'Nions R. K., *et al.* (1997). Evolution of Nd and Pb isotopes in Central Pacific Seawater from ferromanganese crusts. Earth Planet. *Sci. Lett.*, 146: 1~12.

[14] Lee D-C., Halliday A. N., Hein J. R., *et al.* (1999) Hafnium isotope stratigraphy of ferromanganese crusts. *Science*, 285: 1 052~1 054.

[15] Burton K. W., Ling H-F., O'Nions R. K. (1997) Closure of the Central American Isthmus and its effect on deep-water formation in the North Atlantic. *Nature*, 386: 382~385.

[16] Burton K. W., Christense J. N., Lee D. C., *et al.* (1998) The radiogenic isotope chemistry of North Atlantic Deep Water during the Neogene recorded by hydrogenous ferromanganese crusts. *Min. Mag.*, 62A: 263~264.

[17] Christensen J. N., Halliday A. N., Godfley L. V., *et al.* (1997) Climate and Ocean Dynamics and the lead isotopic records in Pacific ferromanganese crusts. *Science*, 277: 913~918.

[18] O'Nions R. K., Frank M., von Blanckenburg F., *et al.* (1998) Secular variation of Nd and Pb isotopes in ferromanganese crusts from the Atlantic, Indian and Pacific Ocean. *Earth Planet. Sci. Lett.*, 155: 15~28.

[19] Reynolds B. C., Frank M., O'Nions R. K. (1999) Nd- and Pb-isotope time series from Atlantic ferromanganese crusts: implications for changes in provenance and paleocirculation over the last 8Myr. *Earth Planet. Sci. Lett.*, 173: 381~196.

[20] Burton K. W., Lee D-C., Christensen J. N., *et al.* (1999) Actual timing of neodymium isotopic variations recorded by Fe-Mn crusts in the western North Atlantic. *Earth Planet. Sci. Lett.*, 171: 149~156.

[21] Abouchami W., Galer S. J. G., Koschinsky A. (1999) Pb and Nd isotopes in NE Atlantic Fe-Mn crusts: Proxies for trace metal paleosources and paleocean circulation. Geochim. *Cosmochim. Acta*, 63: 1 489~1 505.

[22] von Blanckenburg F., O'Nions R. K., Hein J. R. (1996) Distribution and sources of pre-anthropogenic lead isotopes in deep ocean water from Fe-Mn crusts. Geochim. *Cosmochim. Acta*, 60: 4 957~4 963.

[23] Abouchami W., Goldstein S. L., Galer S. J. G., *et al.* (1997) Secular changes of lead and neodymium in central Pacific seawater recorded by a Fe-Mn crust. *Earth Planet. Sci. Lett.*, 61: 3 957~3 974.

[24] Frank M., O'Nions R. K. (1998) Sources of Pb for Indian Ocean ferromanganese crusts: a record of Himalayan erosion. *Earth Planet. Sci. Lett.*, 158: 121~130.

[25] Godfrey L. V., Lee D-C., Sangrey W. F., *et al.* (1997) The Hf isotopic composition of ferromanganese nodules and crusts and hydrothermal manganese deposits: Implications for seawater Hf. *Earth Planet. Sci. Lett.*, 151: 91~105.

[26] Piotrowski A. M., Lee D-C., Christensen J. N., *et al.* (2000) Changes in erosion and ocean circulation recorded in the Hf isotopic compositions of North Atlantic and Indian Ocean ferromanganese crusts. *Earth*

Planet. Sci. Lett., 181: 315~325.

[27] von Blanckenburg F., O'Nions R. K., Belshaw N. S., *et al.* (1996) Global distribution of beryllium isotopes in deep ocean water as derived from Fe-Mn crusts. *Earth Planet. Sci. Lett.*, 141: 213~226.

[28] von Blanckenburg F., O'Nions R. K. (1999) Response of beryllium and radiogenic isotope ratios in Northern Atlantic Deep Water to the onset of northern hemisphere glaciation. *Earth Planet. Sci. Lett.*, 167: 175~182.

[29] Chabaux F., O'Nions R. K., Cohen A. S., *et al.* (1997) ^{238}U ^{234}U ^{230}Th disequilibrium in hydrogenous oceanic Fe-Mn crusts: Palaeoceanographic record of diagenetic alteration. *Geochim. Cosmochim. Acta*, 61: 3 619~3 632.

[30] Eisenhauer A., Gögen K., Pernicka E., *et al.* (1992) Climatic influences on the growth rates of Mn crusts during the Late Quaternary. *Earth Planet. Sci. Lett.*, 109: 25~36.

[31] Huh C-A., Ku T. L. (1990) Distribution of thorium-232 in manganese nodules and crusts: Paleoceanographic implications. *Paleoceanography*, 5: 187~195.

[32] Segl M., Mangini A., Banani G., *et al.* (1984). 10Be-dating of a manganese crust from Central North Pacific and implications for ocean palaeocirculation. *Nature*, 309: 540~543.

[33] Halbach P., Puteanus D. (1984) The inflluence of the carbonate dissolution rate on the growth and composition of Co-rich ferromanganese crusts from Central Pacific seamount areas. *Earth Planet. Sci. Lett.*, 68: 73~87.

[34] Banakar V. K., Hein J. R. (2000) Growth response of a deep-water ferromanganese crust to evolution of the Neogene Indian Ocean. *Mar. Geol.*, 162: 529~540.

[35] Hein J. R., Bohrson W. A., Schulz M. S., *et al.* (1992) Variations in the fine-scale composition of a central Pacific ferromanganese crust: Paleoceanographic implications. *Paleoceanography*, 7: 63~77.

[36] Xu Dongyu (1986) Study on cobalt-rich manganesecrusts in the middle Pacific Seamount region. *Marine Geology & Quaternary Geology*, **6** (1): 63~74.

[37] Liang Hongfeng, Yao De, Liang Dehua, *et al.* (1991) Geochemistry of polymetelallic crust from JianFeng Seamount, South China Sea. *Marine Geology & Quaternary Geology*, **11** (4): 49~57.

[38] Liang Hongfeng, Xu Dongyu, Lin Zhenghong, *et al.* (1994) Element geochemistry of hydrogenic ferromanganese crusts from some areas in the Pacific Ocean. ed. Xu Dongyu, Yao De, Liang Hongfeng, *et al.* Paleoceanographic environment when polymetallic nodule formed. Beijing: Geology Press. 22~41.

[39] Pan Jiahua, Liu Shuqin (1999) Distribution, composition and element geochemistry of Co-rich crusts in the Western Pacific. *Acta Geoscientia Sinica*, **20** (1): 47~54.

[40] Xu Dongyu (1999) Paleoceanographic events and mineralization in Pacific. ed. Xu Dongyu. Proceeding of the 30th International Conference on Geology, Vol. 13, Marine Geolody, Paleoceanography. Beijing: Geology Press. 101~113.

Analysis of Interannual Variations of Inorganic Nitrogen in the Bohai Sea

Shi Qiang (石 强), Gao Zhenhui (高振会), Yang Jianqiang (杨建强)
North Sea Monitoring Center, SOA, Qingdao 266003

Abstract According to the Bohai Sea cross-section data during 1985~1998, the high concentration inorganic nitrogen in the Bohai Sea section bottom layer water nearshore diffused and transferred to the middle of the Bohai Sea year after year. The interannual variations of the concentration of inorganic nitrogen in the Bohai Sea section bottom layer water may reflect the degree of eutrophication more steadily. The nitrate nitrogen and nitrite nitrogen are used to show quasi-equilibrium state interannual variations, but with the aggravation of seawater pollution, the quasi-equilibrium state of interannual variations has been broken and the marine biological-chemical processes can only maintain the secondary part of the interannual variations in a quasi-equilibrium state, but are not sufficient to prevent the main part of interannual variations from deviating from the quasi-equilibrium state. The spatial distributions of inorganic nitrogen would be affected by the reproduction and swarming of marine life.

Keywords Inorganic nitrogen, transference, diffusion, quasi-equilibrium state

1 Introduction

The inorganic nitrogen in the seawater is an important nutrient element that marine organisms must feed on and also one of the major elements participating in the marine biochemical cycle. In the past decade and more, as a result of the large amount of land-based pollutants into the sea along the coast of the Bohai Sea and the increasingly aggravated marine pollution in the Bohai Sea, the normal cyclic process of seawater nutrient elements in the ecological process has been disrupted and the eutrophication of sea water has become more serious. At present, the terrigenous sewage which the Bohai Sea accommodates every year has reached 2.8 billion tons and the pollutants of various kinds have amounted to over 700 000 tons, and the number of marine ecological disasters such as red tide has increased. Since 1990, several dozens of major red tide incidents have been recorded, affecting a sea area up to several thousand square kilometers and causing a direct economic loss of several billion yuan (RMB). It can thus be seen that the distribution and the cyclic process of inorganic nitrogen in the Bohai Sea water have changed significantly and that the natural cyclic process of inorganic nitrogen formed in the past in the Bohai Sea may have been subjected to some variation. Therefore, to study the characteristics of interannual variations of inorganic nitrogen in the Bohai Sea is of significant importance to the research on the variations of the marine chemical cyclic process of inorganic nitrogen in the Bohai Sea and the establishment of the mathematical model for inorganic nitrogen cycle as well as evaluation of the level of eutrophication in the Bohai Sea and recovery of the Bohai marine eco-environment.

Received on July 12, 2002

2 Survey data and analytical methods

The data for analysis are taken from the inorganic nitrogen concentrations at the sea surface and bottom of the Bohai survey sections and the survey stations are shown in Fig. 1. The observation time

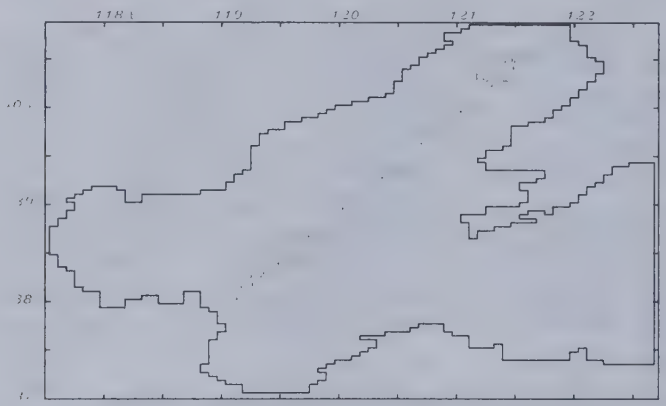

Fig. 1 Schematic sketch of survey section for inorganic Nitrogen in the Bohai

for NO_3-N and NO_2-N at the sea surface and bottom was May in 1985~1995 and August in 1995~1998 and that for NH_4-N was May in 1991~1995 and August in 1991~1998 while the inorganic nitrogen data for August of 1993 are lacking. The analytical instrument used is the marine spectrophotometer and the analytical methods are adopted as provided for in the Marine Survey Specifications of the State Oceanic Administration.

The elements to be analysed are plotted into profile-time views respectively by employing the multi-conicoid objective analysis method based on the radius base function. In order to reduce the noise interference, the Shapiro second-order ideal low-pass filtration is made for the data[1]. To study the space -time analysis of the analytical elements, we have made the empirical orthogonal function (EOF) analysis for each element and chosen the eigenvectors (*EVEs*) and principal components (*PCs*) of NO_3-N, NO_2-N and NH_4-N which are of geochemical significance by applying the N-rule judgement similar to Refs.[2,3].

As the marine surface and bottom waters are adjacent to different media respectively, the surface is close to the atmosphere and the bottom to the sediment. The inorganic nitrogen in the atmosphere over the Huanghai Sea area settles mainly in the form of ammonia nitrogen and nitrate, so they are the main sources of nutrients for the phytoplankton in the upper mixing layer during lamination[4,5]. Field cultural experiment indicates that, as far as the mean flux is concerned, nitrate, nitrite, phosphate and silicate all transport from the sediment to the overlying water and the reverse is true of ammonia nitrogen, *i.e.*, from the overlying water to the sediment[6]. Due to the difference in the form and rate of the nutrient salts as well as photosynthesis and advection transport between the marine surface and bottom waters, the

time-space variation characteristics of their nutrient salts are bound to be somehow different. EOF analysis shows (Table 1) that the analytical eigenvalues of inorganic nitrogen through test at the bottom

Tab. 1 Eigenvectors and principal components with geochemical significance

Month	NO_3-N		NO_2-N		NH_4-N	
	Surface	Bottom	Surface	Bottom	Surface	Bottom
May	E_1, P_1 E_2, P_2	E_1, P_1 E_2, P_2 E_3, P_3	E_1, P_1	E_1, P_1 E_2, P_2	E_1, P_1	E_1, P_1
August	E_1, P_1	E_1, P_1	E_1, P_1	E_1, P_1	E_1, P_1	E_1, P_1 E_2, P_2

Notes: E_1, E_2 and E_3 represent the first, second and third eigenvectors respectively;

P_1, P_2, and P_3 represent the first, second and third principal components respectively.

are slightly more than at the surface, suggesting that the level of geochemical signals of inorganic nitrogen at the bottom is somewhat higher than that at the surface and that the interannual variation characteristics of inorganic nitrogen at the bottom are more stable than those at the surface. Therefore, we mainly make an analysis of the bottom inorganic nitrogen.

3 Analysis of interannual variations of NO_3 -N

In full aeration condition, NO_3-N in sea water is a stable form of compound in the inorganic nitrogen (thermodynamically). The mean water depth of the sections is 19 m, the vertical mixing in the waters is relatively full and there is not much difference in the concentration distribution of NO_3-N between the surface and bottom layers. Figs.2 and 3 are the diagrams of interannual variations of NO_3-N

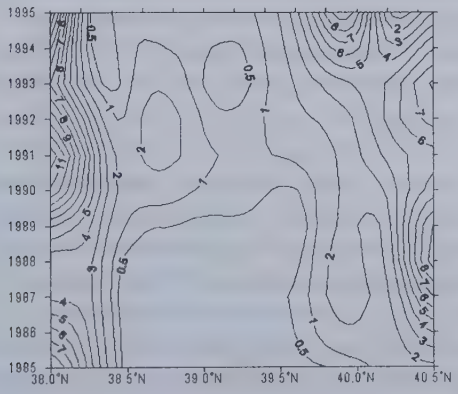

Fig.2 Interannual variations of NO_3-N in the bottom layer water in the Bohai Sea in May (μ mol/L)

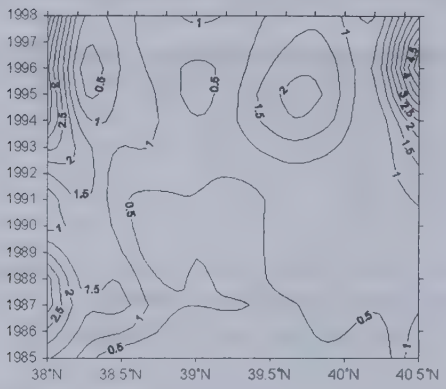

Fig.3 Interannual variations of NO_3-N in the bottom layer water in the Bohai Sea in Augest (μ mol/L)

in the bottom layer water in the Bohai Sea in May and August respectively. In May, the high-value zones of NO_3-N are found in the sea area near the estuary at the two ends of the section. Owing to the transference and diffusion of NO_3-N in the Liaodong Bay and the Huanghe River mouth sea area, the concentration of NO_3-N in the central Bohai Sea has gradually risen, the high-value line of NO_3-N at the end of the Liaodong Bay has persistently moved southwards and the contour line of 110 umol/L has moved about 100 km southwards within 11 years; The NO_3-N in the sea area near the Huanghe River mouth transports to the north in an abrupt way. Such difference can be attributed to the characters of tidal and residual currents in the Bohai Sea. August is the breeding period for organisms such as phytoplankton, bacteria and algae, which take in and excessively store up NO_3-N[7] so that the concentration of NO_3-N in August is lower than that in May. However, as compared with that in 1985, the NO_3-N concentration in the whole section in 1998 has risen quite a lot.

EOF analysis indicates that the seasonal difference in the distribution of the spatial eigenvectors of NO_3-N is distinct in the bottom layer water. In May, the first eigenvectors (EVE_1) are distributed gently with little change in the central Bohai Sea (38.5° N~39.5° N); The cold water mass zone in the Liaodong Bay (40° N~39.5° N) and the nearshore sea area at both ends of the section present an antiphase change (F4a), while, in August, EVE_1 in the majority of areas in the section presents the in-phase change (figure omitted). In May, the second eigenvector (EVE_2) in the southern and northern sea areas of the section with the central Bohai Sea as their boundary presents the in-phase change. (EVE_2 in August is closer to the N-rule criterion and has the similar distribution.) In May, the third eigenvector (EVE_3) presents an obvious in-phase change in the central section (38.7° N) and the sea area at the northern tip (Fig. 4a). The characteristics of the change of principal components are: During 1985~1991, PC_1 presented a quasi-equilibrium state change and after 1991, it has presented the change deviating from the quasi-equilibrium state, while PC_2 and PC_3 still maintain the quasi-equilibrium change (Fig. 4b). To sum up the above-mentioned characteristics, it is clear that in August the biocoenose

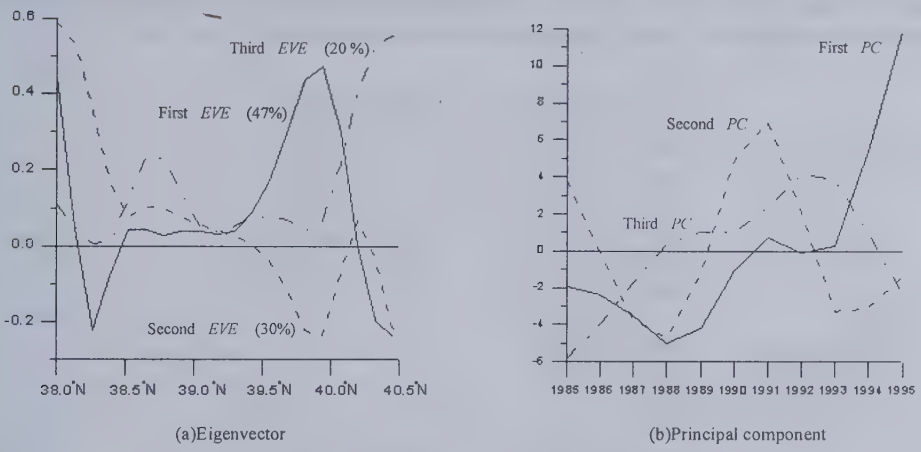

(a)Eigenvector (b)Principal component

Fig.4 Concentration of NO_3-N in the bottom layer water in May

blooms and takes in large amounts of NO_3-N so that the concentration of NO_3-N drops and the spatial distribution structure becomes simple and uniform. In May, the NO_3-N concentration is higher, its spatial distribution pattern is more complicated and the low-temperature environment of the cold water mass in the Liaodong Bay is advantageous to the enrichment of NO_3-N; The highly concentrated phytoplankton in the sea area north of 39° N in the Bohai Sea[8,9] takes in large amounts of NO_3-N, causing the emergence of the component of anti-phase change in the southern and northern Bohai Sea; The input of NO_3-N by the littoral rivers of the Bohai Bay and the Liaodong Bay mainly affects the nearshore sea area of the Bohai Sea section (south of 39° N and north of 40° N). The subject of NO_3-N change in the Bohai Sea section (PC_1) used to be subjected to a quasi-equilibrium state change, but, as a result of the persistent growth of the NO_3-N concentration, the subject of the NO_3-N variations presented a change deviating from the quasi-equilibrium state. However, the secondary parts of the NO_3-N variations (PC_2, PC_3) still maintain the change of a quasi-equilibrium state, and the cyclic periods are approximately 5a and 11a.

4 Analysis of interannual variations of NO_2-N

NO_2-N is an intermediate oxidation state between NH_4-N and NO_3-N. It may appear as a transitional form of NH_4-N oxidation or NO_3-N reduction. These two processes are mainly activated in the ocean by the action of organisms[7]. In the Bohai Sea, the concentration of NO_2-N is lower than that of other inorganic nitrogens. The photoreduction causes the concentration of NO_2-N in the surface layer to be lower than that in the bottom layer and the concentration of algal organisms in summer produces NO_2-N , making the concentration of NO_2-N higher in August than in May. Since the 1990s, the bottom concentration of NO_2-N in August has increased obviously, the high-value line of NO_2-N in the sea area at the end of the Liaodong Bay has extended about 110 km southwards and the high-concentration zone

of NO_2-N in the sea area off the Huanghe River mouth has expanded for about 60 km to the central Bohai Sea. (Fig.5). In May, the high-value line of the NO_2-N concentration in the bottom layer water has extended from the tip of the Liaodong Bay to the central Bohai Sea for about 110 km (Fig. 6).

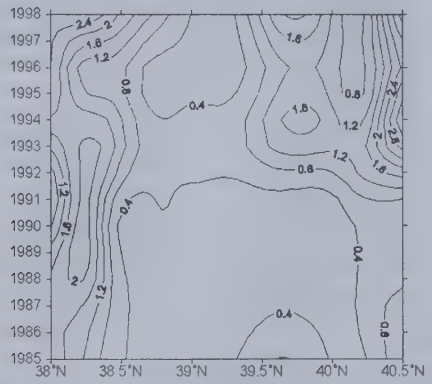

Fig.5 Interannual variations of NO_2-N in the bottom layer water in the Bohai Sea in Augest (μ mol/L)

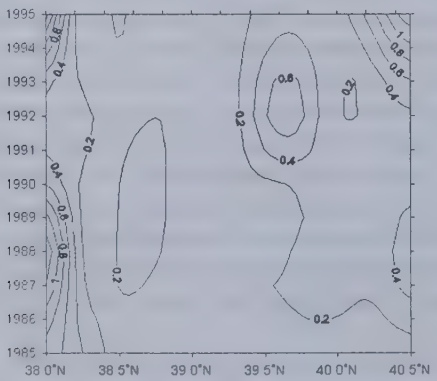

Fig.6 Interannual variations of NO_2-N in the bottom layer water in the Bohai Sea in May (μ mol/L)

Characteristics of EOF analysis: In May, the EVE_1 of NO_2-N in the nearshore areas at both ends of the Bohai Sea section and the central Bohai Sea changes in antiphase while in August, it changes in phase (figure omitted). In May, the EVE_2 of NO_2-N changes in antiphase (Fig.7a). In August, when the PC_1 weight decreased before 1991, the PC_2 weight increased. In May, when the PC_2 weight has continuously increased for 8 years (1985~1992), PC_1 presents the change deviating from the quasi-equilibrium state (Fig.7b).

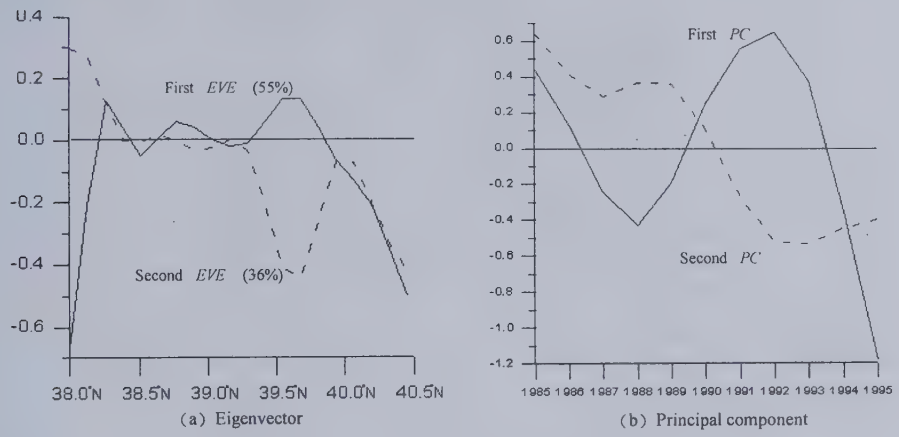

Fig.7 Concentration of NO_2-N in the bottom layer water in May

The above-mentioned characteristics indicate that the interannual and spatial variations of NO_2-N in the section are small in the central Bohai Sea, but large in the sea areas at both ends of the section. The spatial distribution and interannual variations of the NO_2-N concentration are similar to those of NO_3-N and so are their causes, which will not be repeated here.

5 Analysis of interannual variations of NH_4-N

During the growth of phytoplankton, many unicellular algae have a preference of utilizing NH_4-N over NO_3-N and their adsorption rate on NH_4-N is higher than that on NO_3-N. In the surface water of the temperate zone, when the growth of phytoplankton has removed most of NO_3-N, NH_4-N tend to become the most abundant form in the combined inorganic nitrogen. In addition, the dead and aging algal molecules would be subjected to autolysis, which combines with the action of bacteria to release most of the organic nitrogen in the form of NH_4-N which has been bound in the particles[7]. Therefore, NH_4-N is a very important combined form of inorganic nitrogen in the ocean which changes and transforms very quickly.

The concentration of NH_4-N in the bottom layer water rises year by year, which is revealed in the fact that, in May, the high concentration zone of NH_4-N at both ends of the section diffuses and transports toward the central Bohai Sea and that, in August, mainly the NH_4-N concentration in the Sea area north of 38.5° N in the section gradually increases while the diffusion and transference of the high concentration NH_4-N is not evident in the nearshore area (Figs. 8 and 9).

Characteristics of EOF analysis: In August, there exists the component of antiphase change in the EVE_1 of the NH_4-N concentration in the bottom layer water and the antiphase change of EVE_2 is not very evident in the sea area of cold water mass in the Liaodong Bay (Fig. 10a). In August, the PC_1

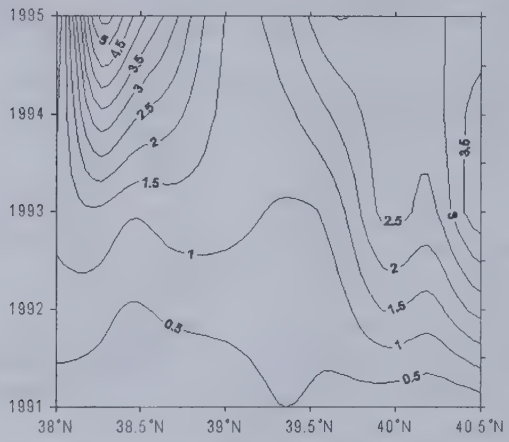

Fig.8 Interannual variations of NH_4-N in the bottom layer water in the Bohai Sea in May (μ mol/L)

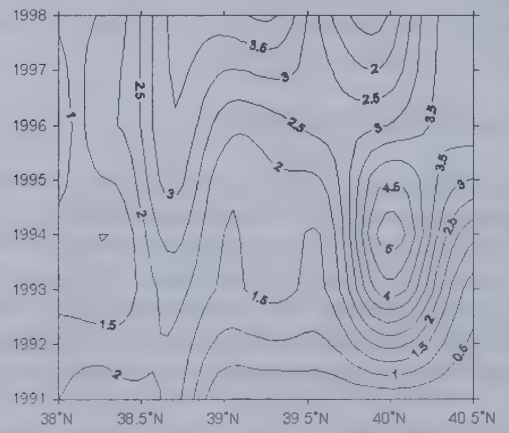

Fig.9 Interannual variations of NH_4-N in the bottom layer water in the Bohai Sea in Augest (μ mol/L)

weight of NH_4-N concentration in the bottom layer water presents an exponential increase, which may be related to the eco-environmental deterioration and the decrease of NH_4-N taken in by plankton. See Fig. 10b for the quasi-equilibrium state change of PC_2. Due to the shorter observational sequence, further analysis of NH_4-N in the Bohai Sea would have to await the accumulation of more observations.

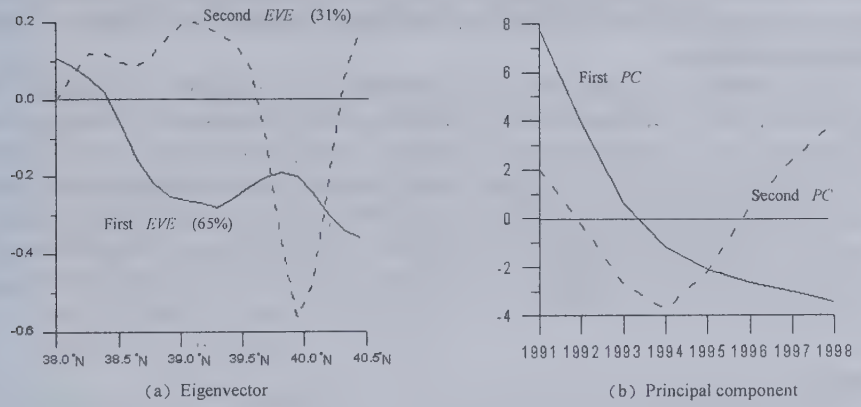

(a) Eigenvector (b) Principal component

Fig.10 Concentration of NH_4-N in the bottom layer water in Augest

6 Conclusions

During 1985~1998, the concentration of inorganic nitrogen was increasing year by year in the sectional waters of the Bohai Sea, and especially since 1991, the inorganic nitrogen in the sectional sea area has increased by several times and eutrophication of sea water has aggravated. The increase of the concentration of inorganic nitrogen in the sectional waters of the Bohai Sea is attributed to the eco-environmental deterioration and the decrease of biomass caused by pollution as well as to the input of inorganic nitrogen in the continental runoff. The water of high concentration inorganic nitrogen transfers and diffuses from the nearshore sea areas at both ends of the section to the central Bohai Sea via the bottom layer water year by year, and the inorganic nitrogen concentration of the surface layer water is prone to transformation and displacement due to the effect of the external physical factors (wind, precipitation, surface current, solar radiation, *etc.*). Therefore, the inorganic nitrogen concentration in the bottom layer water of the Bohai Sea has a more stable character of interannual variations than that in the surface layer and can reflect the level of eutrophication of sea water in a more steady way. *EOF* analysis indicates that the main part of the interannual variations of NO_3-N and NO_2-N in the sectional water of the Bohai Sea was originally the quasi-equilibrium change, which could not be altered immediately by the discharge of continental runoff pollutants. But after the discharged pollutants have increased continuously over many years, the marine eco-environment has been deteriorated, the main part of NO_3-N and NO_2-N variations which once presented a quasi-equilibrium state change has been destroyed, and turned to and maintained at a higher level of concentration. Although the marine biological-chemical process can maintain the secondary part of its interannual variations in a quasi-equilibrium state, it cannot prevent its main part from breaking away from the quasi-equilibrium state.

The reproduction and the concentration density of such marine organisms as phytoplankton and

algae can have significant effect on the spatial distribution of inorganic nitrogen concentrations. In the sea area with highly concentrated organisms such as phytoplankton, the rate of regeneration and consumption of inorganic nitrogen would speed up and the transformation among inorganic nitrogens would become complicated.

In the mid-1980s, the inorganic-nitrogen concentration could still maintain the seasonal[10] and interannual variations of a quasi-equilibrium state, but since the early 1990s, as a result of the aggravated degree of pollution, the natural variation form of inorganic nitrogen in the Bohai Sea has been severely distorted, which, along with the worsening of the Bohai Sea eco-environment, has had adverse effect on the development of marine economy and the improvement of people's quality of life. Therefore, to improve the eco-environment of the Bohai Sea and restore the inorganic nitrogen in the Bohai Sea to its natural variation form is the phase objective of our marine environmental protection work in the near future.

References

[1] Shapiro R. (1970) Smoothing, filtering, and boundary effects. [J]. *Rev. of Geophys and Spac Phys.*, **8**: 359~387.

[2] Preisendor R. W. and Barnett T. P. (1977) Significance tests for empirical orthogonal functions. [C]. *Fifth Conf. Probability and Statistics in Atmospheric Sciences, Las Vegas, Amer. Meteor. Soc.*, 167~172.

[3] Overland.J E and Preisendorfer R W. (1982) A significance test for Principal components applied to a cyclone climatology. [J]. *Mon. Wea. Rev.*, **110**(1):1~4.

[4] Zhang J., Chen S. Z. *et al.* (1999) Factors influencing changes in rainwater composition form urban versus remote regions of the Yellow Sea. [J]. *J.G.R.*, **104**(D1): 1 631~1 644.

[5] Zhang J., Liu M. G. (1994) Observations on nutrient elements and sulfate in atmospheric wet depositions over the northwest Pacific coastal ocean-Yellow Sea. [J]. *Mar.Chem*, 47: 173~189.

[6] Liu S. M., Chen H. T. *et al.* (1999) N, P and Si compounds in the South Yellow Sea. Biogenchemical Processes in the Bohai and Yellow Sea. [M]. *Seoul: The Dongjin Publication Association*, 274.

[7] Riley J.P., Skirrow G. (1975) Chemical Oceanography. [M]. 2nd Edition, Academic Press, **2**.

[8] Kang Yuande (1991) Quantity Distribution and Seasonal Variations of Phytoplankton in the Bohai Sea. *Marine Fisheries Research*, (12): 31~54.

[9] Yu Jianluan and Li Ruixiang (1993) Research on the Ecology of Phytoplankton in the Bohai and Huanghai Seas. [J]. *Bohai and Huanghai Seas Oceanography*, **11**(3): 52~59.

[10] Shi Qiang, Chen Jianglin and Li Chongde (2002) Analysis of Seasonal Cycle of the Nitrate Nitrogen and Nitrite Nitrogen in the Bohai Sea. [J]. *Marine Science Bulltion*, **20**(6): 32~39.

Biogeochemical Character of Dissolved Inorganic Nitrogen and Phosphate at Plume Front in the Changjiang River

Fu Ruibiao (傅瑞彪), Shen Huanting (沈焕庭)
State Key Laboratory of Estuary and Coast, East China Normal University, Shanghai 200062

Abstract Biogeochemical character of dissolved inorganic nitrogen and phosphate at plume front is studied based on the data, which were observed in the Changjiang River Estuary in 1988. The results are as follows: The concentrations of nitrate and phosphate change abruptly at plume front and halocline. The concentrations of NO_2^- and NH_4^+ are very high at 10~25 m depth. The vertical circumfluence transports NO_3^- and PO_4^{3-}, which are released from organisms at the bottom to phytoplankton.

Keywords the Changjiang River estuary, plume front, dissolved inorganic nitrogen, Phosphate, biogeochemical character

1 Introduction

Front is an apparent character of a distinct interface between two conjoint waters with different characters[1]. Plume front usually is formed between mixed estuarine water and oceanic water. Generally there are higher content of chlorophyll *a* and primary production[2-5]. The phytoplankton concentrates at 122° 30′ E nearby in the Changjiang River estuary and appears a remarkable discontinuous phenomenon [6]. Professor Chen Jiyu pointed out that the phenomena are mainly caused by the discontinuity of hydrology and sediments formed by estuarine circumfluence and so on[7]. In order to get some new knowledge about the phenomenon and the mechanism the paper focuses on exploring the biogeochemical character (including distributed, transported, absorbed, regenerated and others) of the dissolved inorganic nitrogen and phosphate. The data, observed on-the spot in 1988, were provided by Professor Fu Fangxi according to the "Estuarine Front" project, supported by the National Natural Science Foundation.

2 Materials and methods

A reconnaissance of the front of the Changjiang River estuary was carried out on a cruise in August 1988 (Figure 1). Methods of collecting and analysing samples are described in Reference [8]. Concentrations of PO_4^{3-}, NO_3^-, NO_2^- and NH_4^+ and salinity are summarized in Table 1.

Received on August 8, 2002

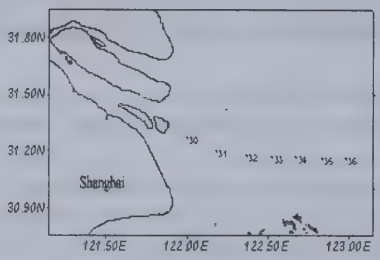

Fig. 1 Sample stations in the Changjiang River estuary

Tab. 1 Concentrations of PO_4^{3-}, NO_3^-, NO_2^-, NH_4^+ and salinity

Station	Depth (m)	PO_4^{3-}	NO_3^-	NO_2^-	NH_4^+	Salinity
		μ mol/L				
30	0.0	0.66	12.00	0.34	2.32	0.3
	5.0	0.66	8.57	0.70	2.36	0.6
	9.0	0.78	9.25	0.29	2.54	0.8
31	0.0	0.06	39.80	0.36	1.94	7.0
	5.0	0.63	36.00	0.46	2.32	11.2
	10.0	0.56	22.10	0.51	2.5	14.7
32	0.0	0.56	25.50	0.54	2.41	10.0
	5.0	0.27	*	1.10	2.52	25.2
	12.0	0.13	*	1.26	2.52	28.7
33	0.0	0.03	0.53	0.28	1.18	26.3
	5.0	0.03	1.24	0.22	1.28	26.5
	10.0	0.03	0.56	0.57	1.84	31.5
	15.0	0.03	1.85	1.18	1.85	32.2
	21.0	0.03	*	1.29	1.19	32.1
34	0.0	0.11	*	0.38	1.78	27.6
	5.0	0.13	*	0.35	1.66	29.6
	10.0	0.11	0.24	0.41	2.46	32.0
	15.0	0.11	2.65	0.69	0.96	33.0
	25.0	0.11	3.64	0.85	1.40	33.0
	33.0	0.13	2.30	0.79	2.69	33.0
35	0.0	*	12.5	0.40	0.43	25.6
	5.0	*	5.12	0.36	*	28.7
	10.0	*	0.06	0.44	*	29.9
	15.0	0.39	0.30	2.24	*	31.3
	25.0	0.83	16.40	0.55	*	32.8
	47.0	1.33	18.70	0.42	0.57	33.6
36	0.0	0.27	*	0.35	*	28.6
	5.0	0.15	*	0.19	*	28.8
	10.0	0.35	7.16	0.65	*	30.8
	15.0	0.85	6.65	0.50	*	32.9
	25.0	1.02	13.70	0.44	*	33.6
	55.0	1.16	14.50	0.31	*	33.2

* under detection limit

3 Results

3.1 Horizontal distribution

The concentrations of NO_3^- and PO_4^{3-} show an obvious discontinuity at the surface between Stations 32 and 33, at the 5 m depth and the bottom between Stations 31 and 32. And the concentrations of NO_3^- and PO_4^{3-} change from 25.5 to 0.53 μ mol/L and from 0.56 to 0.03 μ mol/L at the surface, respectively, from 36.0 μ mol/L to under the detection limit and 0.63 to 0.27 μ mol/L at the 5m depth, respectively, and from 22.1 μ mol/L to under the detection limit and 0.56 to 0.03 μ mol/L at the bottom, respectively.

3.2 Vertical distribution

3.2.1 Phosphate (PO_4^{3-})

The concentration of PO_4^{3-} is very low at Stations 33 and 34, only 0.03 μ mol/L and 0.11~0.13 μ mol/L from surface to bottom, respectively (Figure 2). At Station 35 the concentration of PO_4^{3-} is under the detection limit from the surface to the 10 m depth and increases promptly with depth under the 10 m depth (from under the detection limit to 1.33 μ mol/L, increasing 0.058 μ mol/L per meter). At Station 36 the concentration of PO_4^{3-} is lower than 0.27 μ mol/L between the surface and the 5 m depth and increases with depth under the 5 m depth. Particularly between the 5 m to 15 m depth the concentration of PO_4^{3-} increases promptly (from 0.15 μ mol/L to 0.85 μ mol/L, increasing 0.070 μ mol/L per meter).

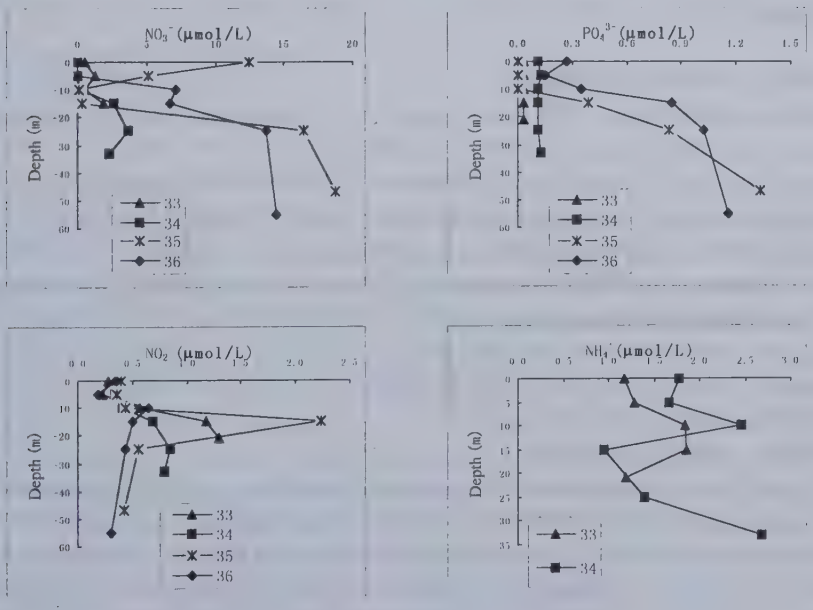

Fig. 2 Vertical variations of concentrations of NO_3^-, PO_4^{3-}, NO_2^- and NH_4^+

3.2.2 Nitrate (NO_3^-)

The concentration of NO_3^- is lower than 2.0 μ mol/L from surface to bottom at Station 33 (Figure 2). At Station 34 the concentration of NO_3^- is also very low, which is under the detection limit between the surface and the 5 m depth. And the concentration of NO_3^- is appreciably increased from the 5 m to 25 m depth, but all are lower than 4.0 μ mol/L. At Station 35 the concentration of NO_3^- reduces quickly from the surface to the 10 m depth (from 12.5 μ mol/L to 0.06 μ mol/L), but increases promptly between the 15 m to 25 m depth (from 0.3 μ mol/L to 16.4 μ mol/L, increasing 1.61 μ mol/L per meter) .At Station 36 the vertical variation of concentration of NO_3^- shows two stages, increasing promptly from under the detection limit to 7.16 μ mol/L (increasing 1.43 μ mol/L.per meter) from the 5 m to 10 m depth and from 6.65 μ mol/L to 13.70 μ mol/L (increasing 0.705 μ mol/L per meter) from the 15 m to 25 m depth.

3.2.3 Nitrite (NO_2^-)

The vertical variation of concentration of NO_2^- is s imilar at every station (Figure 2). The concentration of NO_2^- is lower from the surface to the 10 m depth and from the 25 m depth to the bottom. But from the 10 m to 25 m depth the concentration of NO_2^- is higher, with a maximum of 2.24 μ mol/L.

2.2.4 Ammonium (NH_4^+)

At every station the vertical variation of concentration of NH_4^+ shows an analogy to NO_2^- (Figure 2). The concentration of NO_2^- is lower from the surface to the 5m depth and higher from the 10 m to 15 m depth. And under the 15 m depth the concentration of NO_2^- changes in a much complicated way.

4 Discussion

4.1 Reason for horizontal discontinuity

Concentrations of NO_3^- and PO_4^{3-} reduce greatly maybe due to water mixing and phytoplankton's assimilation. At Station 33 and under the 5 m depth of Station 32 the salinity is in the range of 25.2~ 26.30. And if NO_3^- and PO_4^{3-} behave conservatively, here the concentrations of NO_3^- and PO_4^{3-} will be about 20 μ mol/L and 0.3 μ mol/L, respectively, according to the result of R.C.Tian *et al.*[8]. But the actual concentrations are below the values. So we understand that water mixing is not the main cause of horizontal discontinuity. At the 5m depth of Station 32 and the surface of Station 33 the chlorophyll *a* content is 13.8 and 12.9 mg/m^3, respectively. Thus much phytoplankton would uptake a great deal of NO_3^- and PO_4^{3-}, which causes the concentrations of NO_3^- and PO_4^{3-} to be very low or under the detection limit. In conclusion, phytoplankton's assimilation is the main reason for the horizontal discontinuity of concentrations of NO_3^- and PO_4^{3-}.

4.2 Reason for vertical discontinuity

It is well known that phosphorus and nitrogenous compounds are removed by phytoplankton at the upper layer of ocean[9]. Similarly, at the plume front of the Changjiang estuary (from Stations 33 to 36) chlorophyll *a* content is in the range of 1.6~13.8 mg/m^3 at the upper layer (from the surface to the 10 m depth) and NO_3^- and PO_4^{3-} are used up. Organisms such as plankton's body and excretion sink to the bottom, and decompose to release dissolved inorganic nitrogen and phosphate and consume dissolved oxygen in the course of oxidization. At the stations 35 and 36 the calculated concentrations of NO_3^- and PO_4^{3-} based on apparent oxygen utilization (AOU) are consistent with the observed ones (Table 2).

This indicates that high concentrations of NO_3^- and PO_4^{3-} at the bottom result from organism's oxidization.

At the middle layer (from the 5 m to 25 m depth) is the front of the plume, where the diluted water mixes with the invaded seawater, forming a great gradient of salinity and halocline. The halocline prevents vertical mixing with the result that concentrations of NO_3^- and PO_4^{3-} show discontinuity here. In addition, concentrations of NO_2^- and NH_4^+ appear peak values at the halocline, which has also been observed by Tang Renyou *et al.*[10]. According to the observation of Tang Renyou *et al.*[10] at the plume front the dissolved oxygen is unsaturated undersurface, which indicates that nutrients' regeneration is the main process undersurface. In summer, some organisms decompose while sinking to the bottom and release PO_4^{3-} and NH_4^+ because of high temperature. And part of the regenerated NH_4^+ is nitrified to NO_2^- at the middle layer. So higher concentrations of NO_2^- and NH_4^+ appear at the middle layer.

Tab. 2 Comparisons between calculated and observed concentrations of NO_3^- and PO_4^{3-}

Station	O_2^*	O_2	AOU	$'NO_3^-$	$'PO_4^{3-}$	NO_3^-	PO_4^{3-}	$NO_3^-/'NO_3^-$	$PO_4^{3-}/'PO_4^{3-}$
				μ mol/L					
33	218	118	100	11.6	0.72	≈1.85	0.03	0.16	0.04
34	223	83	140	16.2	1.01	2.30	0.13	0.15	0.13
35	223	67	156	18.1	1.13	18.7	1.33	1.03	1.18
36	218	63	155	18.0	1.12	14.5	1.16	0.81	1.04

$'NO_3^-$ and $'PO_4^{3-}$ represent the calculated concentrations.

NO_3^- and PO_4^{3-} represent the observed concentrations.

O_2^* is the saturated concentration of dissolved oxygen.

4.3 Vertical circumfluence

Why are so low the concentrations of PO_4^{3-} and NO_3^- at Stations 33 and 34? Is there not nutrients' regeneration? This is impossible. Because many phenomena, for instance, the Eh value is lower than -200mv on the sediment surface, dissolved oxygen is unsaturated at the bottom and at Station 34 and the concentration of NO_3^- at the bottom is higher than 2 μ mol/L, result from nutrients' regeneration. But the concentrations of PO_4^{3-} and NO_3^- are far below the calculated concentrations based on AOU. Considering the research findings of other scholars we think that the phenomenon results from vertical circumfluence. Stations 33 and 34 are just where the diluted water mixes with seawater. The diluted water flows to the opensea while mixing with seawater, transferred to down-current by seawater near the isohaline 28, slowly transforming into rightabout current, incorporating into invaded seawater and finally forming up-current, which mixes with the diluted water at the bottom of Stations 33 and 34 (Figure 3). As a result of vertical circumfluence, at Stations 33 and 34 the surface diluted water lacking of nutrients exchanges quickly with the bottom seawater rich in nutrients, transporting a great deal of PO_4^{3-} and NO_3^- from the bottom to the phytoplankton at the surface. So the concentrations of PO_4^{3-} and NO_3^- are very low at Stations 33 and 34.

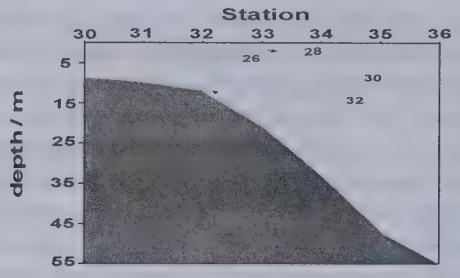

Fig. 3 Cross-section distribution of salinity

5 Conclusions

Plume front of the Changjiang estuary is the confluence of the diluted water, which diffuses outwards to the upper layer, and the seawater invaded from bottom[111], where forms the vertical circumfluence. The vertical circumfluence transports NO_3^- and PO_4^{3-}, which are released from the organism at the bottom to phytoplankton. Horizontal discontinuity of concentrations of NO_3^- and PO_4^{3-} is due to phytoplankton's assimilation. Concentrations of NO_3^- and PO_4^{3-} changing abruptly at the halocline at the plume front are the result of phytoplankton's assimilation at the upper layer and nutrients' regeneration at the bottom. The concentrations of NO_2^- and NH_4^+ are very high at the 10~25 m depth.

Acknowledgements

We wish to thank the National Natural Science Foundation of China which has offerd us the financial support for this research (No: 49736220). We also sincerely thank Professor Fu Fangxi who has provided us with the data and guidance.

References

[1] Baumann M. J. *et al* (1986) Oceanic Fronts in Coastal Processes [M]. (Translated by Liu J. P. and Liu R. Q.). China Ocean Press.

[2] Anderson G. C. (1964) The seasonal and geographic distribution of primary production off the Washington and Oregon Coasts [J]. *Limnol.Oceanogr.*, 9: 284~302.

[3] Milliman J. D. and Boyle E. (1975) Biological uptake of dissolved silica in the Amazon River estuary [J]. *Science*, 189: 95~997.

[4] Revelante N. and Gilmartin M. (1976) The effects of Po River discharge on phytoplankton dynamics in northern Adriatic Sea [J]. *Mar.Res.*, 1: 60~74.

[5] Hobson L. A. (1996) Some influence of the Columbia River effluent on marine phytoplankton during January 1971 [J]. *Limnol.Oceanogr.*, 11: 223~234.

[6] Shen X. Q. and Fu F. X. (1995) The Basic Characteristic of Chlorophyll α Distribution in the Water Area

Outside of the Changjiang River Mouth [C]. *Journal of East China Normal University* (Selections of the Studies of the Turbidity Maximum and Estuarine Front in Changjiang River), 139~158.

[7] Chen J. Y. (1995) The Natural Adaptation and Artificial Control of the Changjiang Estuary [C]. *Journal of East China Normal University* (Selections of the Studies of the Turbidity Maximum and Estuarine Front in Changjiang River), 1~14.

[8] Tian R. C., Hu F. X. and Martin J. M. (1993) Summer Nutrient Fronts in the Changjiang (Yantze River) Estuary [J] *Estuary, Coastal and Shelf Science*, 37: 27~41.

[9] Riley J. P. and Skirrow G. (1982) Chemical Oceanography 2th edition. China Ocean Press, 2: 462~465.

[10] Tang R. Y., Dong H. L. and Wang F. G. (1990) Biogeochemical Behaviour of Nitrogen and Phosphate in the Changjiang Estuary and Its Adjacent Waters [M], "Biogeochemical study of the Changjiang estuary" (edited by Yu G. H., Martin J. M. and Zhou J. Y.), China Ocean Press, 322~334.

[11] Hu F. X., Hu H. and Gu G. C. (1995) Salinity Front of Changjiang Estuary [C]. *Journal of East China Normal University* (Selections of the Studies of the Turbidity Maximum and Estuarine Front in Changjiang River), 84~91.

Distribution and Changes of Specification of Phosphorus in the Yellow Sea

Chen Hongtao (陈洪涛), Chen Shuzhu (陈淑珠), Zhang Jing (张 经), Liu Sumei (刘素美), Wu Qiangming (吴强明)

College of Chemistry & Chemical Engineering, Ocean University of Qingdao, Qingdao 266003

Abstract The studies on the distribution and variation of the specification of phosphorus in the southern part of the Yellow Sea are made. The biogeochemistry of phosphorus in the Yellow Sea is discussed. The phosphorus is slightly higher in the bottom than in the surface waters in the southern part of the Yellow Sea and the dissolved organic phosphorus is the main form. The transfer patterns between various forms of particulate and dissolved phosphorus are different in the bottom and surface, probably due to the contribution of dissolved organic phosphorus. The distributions of dissolved inorganic phosphorus and dissolved organic phosphorus are mainly affected by the biological processes and could act as a prediction factor for the red tide. The supply of N and P in most of the areas in the southern part of the Yellow Sea is sufficient, without apparent limitation of N or P.

Keywords Yellow Sea, phosphorus, specification

1 Introduction

P is an essential composition for the growth and reproduction of marine plankton, and also the fundamental element of marine primary production and food chain. In recent years, more and more scientists have attached importance to the studies of the distribution and variation of the specification of phosphorus in the sea and its cycling in seawater because people pay more attention to the eutrophication of offshore area and P is one of the important controlling factors of it[1-4].

2 Materials and methods

Field observations were undertaken in the southern part of the Yellow Sea using R/V "Xiangyanghong No.9" in May 1998, and occupied 6 sections and 37 serial stations (Fig. 1).

Water samples are collected with a Niskin bottle. Part of the samples is filtered immediately with acetate cellulose 0.45 μ m pore-size filters, and then quickly frozen at -20℃ These samples are used for the determination of dissolved inorganic phosphorus (DIP) and total dissolved phosphorus (TDP); samples without filtration are used for the determination of total phosphorus (TP).

The DIP of filtered sample is determined by the method of phosphomolydate, and the TDP and TP are determined by alkaline potassuim persulphate oxidation[5].

Received on May 29, 2002

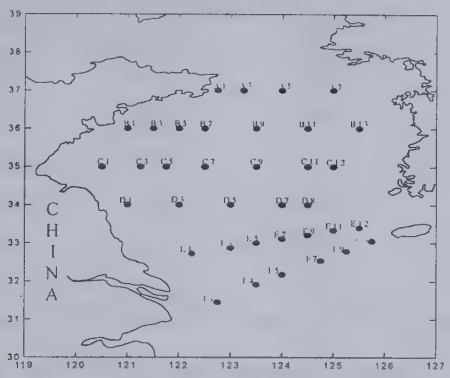

Fig. 1 Sampling stations

3 Results and discussion

3.1 Concentrations of various specifications of phosphorus

The concentration range and average values of TP, TDP, PP, DIP and DOP of the surface and bottom water of the South Yellow Sea in May 1998 are showed in Table 1. It shows that various specifications of phosphorus in the bottom water are all higher than that in the surface water. The biggest difference between bottom and surface is DIP. The average DIP concentration of bottom water is 1.7 times that of surface water. The concentrations of DIP and PP of surface water are close, and the DOP concentration is high. In the bottom water, the DIP concentration is close to DOP, and they are both higher than PP concentration.

Tab.1 Concentration of some forms of phosphorus in the Yellow Sea (μ mol/L)

	TP	TDP	PP	DIP	DOP
Surface	0.83~1.64	0.66~1.21	0.06~0.85	0.05~1.16	0.02~0.97
Average	1.25	0.89	0.37	0.38	0.50
Bottom	1.07~2.51	0.90~1.69	0~1.56	0.06~1.57	0.05~1.01
Average	1.64	1.23	0.41	0.60	0.62
Entire area	0.82~2.51	0.66~1.69	0~1.56	0.05~1.57	0~1.19
Average	1.37	1.07	0.32	0.47	0.60

Yuan reported the DIP data of the South Yellow Sea in 1989 and 1993~1995[6]. Their average values were 0.45, 0.45, 0.71 and 0.32 μ mol/L respectively. Comparison of the above data with this observation (0.47 μ mol/L) shows that the DIP concentration in the South Yellow Sea water is rather stable.

Table 2 shows comparison of the various specifications of phosphorus in the South Yellow Sea

Tab 2. Ratios of phosphorus species (%)

	DIP/TP	DOP/TP	PP/TP	DIP/TDP	DOP/TDP
Surface	3.1~92.8	2.4~84.5	4.8~51.8	4.9~97.5	2.8~95.1
Average	31.3	40.8	27.9	41.9	58.1
Bottom	3.8~88.6	2.2~86	0~62.2	5.6~97.5	0.8~94.4
Average	37.5	39.9	22.6	47.9	52.1
Entire area	3.1~92.8	2.2~90.4	0~62.2	2.8~99.1	0.8~95.1
Average	31.5	47.4	21.9	40.1	59.9

water. With the comparison of organic and inorganic forms, DOP is higher than DIP and the difference is bigger in the surface layer than in the bottom layer. This is because the source of DOP is commonly the product of decomposition and draining of marine organisms. The productivity of Yellow Sea is high in May. Planktons consume a large quantity of DIP while they release organic phosphorus. So, the concentration of DOP is high in this stage. George has reported that in many offshore areas, the DOP concentration of surface water in summer is usually higher than the DIP concentration[7].

From the comparison of dissolved and particulate forms, it is found that TDP is by far higher than PP, and DOP is higher than DIP and DIP is higher than PP. It indicates that phosphorus in the South Yellow Sea water is mainly composed of dissolved form, and the principal form is DOP which accounts for 47.4% of TP, and that the ratio of PP is low.

In the studied areas, DIP is in highly negative correlation with DOP in the surface and bottom layers. DIP has a notable correlation with PP in the bottom layer, while the correlation is not apparent in the surface layer. PP has no correlation with DOP in the surface and bottom layers.

3.2 Horizontal distributions of various specifications of phosphorus

Riley pointed out that TDP and DIP were influenced by the integrated functions of water movement and organism activity, and DOP was mainly controlled by organism activity, because DOP is the product of organism (including secretion of phytoplankton and drainage of zooplankton). Phytoplankton and zooplankton maybe have the same importance in the DOP production[8].

Figs. 2~6 show the horizontal distributions of DIP, DOP, TDP, PP and TP in the South Yellow Sea.

Fig. 2 is the distribution of DIP. Along the coastline, the DIP concentration of surface water increases gradually from north to south. The DIP concentration is low to the north of 34° N, and lower than 0.45 μ mol/L. At the 33° ~ 32° N, its concentration is the highest and ranges from 0.65 to 1.05 μ mol/L, and decreases gradually to south. As can be seen obviously, the DIP concentration increases rapidly from west to east out of the Changjiang River estuary. This should be considered as the influence of the Changjiang River diluted fresh water which is thought of as water with high concentrations of TP and OP and a low concentration of IP[9]. There are high concentration water masses off the southwest of Jizhou Island expanding to northwest, in an direction similar to the Yellow Sea warm current.

Fig. 3 is the distribution of DOP. The DOP concentration in the northeast is low and increases gradually along with the decrease of latitude, and decreases gradually from the middle part of

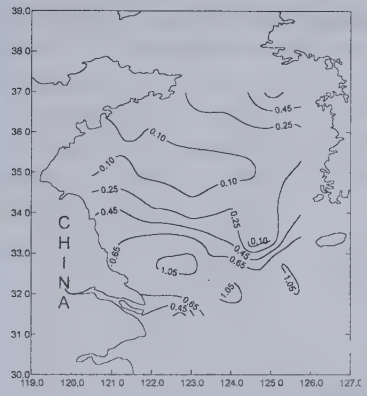

Fig. 2 Horizontal distribution of DIP in the surface water

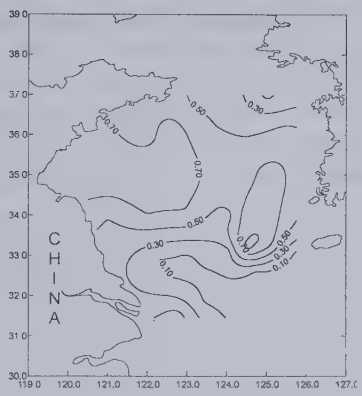

Fig. 3 Horizontal distribution of DOP in the surface water

Yellow Sea to the south. Comparison of the distributions of DIP with DOP shows that the high DIP concentration areas are usually accompanied by low DOP, and vice versa.

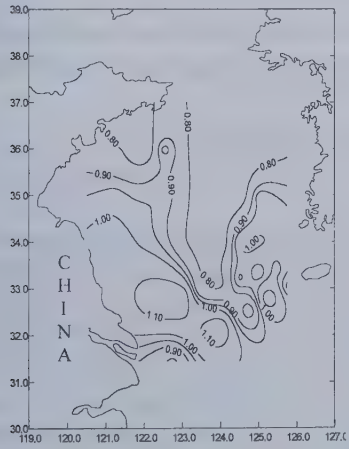

Fig. 4 Horizontal distribution of TDP in the surface water

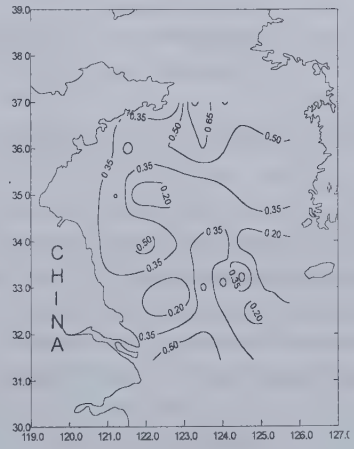

Fig. 5 Horizontal distribution of PP in the surface water

Fig. 4 is the distribution of TDP. The distribution of TDP illustrates that the TDP concentration in the surface water increases gradually from north to south. There is a water tongue in the area of 35° ~ 33° N, 122.5° ~ 124.5° E which is surrounded by high concentration water of two banks.

Fig. 5 is the distribution of PP. The PP concentration in the surface water of the South Yellow Sea

is stable. In most sea areas, the value is about 0.35 μ mol/L. However, there is a high-value area in the vicinity of the Changjiang River estuary and the Chengshan Cape. The value could be as high as 0.5 μ mol/L.

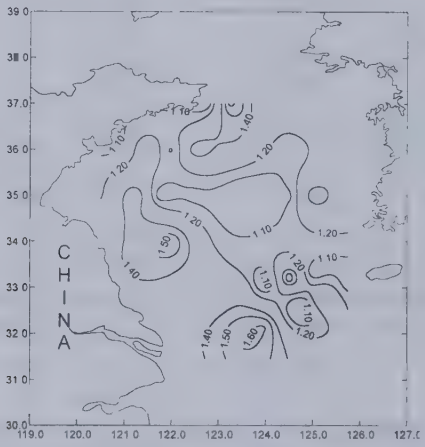

Fig. 6 Horizontal distribution of TP in the surface water

Fig. 6 is the distribution of TP. The TP concentration in the surface water of the South Yellow Sea is also stable. There are two high-value areas in the Changjiang River estuary and coastal Jiangsu province.

3.3 Factors affecting the distribution of various specifications of phosphorus

There are many factors affecting the distribution of various specifications of phosphorus in the South Yellow Sea water. In this paper, we focus on the N: P ratio, *etc.*.

The changes of DIP are relevant to the organism activity and hydrodynamics. Phytoplankton and autotrophic bacteria absorb DIP and reproduce, then IP enters the organism, and the transfer of phosphorus forms begins. The cell of phytoplankton is consumed by herbivores, and the drainage of zooplankton becomes the main source of OP. OP is decomposed to IP by bacteria activity. This kind of mutual transfer process could be supported by the highly negative correlation between DIP and DOP (r =-0.898 in the surface layer, r =-0.901 in the bottom layer). In the course of deposition, particulate OP is deposited to seafloor and part of phosphates is absorbed by suspended material and deposits. In the mixing process, that the waters being stirred causes resuspending of sediment and releasing of phosphorus. Old or damaged cells could release dissolved phosphorus because of autolysis.

Suitable N: P ratio in seawater is favourable for plankton's living and reproducing. On the contrary, lack of certain nutrient elements can limit the growth and reproduction of organisms. The ratio of total dissolved inorganic nitrate (DIN = NO_3^- + NO_2^- + NH_4^+) to DIP during this observation is showed in Fig. 7. In the studied area, the average value of N: P in water is 14.4, slightly lower than the Redfield ratio. It is 8.85 in the surface layer, and 14.8 in the bottom layer. Huminghui *et al.* pointed out that algae's growth is limited by N when N: P is lower than 8; the supply of N and P is both sufficient when

N: P is 8~30. They would be consumed together. Algae's growth is limited by O when N: P is higher than 30[10].From the horizontal distribution of N: P ratio in the surface water of the South Yellow Sea, we can see that it is N limitation on the offshore Korean side and in the northeast sea area of Qingdao. The ratios for other areas are 12 to 24. It illustrates that in most areas of South Yellow Sea it is not limited by N and P.The ratios of N: P in 1989, 1993~1995 and during this observation in the same area are 16.9, 5.1, 4.2, 9.1 and 14.4 respectively. The value of 1989 was close to this observation, but it decreased to a great extent in 1993 and to 4.2 in 1994. The value rose again from 1995, up to the value of 14.4 during this observation.

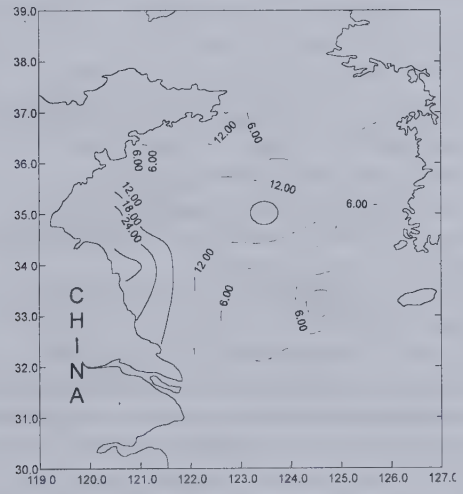

Fig. 7 Horizontal distribution of N:P in the surface water

According to the classification of nutrient levels of water in the "Eutrophication of Hydrosphere and Mariculture"[11] and "Indices of Water Environment"[12] and the evaluating methods of single and multiple indices of "Introduction to Water Environment Pollution"[13], the nutrient status of the South Yellow Sea water can be evaluated roughly as follows.

In the South Yellow Sea water, the average concentration of DIP is 0.47 μmol/L, TP is 1.37 μmol/L and chlorophyll a is 1.43 μg /L. These three indices are all within the range of the medium nutrient sea area. It illustrates that the water quality of South Yellow Sea is still good without an apparent tendency of eutrophication.

4 Conclusions

(1) The phosphorus is slightly higher in the bottom than in the surface waters in the southern part of the Yellow Sea and the dissolved organic phosphorus is the main form.

(2) The transfer forms between various forms of particulate and dissolved phosphorus are different

in the bottom and surface, probably due to the contribution of dissolved organic phosphorus.

(3) The distributions of dissolved inorganic phosphorus and dissolved organic phosphorus are mainly affected by the biological processes and could act as a prediction factor for the red tide.

(4) The supply of N and P in most of the areas in the southern part of the Yellow Sea is sufficient, without apparent limitation of N or P.

Acknowledgments

This study is supported by a fund of China (No. 49736190 and No.G1999043705)

References

[1] Chen S. Z., Zhang J. Z. and Zhang J. (1997) Existing forms of phosphorus and it's content in sediment from river estuaries and the Laizhou Bay. *Costal Engineering*, **16**(2): 41~46.

[2] Hong H. S. (1989) Distributions and transforms of various specifications of phosphorus in Xiamen Harbor-Jiulongjiang Estuary in spring. *Marine Environmental Science*, **8** (2): 1~8.

[3] Shen Z. L., Lu J. P. and Liu X. J. (1987) Inorganic nitrogen and phosphate in the Huanghe River Estuary and its adjacent sea areas. *Studia Marina Sinica*, 30: 51~79.

[4] Zou J. Z., Dong L. P. and Qin B. P. (1983) Preliminary study on eutrophication and red tide of Bohai Gulf. *Marine Environmental Science*, **2**(2): 41~53.

[5] Grasshoff K. (1983) Methods of Seawater Analysis ermany: WILEY-VCH Verlag Gmbh.

[6] Yuan Y. X. *et al* (1996) Study on Huanghai and Bohai Seas environmental quality and ecological changes. Qingdao: Yellow Sea Fisheries Research Institute, Chinese Academy of Fishery Sciences.

[7] George A. J. and Williams P. M. (1985) Importance of DON and DOP to biological nutrient cycling. *Deep-Sea Res.*, 32: 223~235.

[8] Riley J. P. and skilo G. (1982) *Chemical Oceanography*, In:Cui Q C *et al.* eds. Beijing: China Ocean Press.

[9] Huang Z. Q. and Ji W. D. (1994) Changing characteristics and correlations of total phosphorus, organic phosphorus and phosphate in Changjiang River Estuary water. *Acta Oceanologica Sinica*, **16**(1): 51~60.

[10] Hu M. H. and Yang Y. P. (1989) Phosphate limitation of phytoplankton growth in Changjiang River Estuary. *Acta Oceanologica Sinica*, **11**(4): 439~443.

[11] Japanese Society of Scientific Fisheries (1986) Eutrophication of hydrosphere and mariculture (translation of Korea version). Beijing: Agriculture Press.

[12] Gohda K. (1989) Indices of water environment. Beijing: China Environmental Science Press.

[13] Wang H. D. (1984) Introduction of water environment pollution. Beijing: Beijing Normal University Press.

Surficial Sedimentary Diatoms in Okinawa Trough and Its Response to Kuroshio Current

Lan Dongzhao (蓝东兆), Fang Qi (方 琦), Liao Lianzhao (廖连招)
Third Institute of Oceanography, SOA, Xiamen 361005

Abstract This paper describes the relative contents of dominant diatom species and the distributive characteristics of tropical pelagic species and diatom assemblages, and also discusses the relations between the relative content of tropical pelagic species and Kuroshio Current and between the distribution of diatom assemblages and material sources. The results show that the limit of >20% relative content of tropical pelagic species is basically consistent with the demarcation of Kuroshio Current, and that the distributions of dominant diatom species and diatom assemblages reserve the records of their closer relations to material sources.

Keywords sedimentary diatom, Okinawa Trough, Kuroshio Current

The studied area refers to the sea area the major trunk of Kuroshio Current passes through.Since the 1980s, Jin Dexiang *et al.* (1980)[1], Liu Shicheng *et al.* (1983)[2], Wang Caifa *et al.* (1987)[3], Jin Xianglong (1992)[4] and Lü Houyuan *et al.*① (1999) have done some work of analysis and research on the diatom assemblages and species distribution in the surficial and columnar sediments of this area, but the studied stations are fewer in number and no reports have been seen on the response of surficial sedimentary diatoms to Kuroshio Current and the demarcation of the Kuroshio Current extent in the light of the contents of tropical pelagic species. Following the paper entitled "Late Quaternary sedimentary diatom in Okinawa Trough and its paleoceanographic significance", this paper attempts to discuss the extent of influence of Kuroshio Current and alongshore in the area according to the distribution of diatom species and amount in the surficial sediments of Okinawa Trough, so as to provide scientific basis for studying the changes of ancient Kuroshio Current and alongshore current in the area since the late Quaternary period.

1 Material and method

The analytical material is taken from the surficial sediments of 30 stations collected during the survey of the special project 126 by R/V "Dongfanghong 2" of the First Institute of Oceanography, SOA in Sept. Oct.,1998 (Fig.1). For each sample, take 10g of air-dried sample and put it into a high utensil of 50 cm^3. Add distilled water into the utensil and carry out ultrasonic dispersion (150Hz, 2min). Remove the floating fluid through centrifugation by sodium polytungstate with a specific gravity of 1.2 and lastly use the Canada balsam to make whole fixed slices. For each sample, over 300 grains of diatom valve are

Received on February 5, 2002

① Lü Houyuan , Liu Zhenxia,Wu Naiqin, *et al.* Diatom and paleoceanography in domain of Kuroshio Current in Okinawa Trough during the past 20 000a, SOA China, Beijing, 1999, 51~61.

identified and counted, and, in the case of less than 300 grains, three standard slices of 18 mm × 18 mm are counted.

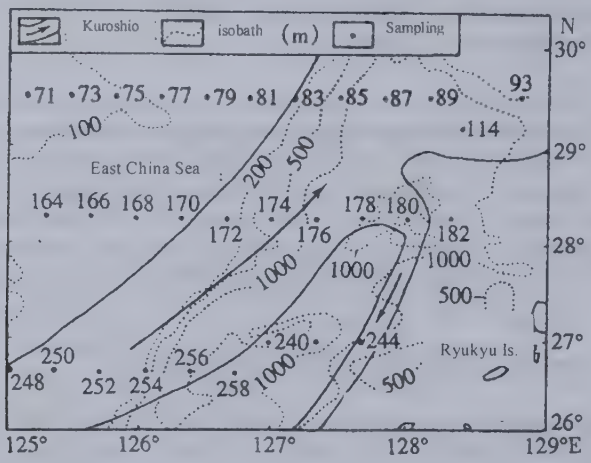

Fig. 1 Sampling stations

2 Results and discussion

2.1 Distribution of major diatom species

From the 30 surficial sediment samples, a total of 74 species and variants falling into 33 genera are identified. Among which 3 species are living in freshwater, 3 species in brackish water and 68 species and variants in seawater. There are 10 dominant species (Fig.2), which are:

Actinocyclus ehrenbergii (Fig.2a): The relative content (hereinafter referred to as content for short) of this species is >10 % and distributed near the demarcations of Kuroshio Current on the east and west sides. The content in individual stations may reach a maximum of over 30 %, while, in the sea area Kuroshio Current passes through, the content is < 10 %.

Actinoptychus undulates (Fig.2b): The content of this species is alternately distributed in a northeast -southwest trending strip. The stations with content >10 % are all located in the sea area to the west of Kuroshio Current. The content in the station No.71 may reach a maximum of 50 %, while it is <5 % in the sea area to the east of Kuroshio Current and even has not been discovered in individual stations.

Actinoptychus splendens (Fig.2c): The >10 % content of this species is only found in a few stations on both sides of the demarcation of Kuroshio Current with a maximum of 14.02 %, while in most stations it is not detected.

Coscinodiscus decrescens (Fig.2d): The content of this species is alternately distributed in a northeast-southwest trending strip, but the >10 % content is only found in the stations Nos.73,81,170 and 254 with a maximum of 25.57 %. It is not detected in a few stations.

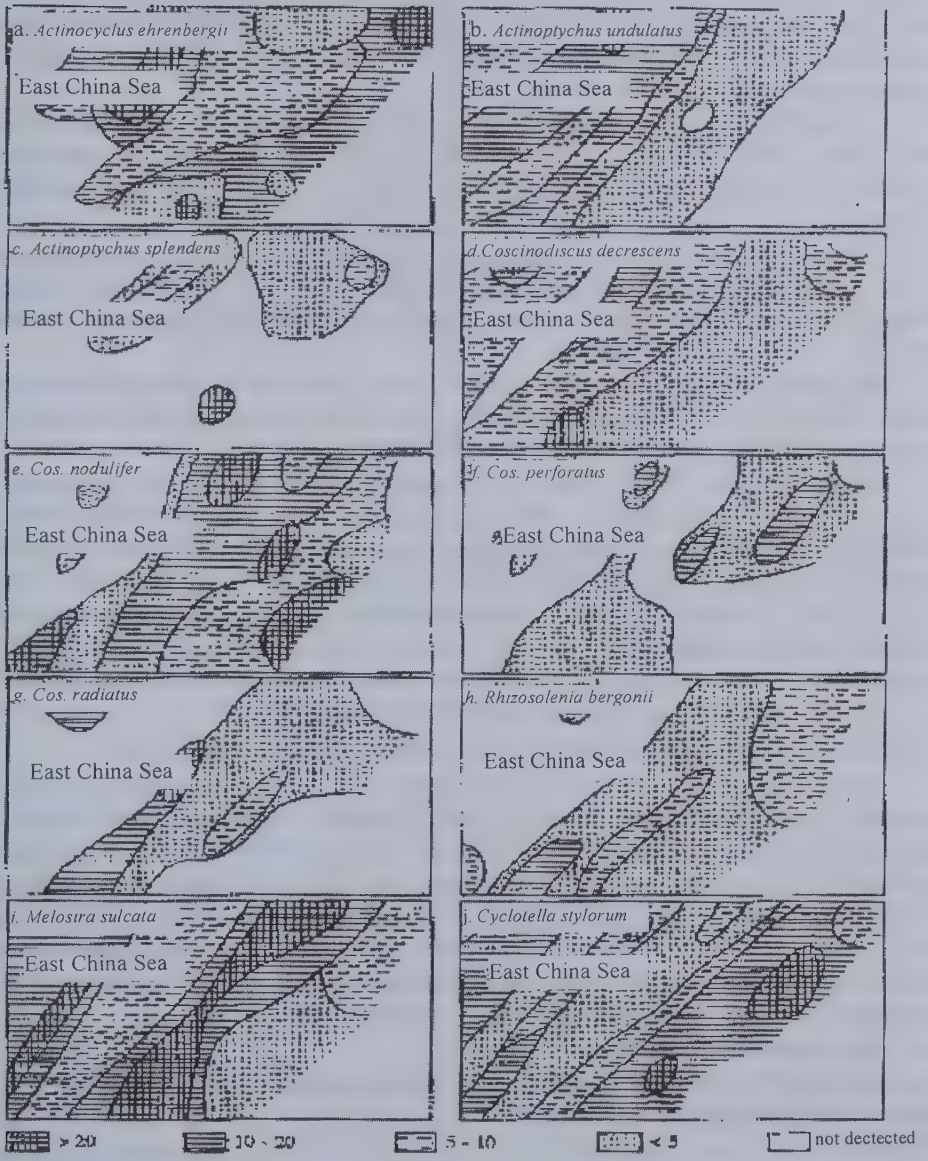

Fig. 2 Distributions of relative content of diminant diatom species in surface sediment from Okinawa Trough

Cos. nodulifer (Fig.2e): The stations with >10 % and >20 % content of this species are all distributed within the limits of Kuroshio Current with the maximum content reaching 40 %; The content of <10 % is found on both sides of the demarcation of Kuroshio Current and it is not detected especially in the most majority of stations on the East China Sea continental shelf of the sea area to the west of Kuroshio Current.

Cos. perforatus (Fig.2f): This species is mainly distributed within the limits of Kuroshio Current. The >10 % content is only found in the stations Nos.81,114,176 and 180, with the maximum reaching 15.25 %; It is not detected on both sides of Kuroshio Current, especially the continental shelf of the East China Sea.

Cos.radiatus (Fig.2g): This species is mainly distributed within the limits of Kuroshio Current.The >10 % content is only found in the stations Nos.172, 252 and 254, with the maximum in station 172, reaching 21.74 %. It is not detected in many stations on both sides of the demarcation of Kuroshio Current.

Rhizosolenia bergonii (Fig.2h): This species is mainly distributed in the sea area Kuroshio Current passes through. The >10 % content is only found in the station No.252. It is not detected in many stations on both sides of the demarcation of Kuroshio Current.

Melosira sulcata (Fig.2i): The benthic attaching species often occur in colonies. The content of the species alternately occurs in northeast-southwest trending strips. The >20 % content is mainly distributed in the sea areas Kuroshio Current passes through and on the continental shelf of the East China Sea with the maximum reaching 78.6 %. The content on the east side of Kuroshio Current is found to be <10 %.

Cyclotella stylorum (Fig.2j): It is a nearshore low-salinity species with the content occurring in northeast-southwest trending strips. The >20 % content is mainly distributed on both sides of the demarcation of Kuroshio Current, with the maximum reaching 31.3 %. It is not detected in the stations Nos. 77, 79, 166 and 248 on the continental shelf of the East China Sea.

2.2 Distribution of tropical pelagic species and their response to Kuroshio Current

Results of the quantitative statistics of the content of 7 tropical pelagic species, namely, *Cos. nodulifer, Rhizosolenia bergonii, Nitzschia marina, Hemidiscus cuneiformis, Roperia tesslata, Cos. africanus,* and *Pesudoeunotia doliolus,* show that the >20 % content of the tropical pelagic species is all distributed in the sea area Kuroshio Current passes through with a maximum of 48 % and an average width of about 111km. The trend of its width and distribution is close to that of Kuroshio Current (Fig.3); while the content of tropical pelagic species on both sides of the demarcation of Kuroshio Current is <20 %. Therefore, the >20 % content of tropical pelagic species may be regarded as the sign showing that the major trunk of Kuroshio Current is passing through.

2.3 Diatom assemblages and their material source

In light of the distribution of dominant diatom species and tropical pelagic species, the studied area may be divided into three diatom zones (Fig.4).

2.3.1 Zone I

It is found on the continental shelf of the East China Sea to the west of the demarcation of Kuroshio Current. The abundance of diatoms is low and each gram of dried sample contains less than 30 grains. This zone is represented by the assemblage of *Melosira sulcata, Actinocyclus ehrenbergii* and *Actinoptychus undulates,* with the contents of 0 % ~ 78.6 %, 0 % ~ 38.46 % and 0 % ~ 33.33 % respectively. In addition, the species of *Cyclotella stylorum, Coscinodiscus decrescens and Actinoptychus splendens*

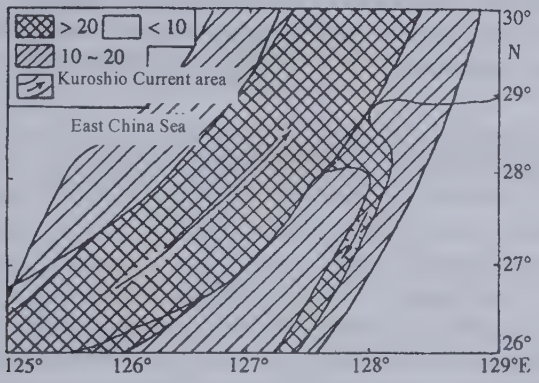

Fig. 3 Distribution of tropical pelagic species content (%)

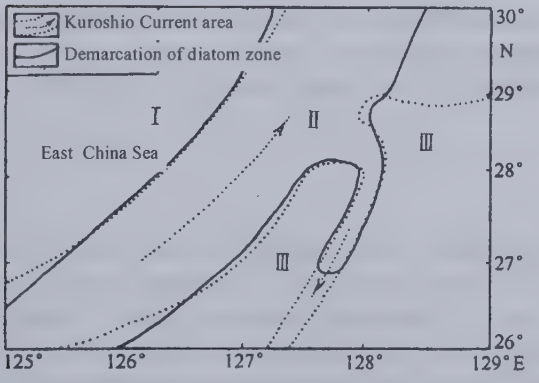

Fig. 4 Distribution of diatom assemblages

are also commonly seen, while the contents of the tropical pelagic species such as *Cos. nodulifer, Nitzschia marina*and *Hemidiscus cuneiformis*are lower. Judging from the characteristics of diatom abundance and diatom assemblage in this zone as well as the fact that the contents of the nearshore benthic attaching species *Melosira sulcata*and the nearshore low-salinity species *Cyclotella stylorum* are alternately distributed in northeast-southwest strips, it is indicated that both accumulation and denudation exist side by side in this zone. The inner shelf matter of the East China Sea comes to this zone together with the alongshore current, with one part accumulating and the other part directly

entering the Okinawa Trough. The sediment accumulated, on the other hand, is subjected to the actions of the bottom current as well as the associated ultra-density current, turbidity current and continental inclined current, thus making the fine matter be transported from the continental shelf to Okinawa Trough and the coarser relict sediment of the late Pleistocene period be left in this zone.

2.3.2 Zone II

Found in the sea area Kuroshio Current passes through, this zone has a diatom abundance of 100~200 grains/g and is represented by the assemblage of *Melosira sulcata - Coscinidiscus nodulifer — Cyclotella stylorum* with contents of 4.4 %~46.9 %, 5.13%~40.6 % and 0 %~19.5 % respectively. Furthermore, *Actinocyclus ehrenbergii, Coscinodiscus decrescens* and *Actinoptychus splendens* as well as the tropical pelagic species *Nitzschia marina, Hemidiscus cuneiformis, Rhizosolenia bergonii, Coscinodiscus africanus* and *Pseudoeunotia doliolus* are also comparatively abundant. These diatom characteristics indicate that in this zone there are not only accumulation of fine-grained matter from the continental shelf of the East China Sea, but also accumulation of the matter brought here by Kuroshio Current. Besides, this zone has the characteristics of bathyal-abyssal deposit.

2.3.3 Zone III

It is found in the sea area to the east of the demarcation of Kuroshio Current. It has a diatom abundance of 50~150 grains/g and is represented by the assemblage of *Cyclotella styloru — Actinocyclus ehrenbergii — Coscinodiscus nodulifer,* with contents of 7.7 %~31.1 %, 9.87 %~23.08 % and 3.13 %~7.85 % respectively. Moreover, the species *Melosira sulcata, Actinoptychus undulatus, Coscinodiscus decrescens, Cos.perforatus* and *Rhizosolenia bergonii* are also commonly seen. These characteristics indicate that in this zone there are not only sediments brought by Kuroshio Current, but also those coming from the nearshore area of the Ryukyu Islands to the east of the demarcation of Kuroshio Current.

3 Conclusions

(1) In the surficial sediment of the studied area, there are ten dominant species, namely, *Actinocyclus ehrenbergii, Actinoptychus undulates, Actinoptychus splendens, Coscinodiscus decrescens, Cos. nodulifer, Cos. radiatus, Cos.perforatus, Rhizosolenia bergonii, Melosira sulcata,* and *Cyclotella stylorum*, which may be divided into 3 diatom zones. The sediments of Zone I are the material from the inner continental shelf of the East China Sea and also the relict sediment of the late Pleistocene epoch; The sediments of Zone II are the fine material for the East China Sea continental shelf and the matter from Kuroshio Current; The sediment of Zone III is the mixed sediment brought by Kuroshio Current and coming from the nearshore area of the Ryukyu Islands to the east of the demarcation of Kuroshio Current.

(2) That the content of tropical pelagic species in the East China Sea is >20 % may be regarded as the sign showing that the major trunk of Kuroshio Current is passing here.

References

[1] Jin Dexiang, Cheng Zhaodi, Lin Junmin *et al* (1980)Surficial Sedimentary Diatoms in the East China Sea. *Act a Oceanologica Sinica*, **2**(1): 97~108.

[2] Liu Shicheng, Jin Dexiang and Lan Dongzhao (1983) Surficial Sedimentary Diatoms in the Southern Yellow Sea and the East China Sea. [J]. *Acta Oceanologica Sinica*, **5**(supplement):927~946.

[3] Wany Kaifa, Sun Yuhua, Zhang Yulan *et al.* (1987) Sedimentary Sporopollen-Algae Assemblage in the East China Sea. [M]. Beijing: China Ocean Press, 1~110.

[4] Jin Xianglong (1992) Marine geology of the East China Sea. [M]. Beijing: China Ocean Press, 1~524.

[5] Lan Dongzhao, Xu Jiang and Chen Chenghui (2000) Late Queternary sedimentary diatom in Okinawa Trough and its paleoceanographic significance. [J]. *Journal of Oceanography in Talwan Strait*, **19**(4): 419~425.

The Functions of China Marginal Sea Sediments in the Cycle of Biogenic Elements

Sun Yunming (孙云明)[1,2], Song Jinming (宋金明)[1]

1 *Institute of Oceanology, Chinese Academy of Sciences, Qingdao* 266071

2 *Qingdao University, Qingdao* 266071

Abstract The contents of biogenic elements in China marginal sea sediments are related to their grain sizes, river transport, et al. In general, the finer the grain size is, the higher the contents of organic matter and OC, N, P are, the lower the contents of S and Si are. The biogeochemical environments of sediments are related to Eh, pH, temperature content of OC, Fe^{3+}/Fe^{2+} radio, water dynamics condition, grain size of sediment, S system in sediment interstitial waters, *et al.*, and they influence the early diageneses and cycle of biogenic elements in sediments. In most regions of China marginal sea, the flux directions of S^{2-}, HS^-, H_4SiO_4, PO_4^{3-}, NH^{4+} across the sediment-water interface are from sediment to the overlying seawater, the flux directions of SO_4^{2-}, HCO_3^-, NO_3^-, NO_2^- across the sediment-water interface are from the overlying seawater to sediment. The irrigation of living things is important in the cycle of the biogenic elements across sediment-water interfaces.

Keywords China marginal sea, sediment, cycle of biogenic element

One important subject of modern chemical oceanography is to study the marine biogeochemical processes relating to global changes, and its key is to study the recycling of biogenic elements in marine ecological systems. The marginal sea sediments play an important role in the recycling of biogenic elements. Studies on transferring, releasing and recycling of biogenic elements in China sea sediments have made a great progress in recent ten years or more, which involves contents and changes of biogenic element C, N, P, Si, S in sediments and in sinking particulates, the recycling of biogenic elements in sinking particulates, the chemical mass transferring and recycling across the sediment-seawater interface, the relations between recycling of biogenic elements and its biological production, etc. The following discussion focuses on the main research findings in the ransferring, releasing and recycling of biogenic elements in China marginal sea sediments.

1 Biogenic elements in China marginal sea sediments

Biogenic elements in marine environments are mainly concentrated on sediments, and their contents are related to grain sizes, river inputs, *etc.* Distributions of the biogenic elements are regulated by the origin of matter, water dynamics and sedimentary grain size, *etc.* In general, the finer the grain sizes are, the higher the contents of OC, N, P and organic matter are, and the lower the contents of S and Si are, too.[1]

Received on May 10, 2002

In China marginal seas, the highest OC contents are found in muddy sediments around the inner continental shelf of southern Yellow Sea and of the East China Sea. The lower OC contents are in the middle regions of Bohai Sea, in southwestern Cheju Island and in Zhujiang estuary, and the lowest are in some sandy sediments, such as in Liaodong beach, outer-bank of Changjiang estuary, Taiwan bank and middle Beibu Gulf. The Eastern Okinawa Trough has a lower content of OC, the others have higher contents of OC. The distributions of N and P are the same as OC and Si, content in shallow sea sediment is higher than that in abyssal sediments. Lower Si contents are found in the inner continental shelf of the East China Sea, the middle southern Yellow Sea, Yellow River estuary, southwestern Cheju Island and eastern Beibu Gulf, *etc.* Lower Si contents are found in the regions such as Taiwan bank, middle Beibu Gulf, Liaodong bank, eastern South Yellow Sea, middle Jiaozhou Bay, outer continental shelf of the South China Sea, and outer big bank of Changjiang estuary, *etc.* The contents of SiO_2% are: continental shelf (68.2)- continental slope (34.93)- abyssal plain (51.30), P_2O_5% are: continental shelf (0.10)- continental slope (0.17)- abyssal plain (0.17). S is enriched in the South China Sea and the Yellow Sea. High S contents are found in the continental shelf of Zhujiang estuary, northeastern Beibu Gulf and middle Southern Yellow Sea, and low S content is found in other sandy regions.

The average abundances of OC, ON, OP in the East China Sea continental surface sediments (not including the Taiwan Straits) are 0.516%, 0.054%, 0.048%, respectively. OC and TN are lower in the northern East China Sea continental shelf surface sediments, higher in the southern and near continental shelf. Medium content of OC, ON and very low content of P are found in the northeastern. High content of P exists in Zhejiang coastal regions[2].

Lower OC, ON, OP contents and higher Si content in the southern Taiwan Straits than that in its nearby regions are determined. Higher Si content is caused by the higher silica content in sedimentary particulates and the less river input. Positive relations between OC, ON and OP contents are found, and negative relations among OC, ON, OP contents and Si content are distinctly found, which shows the dilution of silica. A common characteristic of profile distributions is that the contents of OC, ON, OP and Si decrease with depth, and swiftly decrease in the 20 cm surface layer. This suggests that the decomposition of organic matter mainly occurrs in the surface and subsurface layers[3].

The contents of some biogenic elememts in China marginal sea sediments are listed in Table 1.

Tab. 1 Contents of biogenic elememts in China marginal sea sediments

Regions	C		S/ ($\times 10^{-6}$)			N/($\times 10^{-6}$)	P/($\times 10^{-6}$)	Si/(%)		
	OC/ (%)	IC/(%)	sand	silt	clay			sand	silt	clay
Bohai Sea	0.66	0.66	250	340	520	556	527	33.42	30.13	26.15
Yellow Sea	0.71	0.69	350	420	820	624	522	32.44	30.00	26.48
East China Sea	0.61	1.21	350	530	730	615	516	30.66	29.07	26.17
South China Sea	0.59	1.32	450	580	1 000	620	425	31.04	29.00	26.36
Okinawa Trough	0.97	1.66		730		1 130	630		19.21	

The total characteristic is that the change regularities of OC, TN, TP in China marginal sea sediments are similar. The contents of OC, TN, TP are higher in regions such as Okinawa Trough, Minjiang estuary, lower in the southern Taiwan Straits, and no change in other regions. Sometimes the change of P is not related to C and N, such as in the western Pacific Ocean and near-shore regions of the East China Sea, which results from their different terrigenous inputs in estuary regions. S and Si accord with the role of grain size regulation.

2 Chemical environments of China marginal sea sediments and early diagenesis of biogenic elements

The chemical environments of sediments mainly involve the physical and chemical factors which affect the biogeochemical processes of biogenic elements, such as contents and activities of organic matter, contents of metallic ions correlating with sedimentation and dissolution, redox degree (ROD), pH, temperature, pressure, *etc.*. Organic carbon participates in the consumption of oxygen, reduction of Fe, Mn and S ions in the processes that organic matter is decomposed in the sedimentary environments. The content of organic matter directly reflects the degrees of reaction, pH, Eh, *Es* and concentrations of SO_4^{2-} in the interstitial water are the characteristic functions of sediments, and are also the important factors for appraising redox environments. The influencing degree of organic matter on its regions can be deduced from different characteristic factors.

The driving reaction of early diagenesis is the oxidation of organic matter, and it influences the recycling of CO_2 which is correlative to the global climate and the biogeochemical recycling of biogenic elements by a series of biogeochemical processes, such as denitrification and dissolution of minerials. Unstable organic matter is changed and decomposed into NH_3, CO_2 and H_3PO_4 through deammoniation, decarboxylation, depolymerization, isomerization and redox. In the pH, Eh and interstitial waters, the decomposed products mainly include NH_4^+, HCO_3^- and $\sum PO_4^{3-}$, *etc.*. Accordingly, whether or not the decomposition of organic matter occurs and what its scale is can both be estimated from the changes of the ions in the seabed sediment interstitial water.

Only a few elements such as C, N, O, S, Fe, Mn, *etc.* can participate in redox reactions in marine environment, and the reactions and their degrees directly control and regulate the properties of redox reactions in sediments. The oxidizing agents can be arranged in oxidizing property order according to their standard free energies of decomposing organic matter: O_2> NO_3^-> MnO_2> $Fe(OH)_3$> SO_3^{2-}> CH_2O. China marginal sea sedimentary environments have been systematically researched and it is found that the sedimentary redox environments are not only related to Eh, organic carbon, the ratio of Fe^{3+}/Fe^{2+}, but also to the grain sizes of sediments and sulfur system in the interstitial water. Hereby, a new function — Redox Degree (ROD) is introduced to appraise the redox environments of sediments. The magnitude of ROD quantificationally reflects the degree of redox reactions. The analyses of ROD show that the sedimentary reduction properties of the northern Yellow River estuary are stronger than those of the South Yellow Sea and Okinawa Trough, *etc.* The reducing property of sediment is stronger than that of seawater, and the reducing property in the regions far off the bank is stronger than that in the near-shore area.

S system is one of the main systems to regulate sedimentary redox processes. It participates in a series of diagenesis such as complexation, exchange adsorption, precipitation, *etc.* The existing forms of

S are regulated by environmental pE and pH. S in the East China Sea sediment interstitial water mainly exists in the form of SO_4^{2-}, and it amounts for 99 % of the total S, HS^- amounts for only 1 % of the total S, the others are a little H_2S and S^{2-} *et al.* Sulfate is reduced to sulfide through microbial processes under anoxic circumstances. SO_4^{2-}/ HS^- (S^0) is one of the main redox electrode pairs which regulats marine environments.

The greatest reduction rate of sulfate occurs in the surface layer sediment interstitial water, and it is regulated by the content of organic matter in sediment, and influenced by season. S with -2 value mainly results from the diffusion from the sedimentary interstitial water to overlying waters, and the diffusing flux of HS^- in the Yellow River estuary regions reaches 8.95 μ mol/(m^2 • d)[4].

Behaviors of OC in sediments are mainly controlled by depth and the redox environment. OC from sulfur mineralization accounts for 60 %~80 % of the average net primary production. Phosphorus is controlled by pH and dissolved oxygen of water columns. The higher pH and DO are, the more phosphorus is released. Silicon is mainly controlled by some inorganic dissolution. For example, it can precipitate in the formation of meerschaum mixing with $Mg(OH)_2$, and decrease enormously dissolved solica concentration in the interstitial water. Only a little N in sediments is buried, the others are regenerated through mineralization and are released in the forms of NO_3^-, NO_2^-, NH_4^+, N_2 or N_2O via early diagenesis[5].

Song[5] studied the early diagenesis models of NH_4^+, SO_4^{2-}, PO_4^{3-}, H_4SiO_4 in the East Sea China sediment interstitial water. The decomposition, precipitation and adsorption of ammonium, dissolved silicate, phosphate and sulfate in the interstitial water are ubiquitous, and they could be treated with the first dimension kinetic reaction model. The dissolution of silicate and reduction of sulfate occur in the upper surface layer (0~10 cm). Profiles of silicate in the interstitial water show a decreasing trend with depth. Profiles of sulfate show that the further the distance is, the higher the concentrations of sulfate are. Alkalinity and $\sum PO_4^{3-}$ in the sedimentary interstitial water increase with depth, suggesting that the origin of NH_4^+ is the decomposition of bottom sediments and the release of the decomposed productions, not the diffusion and reduction of NO_3^- in the overlying water. The decomposition of organic matter depends upon the activity of organic matter in the sediment and the efficient actions of electron acceptors under special sedimentary circumstances, which include O_2, NO_3^-, MnO_2 (or Mn_2O_3, MnOOH), Fe_2O_3 (or FeOOH), SO_4^{2-} and C, *etc.*.

The Daya Bay is rich in biological resources. Most of its sediments are soft mud, but contents of nutrients are not high. Daya Bay has high primary production and is prone to bringing about the red tide. The determined contents of NH_4^+, HPO_4^{2-} and H_4SiO_4 are arranged in the order: interstitial water> overlying water>bottom water. No significant change has been found about NO_2^- and NO_3^-, and nor in the concentration profiles of NO_3^-, NO_2^-, HPO_4^{2-} and H_4SiO_4 in the sedimentary interstitial water, but the profiles of NH_4^+ concentrations decrease with depth exponentially. The content of NH_4^+ in the sedimentary interstitial water is 2~3 orders of magnitude greater than those of NO_2^- and NO_3^-, suggesting that the surface sediment of the Daya Bay is in a reducing state. The high concentration of NH_4^+ suggests the recycling utilization ratio of N is very high, and NH_4^+ might have been assimilated before it is converted. The concentration of NH_4^+ in the Daya Bay interstitial water is higher than that in the East China Sea[4,6].

The transferable phosphorus in the natural grain size sediments is in the range of 58.5~69.8 mg /g in the Yellow River estuarine regions, accounting for 9.1 %~11.0 % of the total phosphorus. In

comparison, the phosphorus in the totally-ground sediments is 454.8~529.2 mg /g, accounting for 9.1 %~11.0 % of it. It suggests that the transformed P in the totally-ground sediments mostly could not participate in the biogeochemical recycling. It is found by the survey results in situ from benthos that the biomass of big or small benthos is well correlative to the non-detrital state P in natural grain sizes of sediments. Bad correlations are found between the biological mass and the phosphoric content in the totally-ground sediments. It shows that the transformed P is the P of non-detrital state in natural grain size sediments, and not the P in the totally-ground sediments which have been taken for granted before[7].

Accordingly, the recycling of biogenic elements in China marginal sea sediments is correlated with pH, ROD, temperature, water dynamics and biological activity under sedimentary circumstances. In addition, it is very important whether or not the studying means adopted and its results can really reflect the biogeochemical processes and their contributions to marine changes.

3 Contribution of setting particles to biogenic element recycling in China seas

The sedimentation of marine setting particles is an important source of sediment in seabed, and it plays an important role in sediment-seawater interface processes. It is significant to the researches on the regulation of setting particles on material transferring, transforming and depositing. Fluxes of some biogenic elements in China marginal sea setting particles are listed in Table 2.

Tab. 2 The fluxes of biogenic elements of settling particulates **mg/(m^2 • d)**

Regions		Depth /m	POC	TPC	PON	TPN	POP	TPP	C: N: P	References
Nansha	Xinyi lagoon	5	463.4						50.4: 6.3: 1	Song, 1997
coral	Zhubi lagoon	24	53.38	402.3	8.5	9.8	2.98	4.1	199.1: 9.6: 1	
reef	Zhubi lagoon	16	90.16	575.7	5.6	13.8	1.15	3.07	119.4: 14.9: 1	
lagoons	Yongshu lagoon	5	220.1	2735	32.1	45.9	4.82	12.0		
Nansha Islands		80	193.5							Hong, 1994;
		25	99.25							Hong, *et al.* 1991
Taiwan Straits		50	73.8							
		60	98.5							
Luoyuan Bay		5	5 054				5.64		89.4:11.1:1	
Xiamen Bay		5	856				47.7			Song, 1997
East China Sea		5	213.8		20.1					

The setting fluxes of particle carbons in the euphotic zone of the southern Taiwan Straits region are 73.76 (5 m) and 98.50 (60 m) mg /(m^2 • d), respectively, the annual fluxes in this regions are 2.45×10^9 kg • C/a, the total removal rates in euphotic zone are about 2.5×10^9 kg • C/a, and the total carbons in the euphotic zone of the region are 6.48×10^{10} kg • C/a. Accordingly, the retention period of total carbon in the euphotic zone is estimated 26 years, which shows that the recycling rate of OC in the region is rather quick. The Luoyuan Bay is not rich in inputs of exterior nutrients. The 91 % of N, 97 % of P and 68 % of Si that biological activities need come from their recycles in waters. The contents of POC decrease successively from suspended matter to setting particulates and to surface sediments, and 15 %~40 % of POC in suspended matter has participated in the recycling in the setting process from water to sediment. The annual average content of PP in the Luoyuan Bay waters is (0.342 ± 0.249) μ mol/L, amounting to about 40 % of TP. The distribution of PP is mainly controlled by resuspension and continental inputting processes in winter, and by biological processes in the waters in summer.

Upwelling plays an important role in the recycling of biogenic elements of setting particles in the East China Sea continental shelf, and sometimes it is the main contributor, and the biological activity is less. About 80 % of surface sediments are constituted by suspended matter, so upwelling also influences the interface behaviors of biogenic elements. Upwelling increases the provision of nutrients, and also the biological production. 25 % ~ 40 % of primary production comes from seabed sediments in the processes, and ultimately causes 76 % ~ 83 % of PP to regenerate. Strong upwelling occurs in the near-shore area in summer and exists at the south edge of the Taiwan bank throughout the year. Suspended matters from the 0~10 m upwelling water layer at the south edge of the Taiwan bank mainly consist of biological particles in summer. The PP accounts for 50 % of TP in Xiamen Harbor and Jiulong River estuarine regions in spring, the correlativities between PP and TP are very good. Transformations among different forms of P mainly occur by solution, and are also influenced by biological activities[13].

Resuspension of sediment has a significant influence on the composition of setting particles in the East China Sea continental shelf region. Resuspension of sediments from storm, tides, bottom currents and benthos disturbance is greater in the East China Sea continental shelf region than that in the Changjiang estuary. There are significant differences in the material vertical fluxes in the East China Sea continental shelf regions among different regions and depths. The vertical transferring of C in the regions mainly depends on POC, which accounts for 98 % of TC in the surface waters and 68 % of TC in the bottom water. POC/PON ratios in plankons and suspended particles are both close to 10.6, enormously lower than that in sediments. The particle inorganic carbons (PIC) in plankons and suspended particles account for 0.20 %~1.9 % of PC. PIC/TP value in the bottom layer suspended matter is much greater than that in surface layer suspended matter. Therefore, resuspension of bottom layer matter has a significant influence on the composition, contents and fluxes of setting particles in the East China Sea. The C in the seawater of sediment comes from the CO_2 exchanged across the seawater — air interface, then the DIC is translated into DOC and POC through photosynthesis of phytoplankton and production of zooplankton, which constitutes the main vertical transferring matter and C deposits in the East China Sea continental shelf.

The setting particles in the Nansha Islands coral reef ecosystems are mainly from biological origins, and their setting rates are greater than those in the near-shore regions, which reflects the higher biological production in the regions. C: N: P is 123:10:1 in the particles averagely, having greater difference from the Redfield ratio (106:16:1), and is higher than that in the Luoyuan Bay (89.4:11.1:1).

About 86 %~89 % of OC in lagoon setting particles could be decomposed and released, and about 11 %~14 % of which might be buried. The flux of OC is in direct proportion to TC, and in inverse proportion to water depth. In contrast with it, the fluxes of ON are in inverse proportion to TN, and in direct proportion to water depth. The content of PP in the coral reefs is about 3.13×10^{18} g, which accounts for 96.2 % of TP, and plays an important role in the recycling of P in the ocean. About 86 %~89 % of OC in setting particles has been released before sinking to seabed, which plays an important role in the recycling of OC and in maintaining a higher biological production in the coral reef. The flux of OP is between OC and ON. The recycling rates of setting PP in lagoons are rather quick, 35 days in the Zhubi reef and 7 days in the Yongshu reef. POP in setting particles of Nansha coral reef lagoons accounts for 37.9 %~72.6 % of TP. The releasing ratios of setting PP could be estimated from the contents of TP and POP of setting particles and through surface sediments of lagoons. The releasing ratio of OP is 97.5 % in the Zhubi reef region, which accounts for 90.7 % of TP. Therefore, 97.5 % of OP is released into waters for recycling. The releasing ratio of POP is 81.8 % in the Yongshu reef region. Accordingly, 2.5 %~18 % of OP is buried because of its burial aggradation, IP could also be released to a certain extent, and it mainly comes from the regeneration and dissolution of solid calcium phosphate in bones by bacterial activity. Nansha Islands coral reef ecosystems are the exporter of organic particle and nutrients.

In conclusion, 15 %~40 % of OC and 82 %~97.5 % of OP have been released into the sea water for recycling before biogenic elements in the setting particles reach the seabed in China marginal seas. The researches on biogenic elemental recycling processes in China sea vertical setting particles are not systemic. It is necessary to systematically study the recycling and controlling mechanisms of biogenic elements. Considering the past researches in China seas, biological processes and water dynamical processes must be two important factors.

4 Contribution of China marginal sea sediments to the recycling of biogenic elements

Terrestrial detrital organic matter and suspended particles are the main sources of marine sedimentary biogenic elements and they are brought into the ocean by river runoffs, biological activities and human activities and ultimately reach the seabed. The biogenic elements carry through mass transfer mainly by molecular diffusion across the sediment-seawater interface. Molecular diffusion results from a series of chemical reactions and processes, such as mineralization of organic matter, dissolution and precipitation of minerals, adsorption, exchange of matter, and so on, which alter the compositions of interstitial water, and result in a concentration gradient in the interstitial water. Recycling of biogenic elements between sediments and interstitial water is carried out endlessly along the gradient. The physical chemical environments of sediments play an important regulatory role in the recycling. The mass exchanges between the interstitial water and the overlying water are important material conditions to maintain the ecosystem in surface sediments and in bottom waters.

The diffusing fluxes of biogenic elements across sediment-seawater interfaces mainly depend on the diffusion of concentration difference caused by the concentration gradient near the interfaces. The net diffusing fluxes of biogenic elements across the sediment-water interface in some China sea areas can be estimated by the First Fick Law, and the results are listed in Table 3.

Tab. 3 Diffusion fluxes across the sediment-seawater interfaces in China seas[1)]

Regions	HCO_3^-	SO_4^{2-}	S^{2-}	NH_4^+	NO_2^-	NO_3^-	HPO_4^{2-}	H_4SiO_4
East China Sea	-0.634[2)]~0.387	-2.055~1.214	-0.022~0.141	-34.081~0.193			-1.199~1.938	-324.9~148.8
Liaodong Bay		-0.66	2.24	1.41				
Nansha Islands Lagoon (1993)		-0.39	0.70	630.26	30.22	103.86	9.13	255.10
Nansha Islands Lagoon (1994)		-0.43	14.70	197.61	4.42	212.86	6.71	151.63
Nansha Islands off-reef (1993)		-0.36	0.36	619.77	19.82	345.15	8.35	2637.70
Nansha Islands off-reef (1994)		-0.33	0.22	485.30	14.81	585.05	15.78	1627.32
Xiamen Bay				720.00			7.74	2800.00
Okinawa Trough				-4.488			1.131	2.209
Outer -Wenzhou				-6.640			0.133	111.90
South Yellow Sea				-1.321			-0.102	-55.91
Luoyuan Bay							0.370	314.8
Daya Bay				302.0	-0.06	-1.82	2.53	47.96

1) Unit: HCO_3^- and SO_4^{2-} are mmol/(m^2 • d); S^{2-} is pmol/(m^2 • d); the others are μ mol/(m^2 • d).

2) The minus"-"stands for the flux direction from overlying waters to sediment.

The diffusing behaviors of nutrients depend upon their inner characteristics and the environments of regions. The whole oceanic annual input fluxes of PO_4-P, SiO_4-Si, NH_4^+-N and Mn^{2+} to the overlying water are: 3.8×10^{11} g /a, 1.1×10^{13} g /a, 1.0×10^{13} g /a and 1.4×10^{11} g /a, amounting to 54 %, 2.2 %, 4.8 % and 40 % of the total river inputting fluxes, respectively.

Nutrients released from the organic matter decomposition in bay sediments of China seas contribute 80 % of N and 200 % of P that the plankton needs in the bays. Due to a shallower water depth, stronger seasonal changes of temperature and biogeochemical actions, stronger changes of early diagenesis processes near interfaces and quicker productions or adsorptions of nutrients from sediments in the Bohai Sea, the Yellow Sea and the East China Sea, directions of nutrient diffusions are different in China marginal sea sediments.

Most of the East China Sea continental shelf surface sediments is covered with sandy sediments. Content of H_4SiO_4 in surface sediments is 24 times greater than that in the surface waters, and 23 times greater than that in the bottom waters. The values of PO_4-P are 19 times and 3 times greater, respectively [8~10]. The annual releasing fluxes of P and Si into seawaters from the sediments in the Bohai Sea are 1.02×10^7 kg P / a and 1.91×10^8 kg Si / a, respectively, accounting for 86.4 % of recycling TP and 31.7 % of recycling TSi, respectively. Accordingly, the processes near the sediment-seawater interfaces in the Bohai Sea play an important role in the recycling of nutrients, especially so for P[11]. Liaodong Bay lies in the north of the Bohai Sea. Ammonium and sulfide diffuse from the sediments to the overlying water, and SO_4^{2-} diffuses from the overlying water to the sediments, which reflectes their different chemical diagenesis processes[5].

All the diffusion directions of nutrients near the sediment-seawater interfaces in the Nansha Islands are from the sediments to the overlying water, and their fluxes are greater than those in the Bohai Sea, Yellow Sea and East China Sea. Due to the high water temperature in the Nansha Islands year after year, the apparent active energies of nutrients diffusing and releasing from the sediments decrease, and the sediment activities increase. This results in a great deal of nutrients in the sediments, which diffuse from the sediments to the overlying water.

HS^- concentration in the Nansha lagoon interstitial water is much higher than that in the outer-reef sediment interstitial water. The concentration in the interstitial water of the lagoons with human activities is higher than that in the interstitial water of lagoons without human activities, and is higher in the near-reef sediment interstitial water than that in the off-reef sediment interstitial water. HS^- and S^{2-} diffuse from sediments to overlying seawaters, but it is opposite for SO_4^{2-}. The average diffusing fluxes in the lagoons are higher than those in the outer-reef. H_4SiO_4 is the greatest diffusing composition in the outer-reef nutrient compositions, and NO_3^- and NH_4^+ are the greatest diffusing compositions. The diffusing flux of H_4SiO_4 across the outer-reef sediment-water interfaces is 10.5 times greater than that in the lagoons, and NO_3^- is 3 times greater than that.

All the diffusion directions of S^{2-}, HS^-, H_4SiO_4 are from the sediment to the overlying water in the East China Sea, and the opposites are SO_4^{2-}, NH_4^+, PO_4^{3-}, namely, from the overlying water to the sediments. The different diffusing directions reflect their different early diagenesis processes in the sediments[5].

The diffusion of HCO_3^- from seawater to sediment in the outer-Changjiang estuary and Okinawa Trough regions shows that HCO_3^- must be transferred in the surface layer sediment. The diffusion of HCO_3^- from the sediments to seawaters in the northern Taiwan Straits is due to the short distance of the region from bank, high content of organic matter in sediments, low pH value, and also the dissolution of $CaCO_3$ and the oxidation of organic matter. The diffusion of NH_4^+ is from sediments to seawaters in the outer-Changjiang estuary, Okinawa Trough and northern Taiwan Straits, which reflects the transferring of NH_4^+ through being adsorbed on clay minerals in the East China Sea sediments. There is much solution and diffusion of H_4SiO_4 to seawater from sediments in the Okinawa Trough and the Taiwan Straits because of low pH in the region's sediments. HPO_4^{2-} could be transferred through adsorption or through forming apatite in the Okinawa Trough and the southern Taiwan Straits. HPO_4^{2-} could diffuse from sediment to seawater in Okinawa Trough sediments, which is due to the characteristics of volcano activity and oceanic sedimentation in the region. There is much more organic matter from biological activities in the sediments of Changjiang estuary near-shore, and could decompose and release more NH_4^+ and HCO_3^- to enter the interstitial water, and then diffuse into the overlying waters, which provide more chemical substances for the overlying waters than in the off-shore region. The transferring of Si exists in the sediments of outer-Changjiang estuary. The diffusion of SO_4^{2-} across the sediment-water interface is from the overlying waters to the sediments in the regions of Nansha Islands, Okinawa Trough, Yellow River Estuary and South Yellow Sea, except in outer-Wenzhou. It is due to the stronger reduction of SO_4^{2-} in surface sediments that lead to the consumption and diffusion of SO_4^{2-}. The diffusion directions of S^{2-} and HS^- are from sediments to overlying waters, which reflects the stronger reduction of the two elements in the sediments than that in the overlying waters. S^{2-} from the reduction of SO_4^{2-} diffuses into seawaters. Most of S^{2-} is produced by chemical diagenesis in initial stages when S^{2-} is buried in sediments. Diffusion of S^{2-} into the overlying waters shows that S^{2-} in the surface sediments could be

dissolved and be freed from reduction. The magnitude of transferring fluxes of HS^- reflects the reduction of sediments to a certain degree. The sedimentary reduction could be listed below according to the diffusion fluxes of HS^-: Yellow River outer-shore region> Yellow River near-shore region >southern Yellow Sea region>outer-Wenzhou region> Okinawa Trough region, which mainly depends upon the input of terrigenous matter, especially, of the terrigenous organic matter[5,12].

Luoyuan Bay belongs to a subtropical region, and a typical semiclosed bay. Annually Si and P diffusing into the overlying waters from the bay sediments are 6.61×10^2 g P / a, 4.95×10^5 g Si / a, respectively. The average fluxes of P and Si into the ocean from the river are about 7.13×10^6 g P / a and 1.97×10^9 g Si / a, so the diffusions account for about 10 % of P and 25 % of Si in the input fluxes, respectively. The diffusing fluxes of Si in the Luoyuan Bay sediments are less than those in the Xiamen Bay sediments, and greater than those in the East China Sea continental shelf and outer-Changjiang River. The diffusion fluxes of P in the Luoyuan Bay sediments are less, due to the fact that the content of P in its interstitial water is only 1.0 μ mol. The content is comparable to the contents in the Xiamen Bay sediments, and is tens to millions of times less than those in the world ocean sediments[3,13,14]. The diffusing flux of P into overlying waters in the western Xiamen Bay is 0.9 μ mol / (m^2 • d). The diffusing flux of P across the sediment-seawater interface is 0.026 mg / (m^2 • d) in the Luoyuan Bay and 0.24 mg / (m^2 • d) in the Xiamen Bay, respectively. The fluxes of PP determined from the sampling implements under the euphotic zones are 5.64 mg / (m^2 • d) and 47.7 mg / (m^2 • d), respectively. Accordingly, most of the P released participates in the recycling in the sinking processes. PP that reaches the seabed is strongly adsorbed on solid and only about 0.5% of which diffuses into the waters in the form of solute through early diagenesis processes, even though some P has been released through mineralization of organic matter.

From the Yellow River estuary to the Bohai Sea, the flux of dissolved P is 1.6×10^6 kg / a, the flux of dissolvable P is 2.81×10^8 kg / a, and the flux of buried P is 5.88×10^8 kg / a. The direct contribution of dissolved P to the Bohai Sea is less than the release of dissolvable P from suspended particles and from sediments for the higher suspended matter transportation and lower efflux. About 2/3 of the TP transferring from Yellow River Estuary sinks and is buried in the marine sediments, OP released from the decomposition of river organic matter is the main source of dissolved P and dissolvable P in the region[11,15].

The nutrients supplied from the sediments to the seawaters in the Daya Bay are more important than those in other regions. The cultivated region of Daya Bay is covered with soft mud, the vertical concentration distributions of NO_3^-, NO_2^-, H_4SiO_4, HPO_4^{2-} have no changes in the interstitial water of region, and the distribution of NH_4^+ decreases distinctly with depth. The vertical distribution trend of NH_4^+ is similar to those in the East China Sea, but the content of NH_4^+ in the Daya Bay sedimentary interstitial water is greater than those in the East China Sea. The diffusing fluxes into seawater of NH_4^+, HPO_4^{2-} and H_4SiO_4 in the Daya Bay sediments are much less than those in the Xiamen Bay and the Nansha Islands, but greater than those in many near-shore regions. The diffusing directions of NO_3^- and NO_2^- are from overlying waters to sediments, which shows the enrichment of organic matter near the surface sediment interfaces in the cultivated regions. The content of H_4SiO_4 in the interstitial water of Daya Bay is higher than those in other regions, but changes much less than those in other regions.

In conclusion, the differences of biogenic element diffusing fluxes near sediment-seawater interfaces in different regions are very great, and their directions are not all the same. It reflects the

differences in their early diagenesis processes, interfacial geological circumstances, biological and physical chemical environments.

5 Influences of biological production in China marginal sea sediments on the recycling of biogenic elements

Of all the marine organic matters, the living particle organic matter accounts for 2 %, non-living particle organic matter accounts for 9 %, and dissolved organic matter accounts for 89 %. Life activities are the most active factors in the ocean, and almost involve all the geochemical processes. It is the 2 % of the life organic particles in the ocean that regulats the existence of 89 % of the dissolved organic matter.

5.1 Influences of planktons on the recycling of biogenic elements

Planktons have important contributions to marine primary production. The marine biological production is initiated from photosynthesis of phytoplanktons, which utilize sunlight and CO_2 to synthesize 40 %~50 % of global primary production. 2~20 μm micro-phytoplanktons and those less than 2 μm possess a great proportion in marine primary producers, their contributions sometimes exceed the diatoms - the traditional primary producers, especially in the tropical ocean. The diatoms with tens of μm are the main producers of marine primary production in the past, especially in the spring when algal bloom occurs. The primary production estimated according to chlorophyl-a in the Nansha region is 406 mg / (m^2 • a), and the proportion of the vertical flux of organic carbon in primary production is also estimated. The proportions are 17.7 % in the Nansha Zhubi reef, and 54.2 % in the Yongshu reef. It shows that 17.7 %~54.2 % of primary productions in the lagoons sinks to the seabed through biological particles, and 45.8 %~82.3 % of OC participates in recycling in waters. The values are lower than that in the Luoyuan Bay, and higher than those in general sea regions[15]. The nutrient concentration in the surface layer waters is 0.2 μmol/L, lower than that in the bottom waters, and 0.4 μ mol/L higher than that in offshore region, and, moreover, it increases with depth. The regenerating rate of phosphates between 200 m and 600 m depth is 6.7~20 μmol/L year, and the average sinking rate is 15~80 days[16].

The influences of plankons on recycling of biogenic elements are also embodied in the seasonal changes of the contents and recycling of biogenic elements. The fluxes of amino acids and organic matter in the northern South China Sea setting particles show intense seasonal changes, and the increase and decrease of planktonss such as diatom, coccolith, and foraminifer are similar to the changes of the total flux. The siliceous and calcareous planktons are the main contributors of organic matter. The organic matter is assembled and rapidly settles through mutual actions between organic particles and inorganic particles, decomposed and dissolved by microbes, and causes the particles to return to waters for recycling[17].

Nutrients have an important effect on the growth rate of pelagic diatoms, whereas, the biological production processes of pelagic diatoms also have an important effect on the recycling of biogenic elements[18-20]. The concentrations of nutrients in marine ecosystems not only influence the total biomass, but also lead to the changes of the compositions, structures and characteristics of particles. Some studies show that the waters would become eutrophic when IN>0.2 mg/L, IP>0.045 mg/L, COD>0.2~0.3 mg/L. The optimal nutrient concentration for the growth of cocconeis scutellum Var. Parva is: N: P: Fe: Si=50: 0.25:0.5:2.0; and for that of amphora coffeaeformis is: 2.5:1.0:1.0:2.0; for that of N. millis is:

5.0:0.15:0.5:2.0.

The primary production in estuarine regions reachs 500~1 000 g / (m^2 • a), in contrast to 100 g / (m^2 • a) in the continential shelf regions. The primary production has an important influence on the transferring of OC and on the other biogenic elements. The different microbial and plankton activities, different biogeochemical processes across particle-water interfaces, and different circumstances lead to the changes of forms and the transformation of phases of the biogenic element C, N, P in Changjiang estuary, further alter the surface compositions, properties of particles and the components of medium, consequently influencing the stability of colloidal particle. The biogeochemical process is an important factor and also one of the main mechanisms to regulate the flocculations of particles in the Changjiang estuary region[13].

About 50 % of particle organic matters has been used up before they reach the 5 cm waters above the seabed in the Yongshu reef and the Zhubi reef. The consuming rate is greater in the Yongshu reef than that in the China marginal sea continental shelf. The main source of organic matter in the Yongshu reef is marine plankton[21].

Upwelling in the Taiwan Straits region causes net nutrient fluxes, higher nutrient consumption rates and the net production rates of particle organic matter and dissolved oxygen. POC in plankton provides 25 % of the total POC. POC from the aggradation in euphotic zones is about 2×10 g • C / (m^2 • s), accounting for 35 % of the primary production[3].

In conclusion, plankton is very important in the recycling of setting particles, and its production processes influence the release, burial and transfer of biogenic elements in China seas.

5.2 Influences of benthos on the recycling of biogenic elements

At present, studies on the recycling of biogenic elements in protozoans and minitype animals are not adequate, but studies on the predations of several macrobenthos have been very distinct. Most of the macrobenthos prey on suspensions or sediments, and incept the adsorded sediments (for instance, echinus species), and other species prey on deep-water particles (for instance, star worms). The benthos near marine sediments include microbes (such as bacteria and ephphytes), protozoans, minitype animals and macrobenthos, etc. Their influences on the recycling of biogenic elements in marine sediments are mainly in: (1) influencing the evolution of waters and the transfer of nutrients; (2) influencing the stability and transfer of biogenic elements in sediments; (3) influencing the recycling of global biogenic elements. The benthos near the sediment-seawater interfaces sometimes irrigate their own caves by taking oxygen and food near sediment-seawater interfaces, thereby facilitating the mixing and exchanging of biogenic elements between the surface interstitial waters and the overlying waters[22].

Preying processes are the bases for benthos' ecological functions and biogeochemical processes. Fungi could decompose lignocellulose and chitin , bacteria could decompose particle OC, most of particles are diatoms and animal residues. Hydrolyzing bacteria start this process and create dissolved organic carbons (DOC). DOC could be oxidized to CO_2 by oxidants (O_2, NO_3^-, Mn_4^+, Fe^{3+}, SO_4^{2-} and so on) in sedimentary circumstances, and could be decomposed by zymosis too. The most typical of bacteria are the sulfate deoxidizing bacteria. Mn^{2+}, Fe^{2+} and SO_4^{2-} could be oxidized by some bacteria during the oxidizing processes of OC. Because the processes provide less energy, the production is also limited. However, it is the process that finishes the recycling of C, N, S, Fe and Mn in sediments, and further forms their oxides.

Benthos influence and regulate the recycling of N, and for example, the irrigations of benthos

strongly worked on the content and its vertical distribution of NH_4^+. In general, the concentrations of NH_4^+ in the interstitial water increase with depth until the depth of 5~10 cm or 10~15 cm, reversely, the production rates of NH_4^+ decrease with depth. NH_4^+ from surface sediments diffuses into overlying waters prior to that from deep waters, and the benthos irrigations accelerate the process. The water depth where the benthos locate is in direct proportion to the acting time when the sediments are buried, Thereby, in spite of the lower production rate of NH_4^+ in deeper waters, there is much time for the releasing and accumulating of NH_4^+ from the decomposition of organic matter. Biological processes reduce the gradients between sediment interstitial waters and their overlying waters, and further reduce the ionic diffusing fluxes of NH_4^+ and HCO_3^- calculated by gradient means. On the other hand, due to overestimated quantity of NH_4^+ that enters the overlying waters, the flux calculated by gradient means increases. It further uncovers the relations between distributions of NH_4^+ and HCO_3^- and benthos animal mass[15,22].

The biogeochemical regeneration and transfer of P are two significant controlling factors in primary production, and the biological activities play an important role in the transferring of phosphoric forms. The release of P is especially important to the estuarine and near-shore environments. The regeneration of nutrients in the near-shore sediments evidently provides what primary production needs in the overlying waters[17]. Planktons per se have certain depositing functions to N and P in waters. Due to the decompositions of biological detritus and excretions in the waters under water columns, nutrients such as P and others gain regeneration. Of the nutrients, the regeneration rate of active P commonly is 3.88 μ g / (L • d), and the net biological utilization rate is 3.10 μ g / (L • d), so, the biological inputting and outgoing processes of P are basically in a balanced state[3]. Through *in situ* surveying and laboratory cultivation, it is found that the greatest rates of biological adsorption and excretion of P in the Xiamen Bay and the Jiulong River estuary in spring are 0.191 h^{-1} and 0.063 h^{-1} respectively. The distribution of alkaline phosphatase (ALPase) activities in western Xiamen Harbour sediments and the Hongkang Victoria sediments has certain relativity to the degree of pollution indicated by the microbial characterstic factors, and has a notable relativity to the anaerobic circumstances of sediments[13,23]. The fluxes of nutrients in the Minjiang Estuary are about 3.3×10^{11} g for silicate, 7.7×10^{11} g for phosphate, and 4.6×10^{10} g for DIN, respectively. The average primary production is about 192.4 mg / (m^2 • d) (685 mg / m^2 • d ~ 8.59 mg / m^2 • d). The photosynthesis of planktons is related to the nutrient mass, and C: N: P: Si=106:16:1:15. The consumption of nutrients accounts for 14.5 % N, 53.6 % P and 1.9 % Si of the total river inputs[24].

The recycling of S in sediments is related to biological activities, and the existing forms of S are related to its environment. The reduction of sulfate and the oxidation of sulfide are the two main processes in which S is metabolized in sediments, and the bacteria play a key role in the processes. It is estimated by recordation of the fossils that benthos play a main role in the accumulation of S in sediments. Such a function might be performed by regulating dissolved oxygen and the content of unstable carbons. In the light of the whole world, S is not a limiting element, but it plays an important role in the recycling and in the bacteria evolution. The distribution of S^{2-} is mainly controlled by bacteria, and the ratio of S^{2-}/S_2^{2-} increases from the estuary to the continental shelf. The oxidation of S from S^{2-} to S^0 is also carried out by S bacteria - - a kind of oxidizing bacteria, so the ratio of S^{2-}/S_2^{2-} in the profile of sediments could be used as a measure for estimating the settling rates in modern oceanography[14].

It is obvious that the biological production influences the releasing, burying and transferring of biogenic elements, and it is also an important controlling factor for the recycling of biogenic elements in sediments. Planktons and benthos participate in the biogeochemical processes of biogenic elements in marine sediments, and also influence the oceanic environments and the global marine changes.

In conclusion, the functions of China marginal sea sediments in the recycling of biogenic elements vary greatly with different regions, and are controlled by contents of organic matter, biodisturbance irritations, physical chemical environments, geology, water dynamics, etc. The redox environment of biogenic elements and the ecological character near the sediment-seawater interfaces are two main factors regulating the recycling. In the future, the studies should be emphasized particularly on the distributions, spatial and temporal variabilities, transferring mechanisms of biogenic elements in sediments and on their influences on ecological environments.

Acknowledgement

This study is supported by the National Science Foundation for Outstanding Younger Scientists (No. 49925614).

References

[1] Zhao Yiyang, Yan M. C. (1994) Geochemistry of sediments in China seas. Science Press, Beijing, 15~16; 162~169.

[2] Wang Chenghou (1995) Geochemistry of sediments in East Sea seabed. China Ocean Press, Beijing, 59~72.

[3] Hong Huasheng (1994) Marine biogeochemistry research papers (1986-1993). Xiamen University Press, Xiamen, 2~125.

[4] Qiu J. W., Wang Z. D., Gao H. J. and Peng Y. H. (1999) Diffusive fluxes of nutrients across sediment-seawater in cultural sea area of Daya Bay. *Tropic Oceanology*, **18**(3): 83~90.

[5] Song Jinming (1997) Chemistry of sediment-sea water interface of the China seas. China Ocean Press, Beijing, 9~189.

[6] Gu Deyu, Tang Rongkun and Yu Qun (1995) The nutrient chemistry of inorganic Phosphorus, silicon, Nitrogen in Daya Bay sedimental interstitial waters. *Acta Oceanologica Sinica*, **17**(5): 73~80.

[7] Song J. M. (2000) Transferable phosphorus in sediments of the Huanghe River Estuary adjacent waters. *Marine Sciences*, **24**(7): 42~45.

[8] Bao Gende (1984) A preliminary study on organic matter, nitrogen, phosphorus in East Sea Near-shore shallow water regions. *Donghai Marine Science*, **2**(1): 15~22.

[9] Bao G. (1992) The geochemical characters of some major elements in sediments of Hangzhou Bay and its adjacent sea areas. *Acta Oceanologica Sinica*, **14**(5): 69~74.

[10] Ikehard. K., H. Katayama, Y. Tanaka and Y. Saito (1999) Physical properties of surface sediments of the East China Sea: In Margin Flux in the East China Sea. Edited by Dunxin Hu and Shizuo Tsunogai. China Ocean Press, Beijing, 219~227.

[11] Song J. M., Luo Y. X. (2000) The biogeochemical recycling modes of phosphorus and silicon near Bohai sediment-seawater interface. *Marine Sciences*, **24**(12): 41~43.

[12] Zhang Jing (1996) Study on the biogeochemistry of main estuaries in China. China Ocean Press, Beijing, 1~241.

[13] LinYian, Tang Renyou, Li Yan *et al.* (1995) The relations between the biogeochemical characters of biogenic

elements and their flocculations and sedimentations in Changjiang Estuary. *Acta Oceanologica Sinica*, **17**(5): 65~72.

[14] Chen Cimei, Lin Yueling, Chen Yuwang and Wu Yuduan (1993) The biogeochemical behaviors and environmental capacity of phosphorus in Xiamen western sea area. Acta Oceanologica Sinica, **15**(30):43~48.

[15] Li Y., Yu J. J. (1999) Geochemical characteristics of phosphorus near the Huanghe River Estuary. *Chin.J. Oceanol. Limnol.*, **17**(4): 359~365.

[16] Zhu Ch. J., Shi X. Y. and Li T. (1999) The distribution and regeneration of phosphate in the East China Sea. In Margin Flux in the East China Sea. Edited by Dunxin Hu and Shizuo Tsunogai. China Ocean Press, Beijing, 219~227.

[17] Xu L. Q., Chen J. F., Tang Y. Q. and Zheng L. F. (1997) The fluxes of amino acids in South Sea northern sediments and their biogeochemical functions. *Acta Oceanologica Sinica*, **19**(2): 57~64.

[18] Hong Huasheng, Guo Laodong and Chen Jingqian (1992) Relationships between particle characteristics and biological activities in controlled escosystems. Marine Ecosystem Enclosed Experiments, C.S. Wong and P. J. Harrison ed. 230~243.

[19] Lin Ronggen and Wu Jingyang (1992) Distributions of total, inorganic and organic phosphorus in the sediments near the Huanghe River Estuary, **10**(3): 204~214

[20] Wang Q. H, Li Y. J. and Li M. (1999) Studies on culture conditions of benthic diatoms for feeding Abalone. III. Effects of iron and silicon nutrients and orthogonal combination of nitrogen, phosphorus, iron and silicon on growth rate. *Chin.J. Oceanol. Limnol*, **17**(2): 105~111.

[21] Duan Yi, Song Jinming, Cui Mingzhong and Luo Binjie (1998) Organic geochemical studies of sinking particulate in China Sea area (I) Organic Mtaare fluxes and distributional features of hydrocarbon compounds and fattey acids. *Science in China(Series D)*, **41**(2): 208~214.

[22] Song J. M. (2000) Functions of marine sediments speciles diversity in biogenic element cycling. *Marine Sciences*, **24**(4): 22~26.

[23] Xue X. Z., Hong H. S., Huang B. Q. *et al.* (1995) Distributions, developments of the alkaline phosphatase activities and their relations to every forms of phosphorus in western Xiamen sea area sediments. *Acta Oceanologica Sinica*, **17**(5): 81~87.

[24] Chen S. T. (1997) Biogeochemical behavior of nutrient and their fluxes in the Minjiang River Estuary. *Chin. J. Oceanol. Limnol.*, **15**(2): 150~155.

Fractal Determination of Coastal Types Based on GIS ——A Case Study of China

Zhu Xiaohua (朱晓华)[1], Wu Xiuqin (吴秀芹)[1], Wang Jian (王建)[2]
1 *College of Environmental Science, Beij University, Beijing* 100871
2 *College of Geographical Science, Nanjing Normal University, Nanjing* 210097

Abstract The probability of fractal determination of coastal types based on GIS is preliminarily discussed with China as an example. Finally, some significant conclusions are drawn: (1) The fractal dimension of coastline of the bedrock coast is larger than that of the plain coast on the same scale map; (2) As far as the bedrock coast is concerned, the larger fractal dimension of coastline of the bedrock coast on the same scale map indicates that the bedrock coast is probably not typical; (3) As far as the plain coast is concerned, the smaller fractal dimension of coastline of the plain coast on the same scale map indicates that it is probably the silt plain coast; (4) The different substantial compositions affect the fractal dimensions of coastlines of different coastal types. In general, the coast which lies in the north of the Hangzhou Bay consists of sand mainly, its surface is flat, and it is connected with the coastal plain, its landform is broad shoal, its total change is comparatively homogenous in the tidal dynamic process, and thus, the relatively smaller fractal dimension of coastline results from this. For the bedrock coast, there is more bedrock, the coastline is comparatively smooth and straight, being affected by the faults and ocean dynamic process, which result in the larger fractal dimension.

Keywords GIS, Fractal, Fractal dimension, Determination of coastal type, China

1 Introduction

Studies on coastline have been tried by many researchers. Mandelbrot enunciated the concept of fractal and fractal dimension on the basis of the correlation between the length of coastline of Britain and the measuring yardstick in his famous paper "How long is the coastline of Britain?" published in "Science" in 1967[1]. Goodchild verified the fractal dimensions of different coastlines[2]. Phillips studied the erosion condition of coastline of Delaware Bay in New Jersey in 1986 and considered that the fractal dimension is a good parameter characterizing the erosion changes of coastline[3]. Taking the coastline of Delaware Bay in New Jersey as an example, he also discussed the changes of the shape of coastline resulted from the erosion of coast through the conditions of change of coastline in 38 years. He pointed out that the coastline became more irregular with the increase of the fractal dimension[4]. Qiu studied and proved that different processes through which the coast formed resulted in different fractal dimensions of coastlines. At the same time, the fractal dimension of coastline may be in accord with the different development phases of coastline[5]. Philip S. R. made an attempt to discuss the probable impact of lithologic character and faults on the development of coastline in eastern Britain. He thought that the

Received on May 21, 2002

coastline in eastern Britain was parallel to the faults in some regions[6]. Andrle designed a new approach to calculating the fractal dimension of coastline[7]. Paar calculated the fractal dimension of the coastline of Croatian Island in 1997[8]. Feng *et al.* discussed the geologic significance of fractal dimension of coastline taking the Bohai Sea for example in 1997[9]. Stomczynski discussed the length of coastline of the Atlantic Ocean in 1999[10]. Zhu X. H. *et al.* revealed the fractal characters of boundaries of tidal flat of Jiangsu Province in 2000. They also established the fractal relationship between the length of coastline of Jiangsu Province and the yardstick[11]. Synthesizing related fractal researches on coastline, it may be seen that it is just in a relatively initial phase. Generally, fractal dimensions of coastlines in some regions have been calculated, and the change of fractal dimension of coastline is related with the erosion and deposition of coast. But some problems still remain unsolved. Fractal determination of coastal types based on GIS is preliminarily discussed in this paper with China as an example.

2 Data sources and methodology

2.1 Data sources

The maps used are from the Quaternary Map of China[12] and the Atlas of Geo-Science Analyses of Landsat Imagery in China[13]. Map showing China's coastline is shown in Fig. 1.

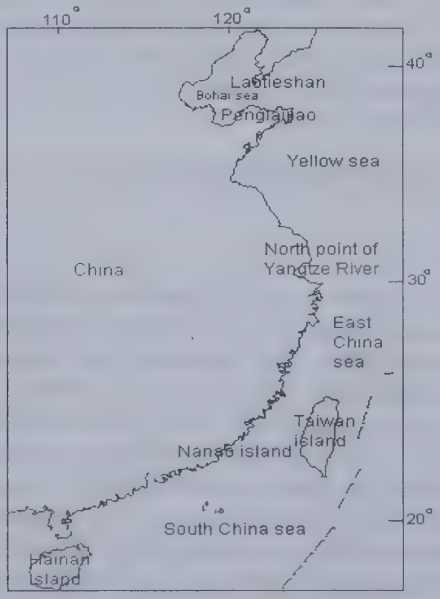

Fig. 1 Map showing China's coastline

2.2 Principles of demarcating the coastline

The coastline under study in China is selected according to the rule similar to that drawn up by the Jiangsu Surveying and Mapping Bureau when the coastline was demarcated in the investigation of land resources of China in 1990.

(1) Principle of demarcating the boundary between land and sea at the river mouth

The harbor character of the large river mouth is retained, the landforms of sand-spit, shoal and lagoon are reflected and the horn shape of the river mouth is displayed. If the river mouth is unsymmetrical, the boundary is marked where the river becomes narrow or where the curvature of the promontory is the largest.

(2) Principle of demarcating the islands

The islands off the bedrock coast and silt coast are not counted. The silt beach land, which protrudes during high tide, is considered as an island. The shoreline is not counted either.

2.3 Methodology

There are two methods of calculating the fractal dimension of a coastline: one is the divider method[14], and the other is the box-counting method[15].

(1) The divider method

To calculate the fractal dimension of a coastline, the coastline is measured by a constant yardstick. The length of coastline $L(r)$ equals to the length of yardstick r multiplied by the number of measurements $N(r)$.

$$L(r) = N(r) \times r \tag{1}$$

If different yardsticks, curve and the complexity of the coastal shape are taken into consideration, the results may vary correspondingly. The smaller the yardstick, the longer the corresponding length of measured coastline, and the closer to the reality the value will be. To be exact, the length of coastline is a variable, which is not a perfect parameter describing coastline. Therefore, an objective parameter should be found, and the fractal dimension is just one.

Supposing the fractal dimension is D (Mandelbrot, 1967), then

$$L(r) = M \times r^{1-D} \tag{2}$$

Where $L(r)$ is the length of coastline measured, r is the yardstick, M is a constant to be determined, and D is the fractal dimension of coastline.

The equivalent equation is

$$\lg L(r) = (1-D) \lg r + C \tag{3}$$

Where C is the constant to be determined, and the slope K is equal to $1-D$.

(2) The box-counting method

The box-counting method is to cover the coastline with the square grid with variable length. The number of grids $N(\varepsilon)$ covering the coastline will vary with the length of sides of square grids ε. According to the fractal theory, then

$$N(\varepsilon) \propto \varepsilon^{-D} \tag{4}$$

The equivalent equation is

$$\lg N(\varepsilon) = -D \lg \varepsilon + A \tag{5}$$

Where A is a constant to be determined, and D is the fractal dimension of coastline.

MapInfo 5.0 and ArcView GIS 3.2a software programs are used in the grid analysis, and then the extracted data are analyzed using the Excel 2000 software. It is self-evident that this data processing method on the basis of GIS is more precise than manual operation. The technological flow for fractal analysis of coastline is shown in Fig. 2.

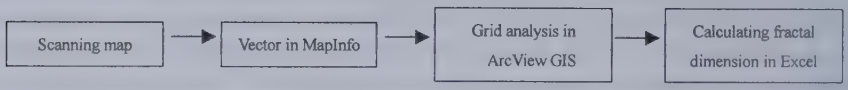

Fig. 2 Map showing technological flow for fractal analysis of coastline

3 Conclusions

3.1 China's coastline is very long, and its shape is various. Therefore, the fractal theory can be applied to the fractal determination of coastal types with China as an example. In this paper, the fractal dimensions of coastlines are calculated in these study areas: Liaodong Peninsula (D_1), Shandong Peninsula (D_2), Zhejiang Province (D_3), Fujian and Guangdong Provinces (From Fuding of Fujian Province to Lufeng of Guangdong Province, D_4), the South of the Hangzhou Bay (D_5), Bohai sea (D_6) and Jiangsu Province (D_7).

The fractal dimensions mentioned above are calculated on the scale 1: 12 000 000 map by the box-counting method. At the same time, the corresponding ones are calculated on the scale 1: 2 500 000 map by the divider method as a comparison. The results are listed in Table1.

Tab. 1 (a) Fractal dimensions of coastlines of different study areas (Box-counting method, the scale is 1: 12 000 000)

	D_1	D_2	D_3	D_4	D_5	D_6	D_7
Fractal dimension	1.009 3	1.019	1.024 7	1.025 4	1.052 8	1.006 9	1.000 4

Tab. 1 (b) Fractal dimensions of coastlines of different study areas (Divider method, the scale is 1: 2 500 000)

	D_1	D_2	D_3	D_4	D_5	D_6	D_7
Fractal dimension	1.081	1.106 2	1.121	1.122 8	1.193 8	1.074 8	1.057 9

The coasts in Liaodong Peninsula, Shandong Peninsula, Zhejiang Province, Fujian and Guangdong Provinces or the south of the Hangzhou Bay are all bedrock ones. Table 1 (a) shows that the fractal dimension of coastline of Liaodong Peninsula is 1.009 3, which is the smallest in the fractal dimensions of coastlines of bedrock coasts. That of the south of the Hangzhou Bay is 1.052 8, which is the largest among those bedrock coasts. As far as the coastal type is concerned, there are plain coasts in Bohai Bay and Jiangsu Province. As shown in Table 1 (a), the fractal dimension of coastline of Bohai Bay is 1.006 9, but that of Jiangsu Province is only 1.000 4. Though the fractal dimension of coastline of Liaodong Peninsula is the smallest among those bedrock coasts (1.009 3), this value is still larger than that of Bohai Bay (1.006 9). A comparison of fractal dimensions of coastlines between the bedrock coast and the plain coast shows that the fractal dimension of coastline of the bedrock coast is larger than that of the plain coast evidently. The conclusion can also be drawn from Table 1 (b).

3.2 The conclusion is drawn by the comparison of the above seven typical coastlines. It is further verified practically with Taiwan Island as an example. Map showing the Taiwan Island's coastline is shown in Fig. 3.

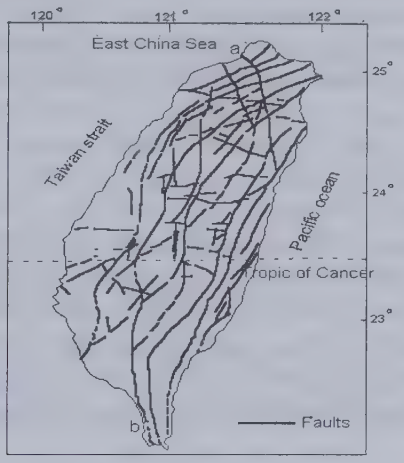

Fig. 3 Map showing the Taiwan Islands' coastline

The plain coast lies in the west of Taiwan Island, whereas the bedrock coast lies in the east. They are demarcated at points a and b, which are shown in Fig. 3. The results are listed in Table 2.

Tab. 2 (a) Fractal dimensions of coastlines of Taiwan Island
(Box-counting method, the scale is 1: 12 000 000)

	Fractal dimension
Fractal dimension of coastline of plain coast in the west of Taiwan Island	1.000 4
Fractal dimension of coastline of bedrock coast in the east of Taiwan Island	1.001 7

Tab. 2 (b) Fractal dimensions of coastlines of Taiwan island
(Divider method, the scale is 1: 2 500 000)

	Fractal dimension
Fractal dimension of coastline of plain coast in the west of Taiwan Island	1.032 3
Fractal dimension of coastline of bedrock coast in the east of Taiwan Island	1.037 3

As shown in Table 2 (a) or Table 2 (b), the fractal dimension of coastline of the plain coast in the west of Taiwan Island is 1.000 4 or 1.032 3, which is smaller than that of the bedrock coast in the east of

Taiwan Island correspondingly. Therefore, this practical verification in Taiwan Island goes a further step to show the conclusion mentioned in 3.1.

3.3 The coasts in Liaodong Peninsula, Shandong Peninsula, Zhejiang Province, Fujian and Guangdong Province are all bedrock ones, but there are still some differences among them. There are typical bedrock coasts in Liaodong Peninsula and Shandong Peninsula. Though the coastal types of Zhejiang Province, Fujian and Guangzhou Province are also classified as bedrock coasts, they are entitled silt coast of bedrock harbor in the Atlas of Physical Geography in China[16]. It shows the difference between them. There is also bedrock coast in Fujian and Guangzhou Provinces, but the biologic coast appears from Fuding. Therefore, the fractal dimensions of the above seven typical coastlines are different. As shown in Table 1 (a), the fractal dimension of coastline of Zhejiang Province is 1.024 7 and that of Fujian and Guangzhou Provinces is 1.025 4, which are larger than those of Liaodong Penisula and Shandong Penisula respectively. A comparison of the fractal dimensions of coastlines between the south of the Hangzhou Bay and Liaodong Peninsula, Shandong Peninsula, shows that the difference is more evident. Table 1 (a) shows that D_3 value (1.052 8) increases by 0.043 5 and 0.033 8 over D_1 and D_2 respectively. These changes are also shown in Table 1 (b). Therefore, as far as the bedrock coast is concerned, the larger fractal dimension of coastline of the bedrock coast on the same scale map indicates that the bedrock coast is probably not typical, and it may be the silt coast of bedrock harbor or others.

3.4 The fractal dimension of Bohai Bay is the largest among those of the plain coasts, whereas that of Jiangsu Province is the smallest. There are delta coasts in Bohai Bay and the west of Taiwan Island, while there are silt coasts in Jiangsu Province. Therefore, as far as the plain coast is concerned, the smaller fractal dimension of coastline of plain coast on the same scale map indicates that it is probably the silt plain coast.

3.5 According to the fractal dimensions of China's coastlines, it is concluded that the fractal dimension of coastline of the bedrock coast is generally larger than that of the plain coast. It has certainly an internal relation to some factors. The research on the fractal character for different boundaries of tidal flat of Jiangsu province's coast has revealed that the fractal dimension of the boundary of the tidal flat in the low tide is the smallest because the silt-fine sand deposit zone consists of silt and fine sand, its surface is low and flat, and its total change is comparatively homogenous in the tidal dynamic process[11]. To some degree it is useful to explain the reason why the fractal dimension of coastline of the bedrock coast is usually larger than that of the plain coast. In general, the coast which lies in the north of the Hangzhou Bay consists of sand mainly, its surface is flat, and it is connected with the coastal plain, its landform is broad shoal, its total change is comparatively homogenous in the tidal dynamic process, and thus, the relatively smaller fractal dimension of coastline results from this. For the bedrock coast, there is more bedrock, and the coastline is comparatively smooth and straight, being affected by the faults and ocean dynamic process, which results in the larger fractal dimension.

4 Discussion

Although some conclusions have been drawn in this paper with China as an example, whether they may be applied to other coasts all over the world still needs to be further studied.

Acknowledgements

We would like to thank Prof. Chen Shupeng, Academician of the Chinese Academy of Sciences, for his guidance. This study owes much to Prof. Zhang Xinrong for his assistance. This research was supported by the Development Fund of the Ministry of Education of China under the grant No. 2001DLXSBJBC12.

References

[1] Mandelbrot B. B. (1967) How long is the coastline of Britain? Statistical self-similarity and fractional dimension. *Science*, **156** (3 775): 636~638.

[2] Goodchild M. F. (1980) Fractals and the accuracy of geographical measures. *Mathematical geology*, **12**(2): 85~98.

[3] Philips J. D. (1986) Spatial analysis of shoreline Erosion, Delaware Bay, New Jersey. *Annals of the association of American geographers*, **76** (-): 50~62.

[4] Philips J. D. (1989) Erosion and platform irregularity of an estuarine shoreline. *Zeitschrift fur geomorphologie supplement*, **73**(-): 59~71.

[5] Qiu H. (1988) Measuring the Louisiana coastline — an application of fractals. The association of American geographers cartography specialty group occasional. Paper 1. Washington D.C: Cartography Specialty Group of the Association of American Geographers, 1~10.

[6] Philip S. R. (1994) Structural an lithological controls on coastline profiles in Fife, Eastern Britain. *Terra Research*, **6** (3): 251~254.

[7] Andrle R. (1996) The west coast of Britain: statistical self-similarity vs. characteristic scales in the landscape. *Earth Surface Processes and Landforms*, **21**(10): 955~962.

[8] Paar V., Cvitan M., Ocelic N., Josipovic M. (1997) Fractal dimension of coastline of the Croatian island Cres. *Acta-Geographica-Croatica*, **32**(-): 21~34.

[9] Feng Jinliang, Zhen Li (1997) Preliminary analysis of the geological significance of the fractal dimension of coastlines. *Marine Geology & Quaternary Geology*, **17**(1): 45~51.

[10] Stomczynski Wojciech (1999) How long was the coast of Atlantics?. *Mathematical Intelligencer*, **21**(1): 38~42.

[11] Zhu Xiaohua, Yang Xiuchun, Xie Wenjun, Wang Jian (2000) On spatial fractal character of coastline — A case study of Jiangsu province. China Ocean Engineering, **14** (4): 533~540.

[12] Zhang zonghu *et al.* (1990) *The Quaternary Map of China.* Beijing: Map Press of China.

[13] Department of Research and Development of National Remote Sensing Center, Institute of Remote sensing Application Academia Sinica (1994) *The Atlas of Geo-Science Analyses of Landsat Imagery in China.* Beijing: Science Press, 196~197.

[14] Mandelbrot B. B. (1982) The Fractal Geometry of Nature. W.H.Freeman and Co, Francisco, California, 468pp.

[15] Grassberger P (1983) On efficient box-counting algorithms. *International Journal of Modern Physics C*, **4**(3): 515~523.

[16] The Northwest Normal college. Map press of China (1984) *The Atlas of Physical Geography in China.* Beijing: Map press of China, 39.

Induction Effect and Genetic Analysis of NG to Conchospores of *Porphyra**

Xu Pu (许 璞)[1], Shen Songdong (沈颂东)[2], Fei Xiugeng (费修绠)[1], Zhang Xuecheng (张学成)[3], Zhu Jianyi (朱建一)[4]

1 *Institute of Oceanography, Chinese Academy of Sciences, Qingdao* 266071

2 *Life Sciences College, Suzhou University, Suzhou* 215006

3 *Marine Life Sciences College, Qingdao Ocean University, Qingdao* 266003

4 *Jiangsu Institute of Marine Fisheries, Nantong* 226007

Abstract The new spreading conchospores of *Porphyra yezoensis*, *P. haitanensis* and *P. katadai* var. *hemiphylla* are induced by N-Methy-N'-Nitro-N-Nitrosoguanidine (NG), a strong mutagen to induce the mutant of chromatophore. It is showed that (1) no mutants have been investigated in all control group. (2) The conchospores of all the three species of *Porphyra* are easy to be induced by NG for they are in the stage of breeding, In the lowest dose (10 μ g/mL) of this experiment, the mutant rate of *P. yezoensis* is up to 57.9%, that of *P. haitanensis* 30.7% and that of *P. katadai* var. *hemiphylla* 51.7%. (3) The mutant rate can not increase obviously by increasing the reagent concentration or prolonging the induction time. Within the scope of experiment, the inducement effects of three species of *Porphyra* ar e much similar, and the mutant rate is near 50%. The optimum induction concentration of NG is 10 μ g/mL, and the optimum induction time is 30 minutes.

Keywords *Porphyra*, Mutant of chromatophore, conchospore, N-Methy-N'-Nitro-N-Nitrosoguanidine (NG), Inducement

1 Introduction

Progress in the induction studies of Porphyra is very limited at present. Experiment of induced breeding on cultivated *Porphyra* (Imada, 1976)[11] has been carried out but gained little attention. Katayama (1983, 1984)[2-3] studied the induction effects of varied chemical mutagens on *Porphyra yezoensis* and *Porphyra tenera*, and found that only colchicines, Ethy l Methanesulphonate (EMS) and N-methy-N'-Nitro-N-Nitrosoguanidine (NG) could successfully induce pigment mutation. Due to the high concentration of mutagen and the long treatment time being used, the mutants do not survive long enough for further studies. Inducing treatments have been carried out on single vegetative cells and protoplasts of *Porphyra yezoensis* and *Porphyra haitanensis* usingcolchicine (Yan and Wang, 1990)[4], X-rays (Dai *et al.*, 1990[5]; Yan, 1992[6]) as mutagens. The results show that profitable culture properties appear in the regenerated blades, and pigmentation mutants appear too. But these studies pay more attention on growth and development, and lack detailed reports on mutation and mutation characters. Using NG as mutagen, Mitman *et al.* (1994)[7] obtained several mutants from cut blade pieces and

Received on April 18, 2002

* Supported by NSFC (C39770593), FMBLC, CAS and Applied Fundamental Project of Jiangsu Province (BJ95182) National Key Fundamental Research Program (G1999012009).

young conchospore blades that have one to several cells. The author simply described the growth and isolation process of pigmentation mutated tissues, and there is no detailed report on the induction process.

The main factors that affect the induction of *Porphyra* are as follows: First is the selection of mutagen. In the inducing studies of pigmentation mutants, only the one treated with NG has attained definite results. Second is the complexity of *Porphyra* life history. A certain kind of mutagen at certain concentrations can only affect a certain stage of the life history. The present study uses NG as mutagen to treat conchospores of *Porphyra yezoensis*, *Porphyra haitanensis* and *Porphyra katadai* var. *hemiphylla*, respectively. Varied pigmentation mutants germinating from conchospores are counted. The research not only is significant to *Porphyra* genetics theory, but also provides direction on *Porphyra* breeding.

2 Materials and methods

2.1 Materials

Porphyra yezoensis, *Porphyra haitanensis* and *Porphyra katadai* var. *hemiphylla* are used in the present study. Fronds of *Porphyra yezoensis* are collected from the semi-floating rafts on the coast of Rudong county, Jiangsu Province. *Porphyra haitanensis* is collected from the natural population growing on reefs of Nanri Island in Putian county, Fujian Province. *Porphyra katadai* var. *hemiphylla* is collected from intertidal puddles in Qingdao. After a period of cultivation, matured conchocelis filaments release conchospores. The conchospores attach to bolting-silk and glass slides, and are used as induced materials.

2.2 Mutagen compounding

N-methy-N'-Nitro-N-Nitrosoguanidine (NG) made in Sweden is used as mutagen in the present study. Dissolve the accurately weighed NG in Formamide (Zhou *et al.*, 1984), then dilute the solution with sterilized seawater to make up stocking solution to a concentration of 1 000 μg /mL. Working solutions are then diluted from the stocking solution with sterilized seawater according to experiment design.

2.3 Inducing treatment

2.3.1 Mutagen concentration and treatment time

The concentration of treatment medium is 0, 25, 50, and 100 μg/mL, respectively. A seawater medium is used as the control. The treatment time is 0, 30, 60, and 120 minutes, respectively.

2.3.2 Inducing treatment

The bolting-silk with conchospores anchored at a density of 30~50 individuals/vision (10 × 20) is selected, cut into small pieces of 1 × 1cm^2, and incubated over night. Before the inducing treatment, the cultivated materials are taken out and kept in the open air at room temperature till the bolting-silk becomes dry. Three pieces of bolting-silk are placed in each treatment medium. All the media are stirred at 20℃. After the treatment the induced materials are washed with sterilized seawater for 3 minutes, and then placed into 60 mL wide-mouth bottles for incubation. In the first three days the culture medium is changed twice a day, in the morning and evening respectively. Then the induced materials are transferred to PES culture medium and cultured under 70~80 μmol photons $m^{-2}s^{-1}$ (12L: 12D). The cultivation temperature varies according to species, *Porphyra yezoensis* is cultured at 18~20 ℃,

Porphyra haitanensis at 21~23℃ and *Porphyra katadai* var. *hemiphylla* at 16~18℃.

2.4 Mutation accounting

After 2 weeks of cultivation the experimental materials are taken out and examined under microscope. Randomly select 150 young gametophytic blades whose cells have divided twice or more, count the number of wild-type blades, single-color mutants, chimeras, survival cells, mutated cells, total color sectors (cells and blades of the same sort are counted as one), and mutated color sectors. Examination and microscopic photography are carried out under a Olympus-BH microscope. The mutation frequency is calculated as follows:

Mutation frequency = Mutated cell sectors / (wild type cell sectors + mutated cell sectors).

3 Results

3.1 Mutation frequency of conchospores

Anchored conchospores are treated with mutagen. After the treatment, color mutation appears in the divided and growing blades of conchospore germlings (Fig. 1 and Fig. 2). Results show that: (1) No mutation occurs in all the control groups. (2) Color mutation appears among conchospore germlings of all the three species. When treated with the lowest dose of 10 μg/mL NG, *Porphyra yezoensis* gains a mutation frequency of 57.9 %, *Porphyra haitanensis* 30.7 % and *Porphyra katadai* var.*hemiphylla* 51.7 %. The mutation frequency is high in all the three species. (3) Mutation frequency does not rise with the increasing of mutagen concentration and treating time. In the tested range of NG concentration and treating time, inducing results are similar in three species and in each treatment. The mutation frequency is close to 50 %. Results show that the optimal inducing condition is to treat with NG 10 μg / mL for 30 minutes.

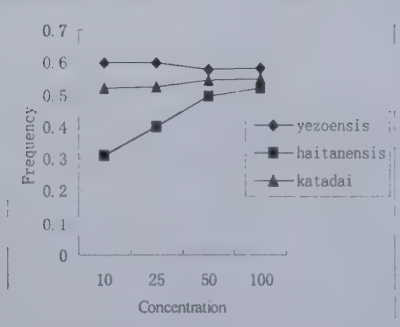

Fig. 1 Inducement effect of NG concentration to conchospore of *Porphyra*

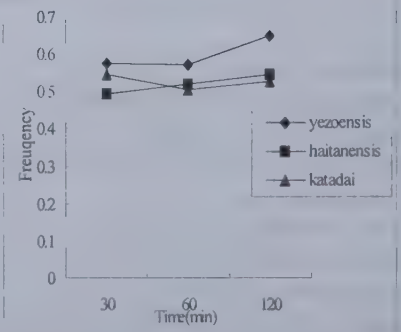

Fig. 2 Inducement effect of NG treating time to conchospore of *Porphyra*

3.2 Growth of mutated conchospore germlings

After treatment with NG, the cell division of conchospore germlings usually stops for 3~5 days. It' s difficult to find out mutated blades or distinguish color mutation at this time. Only when conchospores divide into two cells does color mutation become clear. Most of the mutation types examined are wild type/mutated-type chimeras. After the first division, conchospores may divide again to form the 3~4 cells blades, mutated blades increase significantly, mutation types vary and two or more color-mutated chimeras appear also. But the number of mutants and mutation types do not increase with the division and growth of mutants. Mutated cells divide and develop into multicellular tissues, which form a single-color mutant or a heterozygous cell sector chimera (Fig.3).

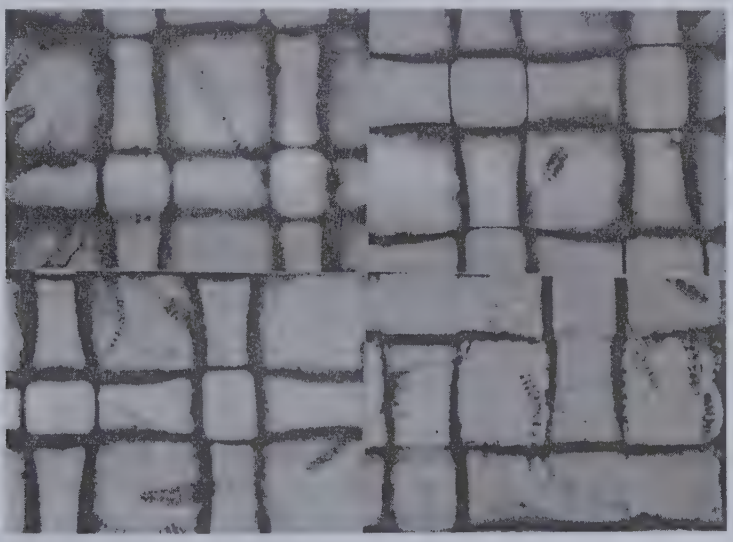

Fig.3 The seedling of induced conchospores of *Porphyra*

3.3 Character of mutated conchospores

As shown in Table 1, after two times of division, mutated conchospore germlings can be distinguished as five types, which are the wild type, single-color type, 2-color chimera, 3-color chimera and 4-color chimera. No chimera of more than 4 colors is observed. Mutant number of each type greatly varies in different treatments. Most mutants are 2-color or 3-color chimeras, then are wild-type and single-color mutants. The number of 4-color chimera is the lowest.

As examined in the present study the mutation of single-color mutants bears no relationship to the cell division frequency, which is similar to wild type blades. 2-color chimera is formed at the first division of conchospores, and mutation causes the separation of hetero-type cells. Therefore 2-color chimera is made by the first division of conchospores and bears no relationship to the second division. The formation of 3-color and 4-color chimeras may be related to the first cell division or not,

Tab. 1 Inducement effect of individual of conchospore seedling of *Porphyra yezoensis*

*Treatment	Tests	Wild types	%	Single color mutant	%	2-chimera	%	3-chimera	%	4-chimera	%
Experiment I											
10/30'	150	15	10.0	18	12.0	45	30.0	51	34.0	21	14.0
25/30'	150	15	10.0	27	18.0	69	46.0	33	22.0	6	4.0
50/30'	150	15	10.0	15	10.0	54	36.0	51	34.0	15	10.0
100/30'	150	36	24.0	30	20.0	36	24.0	42	28.0	6	4.0
50/60'	150	27	18.0	39	26.0	57	38.0	24	16.0	3	2.0
50/120'	150	15	10.0	51	34.0	30	20.0	54	36.0	0	0
Experiment II											
10/30'	150	30	20.0	42	28.0	42	28.0	33	22.0	3	2.0
25/30'	150	36	24.0	48	32.0	39	36.0	21	14.0	6	4.0
50/30'	150	57	38.0	15	10,0	51	34.0	18	12.0	9	6.0
100/30'	150	18	12.0	24	16.0	72	48.0	36	24.0	0	0
50/60'	150	33	22.0	24	16.0	69	46.0	24	16.0	0	0
50/120'	150	42	28.0	30	20.0	45	30.0	24	16.0	9	6.0

* Induction condition: NG concentration (μ g) /induction time (min)

but they must be mutated at the second division. No chimera of more than 4 colors appears in the experimental materials, which indicates that mutation will not occur at the third or more cell division.

According to the results summarized above, we can conclude that after the inducing treatment of *Porphyra* conchospores, mutation usually expresses itself after the first division of conchospores. Most mutation occurs at the first two divisions of conchospores. Thus a conchospore may be mutated twice at most and produce 4 mutated cells, which will develop into a chimera.

4 Discussion

4.1 Description of mutation frequency

Table1 also indicates that: If sorted by the blade types, the wild type blades possess a lower proportion in each treatment, so the mutation frequency varies from the highest of 90 % to the lowest of 62 %. But it doesn' t reflect the true mutation frequency, because most chimeras contain wild type cell sectors. Thus far we can describe mutation frequency according to cell types, and the result is illustrated in Table 2. But this method can' t steadily reflect the character of conchospore mutation. Proper method to describe mutation should reflect the character steadily. So in the present study we describe the mutation frequency by the type of color sectors.

Tab. 2 Inducement effect of cell of conchospore seedling of *Porphyra yezoensis*

[1]Treatments	[2]Tested cells	wt cells	Mutant cells	Mutants
Experiment 1				
10/30'	1 029	528	501	0.487
25/30'	723	300	423	0.585
50/30'	714	342	372	0.521
100/30'	591	231	360	0.609
50/60'	651	270	381	0.585
50/120'	618	201	417	0.675
Experiment 2				
10/30'	852	375	477	0.560
25/30'	777	345	432	0.556
50/30'	765	471	294	0.384
100/30'	699	315	384	0.549
50/60'	690	351	339	0.491
50/120'	666	336	330	0.495

1 Induction condition: NG concentration (μ g)/induction time (min).

2 Total cells of 150 young thalli are counted.

To further explain this question we compare three description methods of mutation frequency and the result is illustrated in Table 3. The result shows that the mutation frequencies described by cell types and color sector types coincide with each other very well, which indicates that the two methods are similar in describing the character and reliability of mutation. As shown in Table 2, most of the examined blades are at 4~6 cells stage, and cells divide for 2~3 times. At this stage the number of varied sorts of cells are about the same and the observed values can describe mutation frequency by cell sorts very well. If cultivated for a longer time or the blades examined are larger, however, the mutation frequency calculated by cell types will decrease, because the wild type blades and sectors grow faster than the mutants under most circumstances. If described by color sector types, the accuracy of mutation frequency is affected by the number and ratios of wild type and single-color mutated blades. But as shown in Table 1, the recorded numbers of wild type blades and mutants are quite similar, and the total number of the two type blades is less than that of chimeras. If only the observation value is more than enough, the deviation could decrease to sufficient low. Most important of all, the method that interprets the mutation frequency by sorts of color sectors steadily describes the character of conchospore mutation. The value of mutation frequency doesn' t correlate to the individual and the size of cell sectors, but mainly to the mutation affair itself. Little effect of other experimental conditions can be observed. Therefore, to interpret mutation frequency by sorts of color sectors is considered to be the most proper.

Tab. 3 Mutant comparation of conchospore seedling of *Porphyra*

*Treatments	Tested	Frequency of mutants		
		In type of individuals	In type of cell	In color of blocks
Test 1				
10/30'	150	0.90	0.487	0.575
25/30'	150	0.90	0.585	0.614
50/30'	150	0.90	0.521	0.630
100/30'	150	0.76	0.609	0.608
50/60'	150	0.82	0.585	0.616
50/120'	150	0.90	0.675	0.722
Test 2				
10/30'	150	0.80	0.560	0.596
25/30'	150	0.76	0.556	0.578
50/30'	150	0.62	0.384	0.500
100/30'	150	0.88	0.549	0.557
50/60'	150	0.78	0.491	0.528
50/120'	150	0.72	0.495	0.566

* Induction condition: NG concentration (μ g)/induction time (min).

4.2 Pigmentation mutants and meiosis

Genetics analysis of pigmentation mutants is first catalyzed by Miura *et al.* (1980)[9]. Cross experiment is done between the red, green and wild type blades, respectively. Results show that in the heterozygous generation of mutants and wild type blades, parental characters segregate in a 1: 1 ratio; in the heterozygous generation of mutants, two recombinant types appear besides the parental types. These are typical characters of the segregation of nuclear genes, though most of the blades appear in chimeras. The chimeras result from conchospore germlings that resemble both parental colors (including recombinant colors). At first this phenomenon is considered to be the result of germination and division of 2~4 monoploidic conchospores. Similar phenomenon has been observed in other Rhodophyte. In the crossing studies of *Gracilaria tikvahiae*, Van der Meer (1977)[10] found that some matured cells of tetrasporophyte didn' t divide to form tetrasporangia as normal, but increased their sizes. When released from the parental blades, they germinated and developed into chimeras that bore both parental colors. But chimeras represented 90~95% of conchospore germlings in *Porphyra* (Migita *et al.*, 1983) [11], which may be correlated to the life history pattern. Ma and Miura (1984)[12] studied the nuclear phase of conchospores in *Porphyra yezoensis* and found that meiosis occurred at the germination of conchospores. Similar results have been obtained in other studies, which include two species of *Porphyra torta* and *Porphyra purpurea* (Burzycki, 1984[13]; Sun and Zeng, 1987[14] Burzycki and Waaland, 1987[15], Ohme and Miura, 1988[16]; Tseng and Sun, 1989[17]; Mitman and Van der Meer, 1994[18]). It can be concluded from the crossing studies of pigmentation mutants that meiosis occurs at the germination of conchospores, which may be the common principle of most (if not all) *Porphyra* species.

References

[1] Imada Koku (1976) Test on making of dissociant of laver genus (*Porphyra* sp.). *Aquatic Breeding Research Society Record.*, 1: 35~38。

[2] Katayama K. (1983) Studies of mutations of *Porphyra* I : employment of some chemical mutagens. *Bull. Fish. Res. Stn., Okayama Pref.*, 57:51~56.

[3] Katayama K. (1984) Studies of mutations of *Porphyra* II : mutations induced by several chemical mutagens. *Bull. Fish. Res. Stn., Okayama Pref.* 58: 43~49.

[4] Yan X. H., Wang S. J. (1990) Effects of colchicine on growth and development of somatic seedlings of Porphyra haitanensis. *Marine Sciences*, 1: 28~32.

[5] Dai J. X., Zhang Q. Q., Bao Z. M., *et al.* (1990) Studies on the pure culture, mutagenization and interspecific fusion of Porphyra protoplasts. *Oceanologia et Limnologia Sinica*, **21**(3): 293~296.

[6] Yan X. H. (1992) Effects of UV irradiation on the development and variations of protoplast progenies in *Porphyra yezoensis. J. Shanghai Fish. Univ.*, **1**(1-2): 71~78.

[7] Mitman G. G. and J. P. van der Meer. (1994) Meiosis, blade development, and sex determination in *Porphyra purpurea* (Rhodophyta). *J. Phycol.* 30: 147~159.

[8] Zhou H. B., Yuan C. F., Li S. G., *et al.* (1984) Induction Studies of N-Methy-N'-Nitro-N-Nitrosoguanidine on *Enterobacter cloacae. Heredity*, **6**(1): 11~14.

[9] Miura A. and Y. Kunifuji (1980) Genetic analysis of the pigmentation types in the seaweed Susabi-nori (*Porphyra yezoensis*). *Iden (Heredity)*, **34** (9):14~20.

[10] Van der Meer J. P. (1977) Genetics of *Gracilaria* sp. (Rhodophyceae, Gigartinalea). II. The life history and genetic implication of cytokinetic failure during tetraspore formation. *Phycologia* 16: 367~371.

[11] Migita S. and Y. Fugita (1983) Studies on the color mutant types of *Porphyra yezoensis* Ueda, and their experimental culture.*Bull. Fac. Fish. Nagasaki Univ.*, 54: 55~60.

[12] Ma J. H. and A. Miura (1984) Observations of the nuclear division in the conchospores and their germlings in *Porphyra yezoensis* Ueda. Jap. *J. Phycol,*. 32: 373~378.

[13] Burzycki G. M. (1984) New evidence regarding meiosis in the red alga *Porphyra. J. Phycol.*, **20**(suppl.): 4.

[14] Sun A. S., Zeng C. K. (1987) Cytology Studies of *Porphyra*—Nuclear division observation of sporangium and conchospore. *Oceanologia et Limnologia Sinica*, **18**(4): 328~332.

[15] Burzycki G. M. and J. R. Waaland (1987) On the position of meiosis in the life history of *Porphyra torta* (Rhodophyta). *Bot. Mar.* 30: 5~10.

[16] Ohme M. and A. Miura (1988) Tetrad analysis in conchospore germlings of *Porphyra yezoensis* (Rhodophyta, Bangiales). *Plant Sci.*, 57: 135~140.

[17] Tseng C. K. and A. Sun (1989) Studies on the alteration of the nuclear phases and chromosome numbers in the life history of some species of *Porphyra* from China. *Bot. Mar.*, 32: 1~8.

[18] Mitman G. G. and J. P. van der Meer (1994) Meiosis, blade development, and sex determination in *Porphyra purpurea* (Rhodophyta). *J. Phycol.*, 30:147~159.

[19] Van der Meer J. P. (1987) Using genetic markers in phycological research. *Hydrobiologia*, 151/152: 49~56.

Induction Effect and Genetic Analysis of NG to Thallus of *Porphyra**

Xu Pu (许 璞)[1], Shen Songdong (沈颂东)[2], Fei Xiugeng (费修绠)[1], Zhang Xuecheng (张学成)[3], Zhu Jianyi (朱建一)[4]

1 *Institute of Oceanography, Chinese Academy of Sciences, Qingdao* 266071

2 *Life Sciences College, Suzhou University, Suzhou* 215006

3 *Marine Life Sciences College, Qingdao Ocean University, Qingdao* 266003

4 *Jiangsu Institute of Marine Fisheries, Nantong* 226007

Abstract The young thalli of *Porphyra yezoensis* and *P.haitanensis* are induced by N-Methy-N'-Nitro-N-Nitrosoguanidine (NG), a strong mutagen to induce the mutant of chromatophore. It is showed that no mutants have been investigated in all control groups, while in the induced groups, it is easy to find mutant cells or mutant cell masses in the thallus. The pigmentation mutants may be the result of NG inducement. The mutant rate increases obviously with the mutagen concentration or by prolonging the induction time. Within the scope of experiment, the inducement effects of *Porphyra yezoensis* are raised from 11.2% to 28.7%, and those of *P. haitanensis* from 10.1% to 20.2%. According to our experiments, the amount of mutant cells in the same area does not increase with the induction intensity The amount of mutant cells in every group of inducement of both species of *Porphyra* changes very little with the fixed fields check method. The lowest dose (25 μ g/mL) of this experiment has a high mutant rate. The mutant rate shows the percentage of mutant cells in all the survived cells, while the amount of mutant cells reflects the effect of inducement. Thus the optimum induction concentration of NG is 25 μ g/mL, and the optimum induction time is 30 minutes.

Keywords *Porphyra*, Mutant of chromatophore, N-Methy-N'-Nitro-N-Nitrosoguanidine (NG), thallus, Induction, Genetic analysis

1 Introduction

Pigmentation mutants in *Porphyra* have been noticed as early as the 1970s (Miura *et al.*, 1974[1]; Aruga, 1974[2]; Miura, 1976, 1977[3-4]). At first they are observed in the cultivated populations, first in *Porphyra yezoensis*, then in *Porphyra tenera*. Two kinds of thalli different in color can be easily distinguished. They are called the red-type and green-type, respectively. Miura *et al.* (1974)[1] reported that the red thalli in the culture population are spontaneous pigmentation mutants, and has heredity, while the green thallus is still a kind of wild type. A lot of color mutation occurs in chimeras. Pigmentation mutants in *Porphyra tenera* show the same tendency, and the frequency of chimeras varies with the cultivation method.

Apart from the red and green type mutants, crosses between the mutants of red and green type yield

Received on April 18, 2002

* Supported by NSFC (C39770593), EMBLC, CAS and Applied Fundamental Project of Jiangsu Province (BJ95182) National Key Fundamental Research Program (G1999012009).

the yellow type, and crosses between the mutants of red and yellow type yield the orange type (Miura, 1978[5]; Migita *et al.*, 1983[6]). Miura(1985)[7] obtained light-red, light-green and light-yellow type mutants. Niwa*et al.* (1993)[8] reported purple type and a new pigmentation mutant. All these newly observed pigmentation mutants occur in laboratory or spontaneously, and all are recessive nuclear genes mutants.

Inducing treatment is expected to yield mutants in *Porphyra.* Katayama (1980, 1984)[9~10] examined the inducing effects of varied chemical mutagens on *Porphyra yezoensis* and obtained red and green color young gametophytes blades.Yan and Wang (1990)[11] treated the vegetative cells of *Porphyra haitanensis* with colchicine and obtained some deeper color mutants. Yan X. H. (1992)[12] treated the protoplasts of *Porphyra yezoensis* with X-rays and obtained some regenerated pure red-color mutants. In the genetic analysis of *Porphyra purpurea*, using NG as mutagen, Mitman *et al.*(1994)[13] obtained 5 types of color mutants, which were the yellow, red, green and two pink-color types. Among these mutants, the yellow and red types and one pink type are nuclear mutants, while the other two types are cytoplasm mutants.

It is very common that the blade color of *Porphyra* varies with age and culture conditions. How to distinguish the periphery pigmentation mutants from the wild type blades? Or what is the stable character of pigmentation mutants? Aruga *et al.* (1984)[14], Kato*et al.* (1984)[15] and Niwa *et al.* (1993)[8] examined the absorption spectra and pigment contents of the five color mutants (red, green, yellow, orange and purple) under the same culture conditions in laboratory. Results show that these pigmentation mutants have steady characters of their own. Kikuchi *et al.* (1979)[16] studied the phycobiliprotein of 3 mutants and the wild type strain of *Porphyra yezoensis,* and found that phycobiliprotein showed distinct characters in each pigmentation mutant. Similar results have been reported in other studies.

In the present study thalli of *Porphyra yezoensis*and *P. haitanensis* are treated with NG. After the treatment, varied pigmentation mutants are examined and counted. The research will not only provide important evidence for *Porphyra* genetics study, but also improve *Porphyra* cultivars and breeding technique.

2 Materials and methods

2.1 Materials

Porphyra yezoensis and *Porphyra haitanensis* are used in the present study. Fronds of *Porphyra yezoensis* are collected from the semi-floating rafts on the coast of Rudong county, Jiangsu Province. *Porphyra haitanensis* is collected from the natural population growing on reefs of Nanri Island in Putian county, Fujian Province.

2.2 Mutagen compounding

N-Methy-N'-Nitro-N-Nitrosoguanidine (NG) made in Sweden is used as mutagen in the present study. Dissolve the accurately weighed NG in formamide (Zhou H. B. *et al.*1984)[17], then dilute the solution with sterilized seawater to make up stocking solution to a concentration of 1 000 μg / mL. Working solutions are then diluted from the stocking solution with sterilized seawater according to experiment design.

2.3 Inducing treatment

2.3.1 Mutagen concentration and treatment time

The concentration of treatment medium is 0, 25, 50, and 100 μg / mL, respectively. A seawater medium is used as the control. The treatment time is 0, 30, 60, and 120 minutes, respectively.

2.3.2 Inducing treatment

Young blades of about 1cm in size are selected and kept in the open air for 30 minutes. 10 blades are allocated to each treatment and stirred at 20 ℃ . After being treated for designed time the experimental materials are collected by net, washed with flowing sterilized seawater for 3minutes, then are placed into triangle flasks or glass containers for incubation. In the first three days the culture medium is changed twice a day, in the morning and evening respectively. Then the induced materials are transferred to PES culture medium and cultured with aeration at 70~80umol photons $m^{-2}s^{-1}$ (12L: 12D). The cultivation temperature varies according to species, *Porphyra yezoensis* is cultured at 12~15℃ and *Porphyra haitanensis* at 17~20℃.

2.4 Mutation accounting

After 2 weeks of cultivation 3 young blades are randomly taken out from each treatment and examined under a microscope at 15 × 20. Each blade is examined for 10 visions, so each treatment has 30 visions tested in total. The number of survival cells and mutated cells are recorded. Examination and microscopic photography are done under Olympus-BH microscope. The mutation frequency is calculated as follows:

Mutation frequency = Mutated cell numbers/survival cell numbers.

3 Results

3.1 Mutation frequency of thallus

Vigorously growing young thalli of about 1cm are used in the present study. After treatment with mutagen, mutated cells of varied colors and mutated sectors of varied sizes (or consisting of different numbers of mutated cells) are formed on the thalli. Inducing results of *Porphyra yezoensis* and *Porphyra haitanensis* are summarized in Fig. 1 and Fig. 2. The results show that :(*i*) No mutation occurs in all of the control groups, while mutated cells or cell sectors can be easily observed in each treatmentunder the same conditions, which indicates that the mutation observed results from induction. (*ii*) Mutation frequency rises with the increasing of mutagen concentration and treating time. In the tested ranges, with the increasing of inducing intensity mutation frequency of *Porphyra yezoensis* is raised from 11.2% to 28.7%, and that of *P. haitanensis* rises from 10.1 % to 20.2 %. (*iii*) On the thalli of the same size mutated cell numbers do not increase with inducing intensity. Mutated cell numbers of the two species are similar in each treatment. Much higher mutation frequency occurs in the lowest doses of treatment. Since mutation frequency represents the ratio of mutated cells to survival cells, therefore mutated cell numbers on a certain area of thalli reflects the inducing effects in the present study. Treatment with 25 μg/mL NG for 30minutes may be considered optimum.

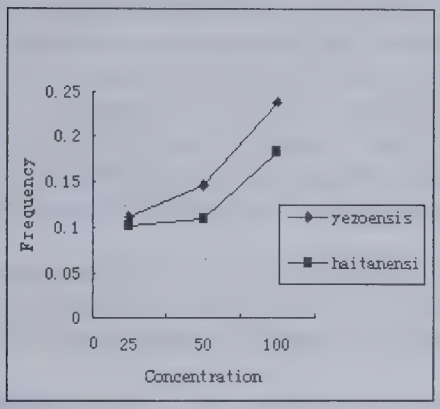

Fig. 1 Inducement effect of NG concentration to thallus cells of *Porphyra*

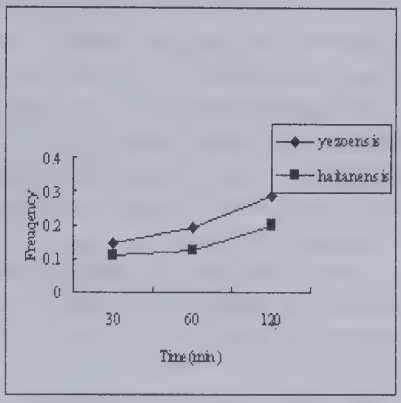

Fig. 2 Inducement effect of NG treating time to thallus cells of *Porphyra*

3.2 Growth and development of induced thalli

After a week of cultivation some cells of lighter color appear on the induced thalli. Some linked or sectored discolored cells are dead because of induction, which occurs much more often in the treatment

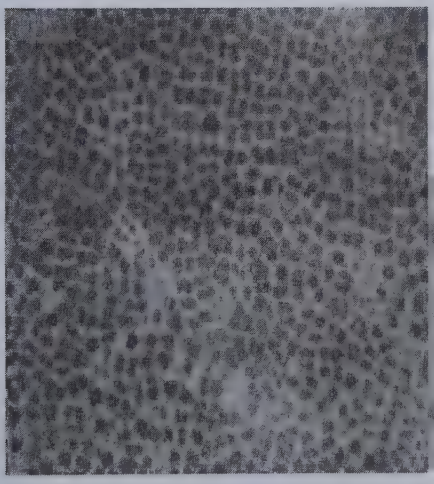

Fig. 3 Pigment mutants of adult thallus

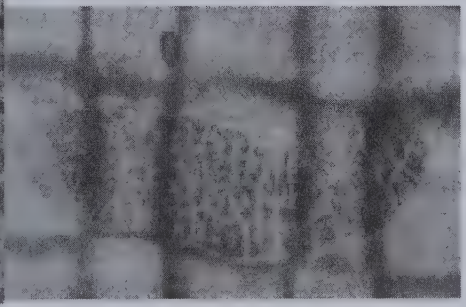

Fig. 4 Pigment chimaeras of young thallus

of higher concentration and longer time. Most of the single dotted cells survive and their star chromosomes are still clear and distinctive. Later on the colors of these single survived cells begin to change and show some mutation characters. The green and red color mutations are distinguishable at the early stage, while the yellow, brown and purple color mutations are distinguishable after cell divisions, when it is obviously controllable to the periphery wild type cells. With the division and growth of these mutated cells some mutated sectors appear on the blades. These mutated sectors vary in shapes and sizes, but consist of cells of the same shape and color. One sector represents one mutated color, which indicates that each sector is formed by mutated cells of the same type and results from one mutation of one mutated cell.(Fig. 3)

To test the results illustrated above we select young blades of 4~10 cells for further induction and observation. It' s found that a lot of heterozygous cell chimeras appear on these blades. The total number of chimeras is no more than the original cell number of the blade. Each chimera consists of the same kind of cells.(Fig.4)

Thus it can be concluded that mutation occurs on single vegetative cells of *Porphyra* gametophytic blade after inducing treatment. One mutated cell can develop into one kind of mutated tissue, and several different mutated cells can form several kinds of mutated tissues. Mutation usually produces a lot of heterozygous chimera blades.

4 Discussion

4.1 Application of pigmentation mutants in cellular culture and protoplast fusion

Some valuable results have been achieved in the application study of pigmentation mutants in the cell culture and protoplast fusion of *Porphyra*. Fugita *et al.* (1987)[18] isolated a heterozygous protoplast from the green and wild type mutants of *Porphyra yezoensis*. The protoplast develops into callus-like after cultivation. A lot of irregular chimeras of the green and purple-red color sectors occur on the blades regenerated from these calli-like. The conchocelis developed from these matured thalli appear green in color. Most of the F1 gametophytic blades they yield are green in color, others are purple-red in the basal part and green in the other part of blade. Araki(1987, 1993)[19-20] studied protoplast fusion between *Porphyra tenera* and *Porphyra yezoensis*, and obtained heterozygous fusion cells using green type *Porphyra tenera* as a marker. In the blades regenerated from calli-like appear wild type, green type and chimeras of the wild and green color type. Most monospores released from green type blades germinate and develop into the wild and green type chimeras. Iwabuchi (1995)[21] obtained wild type protoplasts from digested culture blades. The protoplasts develop into thalli of 15cm long after a period of cultivation. 200 blades are examined, among which 6 blades are pigmentation mutants, including 4 blades of single red-color mutants and 2 blades of red and wild type chimeras. Red color cell sectors of varied sizes irregularly distribute among the wild type sectors on these chimeras.

In the studies discussed above the authors do not describe the genetics character of materials used and whether the color mutation is nuclear or cytoplasm. A common point of their observations is that mutations appearing in their cultivars all correlate to the formation and isolation of calli, which may indicate a special genetic transmission process.

4.2 Pigmentation mutants and *Porphyra* genetics breeding

Studies of cross pigmentation mutants show that new recombinant phenotypes may be produced by chromosome exchanging during meiosis process of *Porphyra*. Miura *et al.* (1989)[22] has developed an important breeding technique from crosses between pigmentation mutants. Crosses between the red and green pigmentation mutants are performed and F1 gametophytic blades are obtained after cultivation. Recombinant wild type tissues with remarkable growth potential and deeper color are isolated from 2-color and 4-color chimeras that do not bear two parental color phenotypes. The isolated recombinant wild type tissues are co-cultured and yielded storing strains after maturation, which are called ZGRW. New strains of ZGRW show remarkable superiority in growth rate, production and blade quality (including contents of chlorophylla and phycocyanin). This is the first successful record of applying genetic recombinant technique in *Porphyra* breeding.

References

[1] Miura A., Y. Aruga and M. Fuseya (1974) Thremmatological studies of the cultivated *Porphyra* II. Effect of selection on the form and color of folise thalli in *Porphyra yezoensis* form narawaensis. *Nippon Suisan Gakkai*, 1974 Spring Annual Meeting Abstract: 93.

[2] Aruga Y. (1974) Color of the cultivated *Porphyra*. *W. Kushitachi on Nori Kenkyu*, 23:1~14.

[3] Miura A. (1976) Genetic studies of cultivated *Porphyra* (Nori) improvement. *Mar. Sci.* 8: 15~21.

[4] Miura A. (1977) Chimera variegation found in *Porphyra*. *J. Phycol.*, **13**(suppl): 45.

[5] Miura A. (1978) Color variants and heredity of color in *Porphyra*. *Iden (Heredity)*, 32:11~16.

[6] Migita S. and Y. Fugita (1983) Studies on the color mutant types of *Porphyra yezoensis* Ueda, and their experimental culture. *Bull. Fac. Fish. Nagasaki Univ.*, 54: 55~60.

[7] Miura A. (1985) Genetic analysis of variant color types of light red, light green and light yellow phenotypes of *Porphyra yezoensis* (Rhodophyta, Bangiaceae). pp.270 284. In: H Hara (ed). Origin and evolution of diversity in plant and plant communities. *Academia Scientific Book Inc.*, Tokyo.

[8] Niwa K., A. Miura, J. A. Shin and Y. Aruga (1993) Characterization and genetic analysis of the violet type pigmentation mutant of *Porphyra yezoensis* Ueda (Bangiales, Rhodophyta). *Korean J. Phycol.*, **8**(2): 217-230.

[9] Katayama K. (1983) Studies of mutations of *Porphyra* I : employment of some chemical mutagens.*Bull. Fish. Res. Stn.*, Okayama Pref.., 57:51~56.

[10] Katayama K. (1984) Studies of mutations of *Porphyra* II : mutations induced by several chemical mutagens.*B ull. Fish. Res. Stn.* Okayama Pref.., 58:43~49.

[11] Yan X. H., Wang S. J. (1990) Effects of colchicine on growth and development of somatic seedlings of Porphyra haitanensis. *Marine Sciences*, 1: 28~32.

[12] Yan X. H. (1992) Effects of UV irradiation on the development and variations of protoplast progenies in *Porphyra yezoensis*. *J. Shanghai Fish. Univ.*, **1**(1-2): 71~78.

[13] Mitman G. G. and J. P. van der Meer (1994) Meiosis, blade development, and sex determination in *Porphyra purpurea* (Rhodophyta). *J. Phycol.*, 30:147~159.

[14] Aruga Y. and A. Miura (1984) In vivo absorption and pigment contents of the two types of color mutants of *Porphyra*. *Jap. J. Phycol.*, 32: 243~250.

[15] Kato M. and Y. Aruga (1984) Comparative studies on the growth and photosynthesis of the pigmentation mutants of *Porphyra yezoensis* in laboratory culture. *Jap. J. Phycol.*, 32: 333~347.

[16] Kikuchi R., K. Ashida and S. hirao (1979) Phycobil different color types of *Porphyra yezoensis*. *Bull. Jap.*

Soc. Sci. Fish, 45:1461~1464.

[17] Zhou H. B., Yuan C. F., Li S. G., *et al.* (1984) Induction Studies of N-Methy-N'-Nitro- N-Nitrosoguanidine on *Enterobacter cloacae. Heredity,* **6**(1): 11~14.

[18] Fugita Y. and S. Migita (1987) Fusion of protoplasts from thalli of two different color types of *Porphyra yezoensis* Ueda and development of fusion products. *Jap. J. Phycol.*, 35: 201~208.

[19] Araki T., T. Aoki and M Kitamikado (1987) Preparation and regeneration of protoplasts from wild type of *Porphyra yezoensis* and a green variant mutant of P. tenera. *Bull. Jap. Soc. Sci. Fish.*, 53:1623~1627.

[20] Araki T. (1993) Isolation and regeneration of protoplast in the genus *Porphyra. Kaiyo*, 25: 696~703.

[21] Iwabuchi (1995) Color mutant in regenerated thalli of isolated protoplasts from *Porphyra yezoensis. Bull. Fukuoka Fish. Mar. Technol. Res. Cent.*, 4: 57~58.

[22] Miura A. and J. A. Shin (1989) Crossbreeding in cultivars of *Porphyra yezoensis* (Bangiales, Rhodophyta) preliminary report. *Korean J. Phycol.*, 4: 207~211.

Cloning and Structural Analysis of Calmodulin Gene from the Mangrove Plant *Sonneratia Paracaseolaris**

Xiong Lingyuan (熊玲媛), Lin Tao (林 涛), Zhou Hantao (周涵韬), Xu Jinsen (徐金森), Ge Yunsheng (葛运生), Chen Muchuan (陈睦传), Chen Liang (陈 亮)
School of Life Sciences / The Key Laboratory of the Ministry of Education for Cell Biology and Tumor Cell Engineering, Xiamen University, Xiamen 361005

Abstract Calmodulin is a calcium binding protein that modulates the activity of diverse groups of protein including some protein kinase, adenylate cyclases and ATPase. Here we use the total DNA of *Sonneratia paracaseolaris* as the template of the polymerase chain reaction (PCR). The PCR primers have been designed and synthesized according to the 5-and 3-terminal oligonucleotide sequences of Calmodulin gene of plants in Genbank and ligated with cloning vector pBsk(+).The recombinant clones have been obtained from the selected medium. The results of DNA sequences analysis show that the nucleotide sequences of ORF share more than 85% homologies as compared with those of calmodulin genes of several other plants.Similar to rice and apple, the ORF is interrupted by an intron behind the 75th nucleotide.

Keywords *Sonneratia paracaseolaris*, calmodulin gene, polymerase chain reaction (PCR)

In 1967, Ebashi *et al.* first pointed out that there exists a calcium-binding protein which can transmit calcium signals. Then Cheung found a kind of phophodiesterases which can bind with calcium. Further studies have indicated the protein also has functions of activating adenylate cyclases, calcium-depended ATPase, protein kinases. Cheung denominated it Calmodulin. Now calmodulin is known to mediate many biological processes including: regulating enzyme activity, cell division and differentiation, movement of cell skeleton and cell, cell secreting, modulation of osmosis, photosynthesis, pollen bourgeoning, reaction of hormone, intranuclear enzyme system, gene expression, and so on. The experiment proved Calmodulin also mediates the signal thansduction induced by salinity stress. Using TCH-1 of Arabidopsis as probe, Botella and Arteda(1994) isolated two CaM cDNA (MBCaM-1 and MBCaM-2) from sainfoin cDNA gene library. When the plant is under salinity stress, the expression level of MBCaM-1 increases after 2 hours, and gets to the maximum level after 4 hours, while the level of MBCaM-2 doesn' t change all time. Because of its important function, Camodulin gets more and more attention.Many calmodulin genes in animal, epiphyte andprotozoan have been isolated and cloned. Calmodulin genes in barley, pea, sugarcane, rice, maize, potato, capsicum and yeast have been cloned too. They share high homologies as compared with those of Calmodulin genes of animals. *Sonneratia paracaseolaris*, a kind of mangrove plant occurring primarily in the tropical regions around the world, survives under envonmental stress due to high saline conditions and has adapted itself to it. So

Received on June 6, 2002
*Supported by the national science and technology ministry plant transgenic and industrialization foundation of China (J00-B-14), the foundation of Key Laboratory of halobios engineering, SOA

it is very important to isolate and clone calmodulin gene of it and study the role of the calcium signal system in its salinity tolerant process.

1 Materials and methods

1.1 Materials

The leaves of *Sonneratia paracaseolaris* have been collected fom Dongzhai Harbour Mangrove Reserve in Hainan. Escherichia coli DH 5α and pBsk(+) are kept in our laboratory.

1.2 Reagent

Restriction endonucleases Bam HI and EcoR I, T4 DNA ligase, PCR amplifying kit and gel extraction mini kit have been purchased from Sangon Biotech (Shanghai, China). The other reagents are all analytic pure. Primers are synthesized by Sangon Biotech.

1.3 Total DNA extraction

Total DNA is extracted from *Sonneratia paracaseolaris* leaves by using the CTAB method.

1.4 PCR amplifying

The PCR primers have been designed and synthesized according to the 5' -ahd 3' -terminal oligo nucleotide sequences of Calmodulin gene of plants in Genbank, the sequences are:

5' - terminal: 5' -GCGCGAATTCGGCATGGCGGATCCGCTCACCGAC-3'
3' - terminal: 5' -GGCCGGATCCTCCCATGGCCATCATGACCTTGA-3'

The underlined indicates restriction endonucleases Bam HI and EcoR I site.

PCR is amplified using the total DNA of S. *paracaseolaris* as the template. The thermal cycling parameters are: 94℃ for 45s, 55℃ for 1 min, 72℃ for 1 min, 35 times, and a final 72℃ for 10 min. Then it is kept in 4℃.

1.5 Cloning of PCR production

After being detected by agarose gel electrophoresis, the PCR reaction mixtures are deposited and extracted with 1/10 V 3 mol/dm^3 NaOAc (pH=5.2) and 2V absolute alcohol. The PCR production and the plasmid pBsk(+) are digested with EcoR I and Bam HI and purified with gel extraction mini kit and ligated with each other by T4 DNA ligase. Then transfer them to Escherichia coli DH 5α : Take 5mm^3 ligation, mix it with 40 mm^3 Escherichia coli DH 5α .Incubate it on ice for 30 min. Then heat activate it for 90s at 42℃, cool it down on ice for 2 min. Transfer all bacteria to 360 mm^3 of LB medium and incubate it at 37℃ for 1 h. Spread 100 mm^3 to LB agar plate (with AMP and X-gal). Incubate it at 37℃ overnight.

1.6 Screening colonies

Choose colonies containing recombinant by white selection from the selected media. Extract plasmid DNA by Alkaline lysis with SDS and detect it by PCR amplifying and digesting with restriction endonucleases. Screen out colonies with the target DNA to sequence and analyze the result with Blast software.

2 Results and analysis

2.1 PCR amplifying of Calmodulin gene

Using purified total DNA of *S. paracaseolaris* as template, after PCR amplifying for 35 cycles, we have got a DNA fragment of about 1.3kb (Fig. 1A).

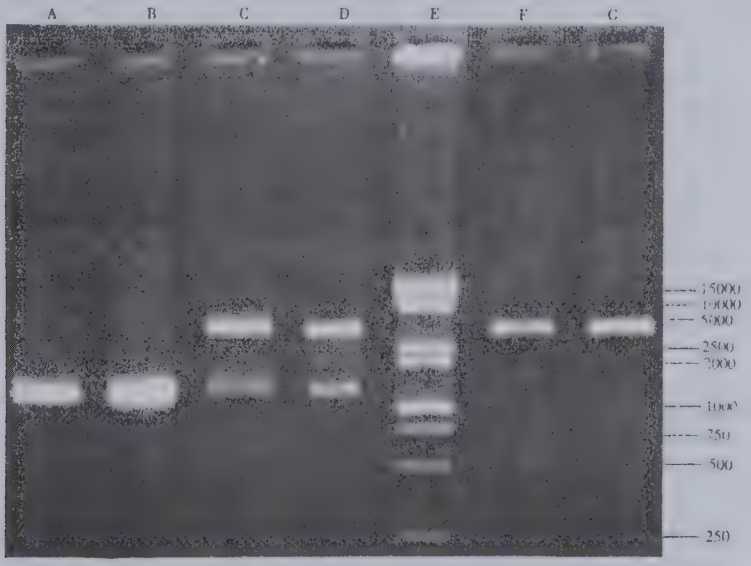

Fig. 1 Agarose gel electrophoresis of PCR product and pBsk(+)

A. PCR production of total DNA B. PCR production of pBsk(+)-CaM
C, D. pBsk(+)-CaM /EcoRI+BamHI E. DNA marker 2 000-15 000.
F. pBsk(+)/EcoR I. G. pBsK(+)/EcoRI+BamHI

2.2 Cloning of PCR production and screening of recombinant

Purify the 1.3kb DNA PCR production after digested with restriction endonucleases EcoR I and Bam HI. Then ligate them with pBsk(+) which is treated in the same way. Introduce it to Escherichia coli DH 5 α . Screen 12 white colonies from LB agar plate (with AMP and X-gal). Detect them by PCR amplified and digested with restriction endonucleases. The result shows that eight of them have been cut into two fragments after being treated with EcoR I and Bam HI. One has the same weight as the vector and the other just has the same weight as PCR production which is approximate to 1.3kb (Fig. 1 C, D). So the eight colonies might be the recombinant with the target DNA. Select one of them to sequence. The result is showed in Fig. 2.

GGCATGGCGGATCCGCTCACCGA CGACCAGATCTCCGAGTTCAAGGAG
GCCTTCAGCCTCTTCGACAAGGACGGAGACG*GTCTCTCTCTCTCTCTC*
TCGCTATCAGATCTCCCCTTTTCTTACCCACAATGTTTCGTTCTGATTTTCAA
TTCTGAGATCACATACTTCTGATGCTGTTTTCTAATCACGGTGGTGATGTCT
CGGTCGTTGTCCTGTCGTTGCTAATATTCATCGCATTGTTGATCAGCGGCTT
CGTCTAGTGTTTATCGTATTTATGGCTTTTGTCTTCGGTTCTTAAGCTAAGGT
AACGCGGTTTGTGATTCATTGTTTGTGCTGTATTCCCTTTGATCTCATCTGCT
GGGATCTATTTAAGCATTGCGTGCTCTCCGATTTCATCTCATTGTTTTTTTTT
GGGGGGGCCATTTTGGCAACTCTTTTGTTGTTCTGATTGCAGTTGCTCTAG
CATTAGGATATCCTTGACTTGCACGTTTGGTGTTAAGATTTATTTTCCTAGCT
TACTGTTATTTCGATTATTTCAAGATAAAGATATCTGCGTCCTATTAGTTTTAT
GTTGGACTCTTTGAAGGTGAAACCCATGTCCCAGTATTTAGCAGCGGTTTTA
CCTGCAATTGTTGGTACCCCTCTGTTTAAATCATTTGGGGTTCATGAATTTC
CTTTAGCTTCTCCCTGTCAATCCCATCATTAAATCGGTGATTAACACAGTCC
TTTCTGCTCTTCCCTGAATTTTTGTAAATGGATATAATCTCTTCCTGGACCTG
GAGGTGAAGATGATGGCATGTGAAATGTACAGTAAATGGATATACGTATCAT
GTTTCTCCTTCATTAGTCCAGGGAATCTTCGATTTCACGTTCAGCGCCTTAT
TGATGGTGTTTCTTTTTTCCAAACTATATATCTACAG GTTCCATCACAACCA
AGGAGCTTGGAACTGTTATGCGGTCACTGGGGCAGAACCCAACGGAGG
CAGAGCTTCAGGACATGATCAATGAGGTTGATGCTGACGGTAACGGTA
CCATCGATTTCCCAGAGTTTCTTAACCTGATGGCTAGGAAGATGAAGGA
CACTGACTCGGAGGAAGAGCTCAAGGAAGCTTTCCGAGCTTTCGACAA
GGACCAAAATGGCTTGATTTCTGCTGCTGCTGAGCTTCGCCATCTCATG
ACAAACCTCGGTGAGAAGTTGACCGATGAGGAAGTTGATGAGATGATC
CGAGAAGCTGATGTGGATGGTGATGGCCAGATCAACTATGATGAGTTCG
TCAAGGTCATGATGGCCATGGGA

Fig. 2 Nucleotide sequence of S.caseolaroids calmodulin gene
The underlined part indicates primer, and the italicized part indicates intron.

2.3 Analyzing the PCR amplifying DNA sequence

The results of DNA sequences analysis show that the DNA fragment is 1299bp including an intron of 844bp nucleotide and located behind the 75th nucleotide of the ORF (Fig. 2, italic). ORFof it includes 453bp nucleotide. the nucleotide sequences of ORF share more than 85% homologies as compared with those of calmodulin genes of several other plants such as bean, barley, rice, maize, tobacco, and Arabidopsis thanliana (Fig. 3). Its encoding amino acid sequences share more than 95% homologies as compared with those plants.

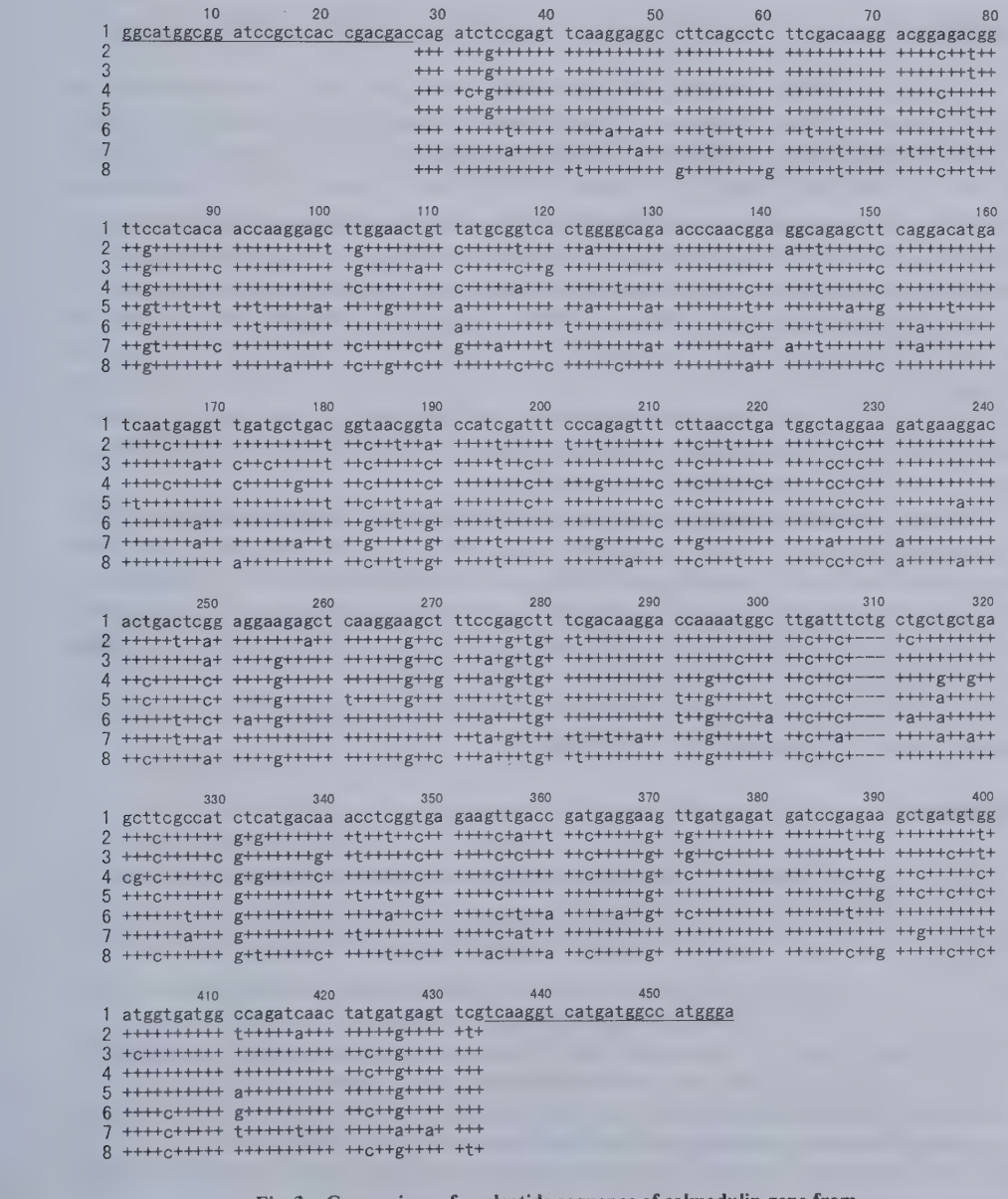
10 20 30 40 50 60 70 80
1 ggcatggcgg atccgctcac cgacgaccag atctccgagt tcaaggaggc cttcagcctc ttcgacaagg acggagacgg
2 +++ +++g++++++ ++++++++++ ++++++++++ ++++++++++ ++++c++t++
3 +++ +++g++++++ ++++++++++ ++++++++++ ++++++++++ +++++++t++
4 +++ +c+g++++++ ++++++++++ ++++++++++ ++++++++++ ++++c++++
5 +++ +++g++++++ ++++++++++ ++++++++++ ++++++++++ ++++c++t++
6 +++ +++++t++++ ++++a++a++ +++t++t+++ ++t++t++++ +++++++t++
7 +++ +++++a++++ +++++++a++ +++t+++++ +++++t++++ +t++t++t++
8 +++ ++++++++++ +t++++++++ g++++++++g ++++++t++++ ++++c++t++
90 100 110 120 130 140 150 160
1 ttccatcaca accaaggagc ttggaactgt tatgcggtca ctggggcaga acccaacgga ggcagagctt caggacatga
2 ++g+++++++ ++++++++++ +g++++++++ c++++++++ ++a+++++++ ++++++++++ a++t+++++c ++++++++++
3 ++g++++++c ++++++++++ +g++++++a++ c++++++c++g ++++++++++ ++++++++++ +++t+++++c ++++++++++
4 ++g+++++++ ++++++++++ +c++++++++ c++++++a+++ ++++++t++++ +++++++c++ +++t++++++c ++++++++++
5 ++gt+++t++t ++t+++++a+ ++++g++++ a++++++++ ++a+++++a+ +++++++t++ ++++++a++g ++++++t++++
6 ++g+++++++ ++t++++++ ++++++++++ a++++++++ t++++++++ +++++++c++ +++t++++++ ++a+++++++
7 ++gt+++++c ++++++++++ +c++++++c++ g+++a+++++t ++++++++a+ +++++++a++ a++t++++++ ++a+++++++
8 ++g+++++++ +++++a++++ +c++g++c++ ++++++c++c +++++c++++ +++++++a++ ++++++++++ ++++++++++
170 180 190 200 210 220 230 240
1 tcaatgaggt tgatgctgac ggtaacggta ccatcgattt cccagagttt cttaacctga tggctaggaa gatgaaggac
2 ++++c+++++ +++++++++t ++c++t++a+ ++++t+++++ t++t++++++ ++c++t++++ +++++c+c++ ++++++++++
3 +++++++a++ c++c+++++t ++c+++++c+ +++++t++c++ ++++++++++ ++c+++++++ +++++cc+c++ ++++++++++
4 ++++c+++++ c+++++g+++ ++c+++++c+ +++++++c++ +++g+++++c ++c+++++c+ ++++cc+c++ ++++++++++
5 +t++++++++ +++++++++t ++c++t++a+ +++++++c++ +++++++++c ++c+++++++ +++++c+c++ ++++++a+++
6 +++++++a++ ++++++++++ ++g++t++g+ ++++t+++++ +++++++++c ++++++++++ +++++c+c++ ++++++++++
7 +++++++a++ +++++++a++t ++g+++++g+ ++++t+++++ +++g+++++c ++g+++++++ ++++a+++++ a++++++++
8 ++++++++++ a++++++++ ++c++t++g+ ++++t+++++ ++++++a+++ ++c+++t+++ ++++cc+c++ a+++++a+++
250 260 270 280 290 300 310 320
1 actgactcgg aggaagagct caaggaagct ttccgagctt tcgacaagga ccaaaatggc ttgatttctg ctgctgctga
2 +++++t++a+ +++++++a++ ++++++g++c +++++g+tg+ +t++++++++ ++++++++++ ++c++c+--- +c++++++++
3 ++++++++a+ ++++g+++++ ++++++g++c +++a+g+tg+ ++++++++++ ++++++c+++ ++c++c+--- ++++++++++
4 ++c+++++c+ ++++g+++++ ++++++g++g +++a+g+tg+ ++++++++++ +++g++c+++ ++c++c+--- ++++g++g++
5 ++c+++++c+ ++++g+++++ t+++++g+++ +++++t+tg+ ++++++++++ t++g++++++ ++c++c+--- ++++a+++++
6 +++++t++c+ +a++g+++++ ++++++++++ +++a+++tg+ ++++++++++ t++g++c++a ++c++c+--- +a++a+++++
7 +++++t++a+ ++++++++++ ++++++++++ ++ta+g+t++ +t++t++a++ +++g++++++ ++c++a+--- ++++a++a++
8 ++c+++++a+ ++++g+++++ ++++++g++c +++a+++tg+ +t++++++++ +++g++++++ ++c++c+--- ++++++++++
330 340 350 360 370 380 390 400
1 gcttcgccat ctcatgacaa acctcggtga gaagttgacc gatgaggaag ttgatgagat gatccgagaa gctgatgtgg
2 +++c++++++ g+g+++++++ +t++t++c++ ++++c+a++t ++c+++++g+ +g++++++++ ++++++t++g ++++++++t+
3 +++c+++++c g+++++++g+ +t++++++c++ ++++c+c+++ ++c+++++g+ +g++c+++++ +++++++t+++ +++++c++t+
4 cg+c+++++c g+g+++++c+ +++++++c++ ++++c+++++ ++c+++++g+ +c++++++++ ++++++c++g ++c+++++c+
5 +++c++++++ g+++++++++ +t++t++g++ ++++c+++++ ++++++++g+ ++++++++++ ++++++c++g ++c++c++c+
6 ++++++t+++ g+++++++++ ++++a++c++ ++++c+t++a +++++a++g+ +c++++++++ ++++++t+++ ++++++++++
7 ++++++a+++ g+++++++++ +t++++++++ ++++c+at++ ++++++++++ ++++++++++ ++++++++++ ++g+++++t+
8 +++c++++++ g+t+++++c+ ++++t++c++ +++ac++++a ++c+++++g+ ++++++++++ ++++++c++g +++++c++c+
410 420 430 440 450
1 atggtgatgg ccagatcaac tatgatgagt tcgtcaaggt catgatggcc atggga
2 ++++++++++ t+++++a+++ +++++g++++ +t+
3 +c++++++++ ++++++++++ ++c++g++++ +++
4 ++++++++++ ++++++++++ ++c++g++++ +++
5 ++++++++++ a+++++++++ +++++g++++ +++
6 ++++c+++++ g+++++++++ ++c++g++++ +++
7 ++++c+++++ t++++++t+++ +++++a++a+ +++
8 ++++c+++++ ++++++++++ ++c++g++++ +t+

Fig. 3 Comparison of nucleotide sequence of calmodulin gene from *Sonneratia paracaseolaris* and other plants

1, 2, 3, 4, 5, 6, 7, 8 indicate nucleotide sequence of *S. paracaseolaris*, rice, barley, maize, soybean, tobacco, Arabidopsis and lily calmodulin gene respectively. + indicates the identical sequence with the first row. PCR primers are indicated by the underlined part.

3 Discussion

Calmodulin, a highly conserved and ubiquitous protein in eukaryotes, plays a very important role in life. The mutant of it is fatal. Camparing Calmodulin amino acid sequences of spinach are compared with those of Triticum, Alfalfa, potato and Arabidopsis, and the results show they share high homologies (For Triticum, Alfalfa, and Arabidopsis, it is about 97 %~99 %, and for potato, 92 %). It is indicated that its highly conserved among endogen and dicotyledon. The amino acid sequences derived from plants calmodulin cDNA also share high homologies as compared with those of mouse calmodulin cDNA. It seems that it's conserved between animals and plants. Present study has showed that there exists isoform of calmodulin DNA. In Arabidopsis exist three isoforms of ACaM-1, ACaM-2, and AcaM-3. There are some differences among their nucleatide sequences (86 % homologies). ACaM-2 and ACaM-3 encodes the same protein. This protein is different from ACaM-1 on the conserved site out of calcium-binding domain. There are also differences in the expression of the three genes. In the roots only ACaM-1 mRNA has been dectected. It indicates ACaM-1 can express normally while ACaM-2 and ACaM-3 don't express or express little. The significance awaits further study.

In AcaM-3, the ORF is interrupted by an intron located behind the 75th nucleotide. Similarly, from rice, two Calmodulin genes (CaM-1, CaM-2) have been isolated. The amino acids derived from them share high homologies. Only one amino acid (139th) has been substituted between the two isoforms. In CaM-1 exists an intron of 1 400 bp, and in CaM-2, 770 bp. They both locate behind the 75th amino acid. Similarly, there is a 860 bp intron behind the 75th amino acid in apple. There are 5 introns in calmodulin gene of Chlamydomonas. The first of them is behind the 75th amino acid. Our results are similar to it too. It is obvious that the location of intron in the higher plants is conserved. But the biological role of the intron in calmodulin gene expression is still unknown.

References

[1] Cheung W. Y. (1967) Cyclic 3, 5-nucleotide phosphodiesterase pronounced stimulation by snake venom. [J]. *Biochem. Biophy. Res. Commu.*, 29: 478~482.

[2] Wang Zhaohui, Sun Dayc (1997). Advances of the studies on plant calmodulin. *Chinese bulletin of Botany.*, **14** (1): 1~7.

[3] Griess E. A., Igloi GL., Feix G. (1989). Isolation and sequences encoding the calcium-banding protein, calmodulin,from barley (Hordeum vulgare L). *Plant Physiol.*, 90 : 714~719.

[4] Yao Jin, Cao Xiao feng, Liu Zhi hua, *et al.* (1994). Cloning of calmodulin gene of Pea (Pisum Sativum) by PCR and comparison of its coding sequences in different speices. *Acta Botanica sinica.*, **36** (2): 81~86.

[5] Lin Junfang, Chen Rukai, Jin Zhiqiang, *et al.* (1993).Amplification of Calmodulin gene of Sugarcane by polymerase chain reaction and its sequence analysis. *Acta Agronomica Sinica*, **9** (4): 309~313.

[6] Liu zhihua, Wu Xiangyu, Pan Naisui, *et al.* (1994) Cloning and structural analysis of calmodulin gene from Rice, **24** (1): 28~33.

[7] Eike A. Griess, Gabor L. Igloi, Gunter Feix (1994). Isolation and Sequence Comparison of a Maize Calmodulin cDNA. *Plant Physiol.*, 104: 1467~1468.

[8] Pieterse C. M.,Verbakel H. M.,Spaans J. H., *et al.* (1993). Increased expression of the calmodulin gene of the late blight fungus Phytophthora infestans during pathogenesis on potato. *Mol. Plant Microbe Interact*, **6** (2):

164~172.

[9] He Shuilin, Lai Zhongxiong, Guan Deyi, *et al.* (2000). Cloning of calmodulin cDNA of Capsicum ammuum. *Journal of Agricultural Biotechnology*, **8** (2): 151~154.

[10] Vis T. N., Urdea M. S., Masiarz F. R., *et al.* (1986).Isolation of the yeast calmodulin gene:calmodulin is an essential protion. *Cell*, 47: 423.

[11] Frederick M., Ausubel, Robert E. Kingston, J.G. Seidman, *et al.* (translated by Yan Ziying, Wang Hailin, 1998). Short Protocols in Molecular Biology. Beijing: Science publishing company, 37~38.

Mechanism of Gonadal Precocity in Cultured Large Yellow Croaker, *Pseudosciaena Crocea* : A Study of Microstructure and Submicrostructure of Leydig Cell and Sertoli Cell in Testis

Fang Yongqiang (方永强)[1], Weng Youzhu (翁幼竹)[1], Zhou Jing (周 晶)[1], Xie Fangjing (谢访靖)[2], Liu Jiafu (刘家富)[2]

1 *Third Institute of Oceanography, SOA, Xiamen* 361005

2 *The Experimental Farm of Aquaculture Technology Extension Station, Ningde* 352100

Abstract Microstructure and submicrostructure of Leydig cell and Sertoli cell in the testis of gonadal precocity and immaturation in cultured large yellow croaker, *Pseudosciaena crocea*, are studied using histology and electron microscopic technique. The results indicate that the fine structure of the two kinds of cells in different development stages presents an obvious difference. The smooth endoplasmic reticular and tubular mitochondria of Leydig cell and Sertoli cell are well developed in the testis of gonadal precocity, but poorly developed in the testis of immaturation. We suggest that the reason for gonadal precocity in the large yellow croaker may be related to the earlier development and maturation of Leydig cell and Sertoli cell.

Keywords *Pseudosciaena crocea*, testis, Leydig cell, Sertoli cell, gonadal precocity

The authors[1] have reported the seriousness of gonadal precocity in net box-cultured *Pseudosciaena crocea* from Ningde and and its surrounding area. The gonadal precocity in male is more serious than in female, and has reached a rate of about 60-70%. In addition, the cause of gonadal precocity, which had been demonstrated to be the development and entry into secretary activity of GtH cells in pituitary, was documented in the article "the mechanism of inhibitory gonadal precocity of GnRH-A and Ziqi in cultured *Pseudosciaena crocea*"[2]. It is suggested that the development and maturation of body cells producing steriod hormones in testis because of GtH cells secretory activity may be an important cause inducing gonadal precocity. To verify the reliability of this suggestion, we have studied the histology and ultrastructure of testes of gonadal precocity and immaturation in *Pseudosciaena crocea* by histology and electron microscope technique, and compared the difference in development and maturity of various organelle of Leydig cell and Sertoli cell in different development stages of testes, and found out the factors related with gonadal precocity in male. On the other hand, while the testis development cycle and histological character of different stages of spermatogenic cells in male*P.crocea* had been described by Lin *et al.*[3] in the article "Study on the gonad development cycle in cultured*Pseudosciaena crocea*", the ultrastructure of spermatogenesis and maturation were not mentioned. The present study not only provides the understanding of regulation mechanism on testis development and maturation and accumulates basic data for reproduction physiology of male *P.crocea*, but also clarifies the mechanism of gonadal precocity in P.crocea, and thus has value both in theory and practice.

Received on July 30, 2002

1 Material and methods

1.1 Material

Male *P.crocea* are collected from the Experimental Farm of Aquaculture Technology Extension Station, Ningde. The fish came from the fry bred in the spring 1999 and have been cultured in the net cage for 6 to 10 months. 40 animals were collected from the net cage and measured 14~23 cm in length and 35~360 g in body weight after anaesthesia with eugenol.

1.2 Methods

1.2.1 Preparation of histological specimens

Testes are isolated from dorsal side of abdominal cavity of *P.crocea* and their development stage are distinguished by the naked eye. Immature testis are thin string-shaped or flat band-shaped, while precocious testis is white fat long slice-shaped. Testes are fixed with Bouin-Holland for 8~12 h, dehydrated in a graded series of alcohol. After transparence is made by xylene, specimens are embedded in paraplast. Sections are cut at 6~7 μ m and stained with hematoxylin-eosin to determine the development stage of testes and the development level of Leydig cell and Sertoli cells in the precocious and immature large yellow croaker.

1.2.2 Preparation of electron microscopic specimens

For electron microscopic observation, the immature and precious testes which are collected at the same time of preparation of histological specimens are fixed in ice-cold 2.5 % paraformaldehyde for 4~6 h, and then washed in 0.1 mol/L (pH 7.2~7.4)phosphate buffer 3 times. After postfixation in 1 % (*m/m*) osmic acid for 1~2 h, specimens are embedded in epoxy resin 812. Ultrathin sections at 1 um thick are made with LKB 8800III and located after being stained with 1 % (*m/m*) aniline blue. Photographs are taken with the HV-12A transmission electron microscope.

2 Results

2.1 Histological structure of testis in *Pseudosciaena crocea*

The testis of large yellow croaker, like that of the great majority of teleost fish, is of the lobular type. The observational results of histological sections in testes of gonadal precocity and immaturity in the cultured large yellow croaker indicate that the testicular development of the gonadally precocious large yellow croaker are at the stages IV-V characterized by different well-developed stages of spermatogenic cells including spermatogonia, primary and secondary spermatocytes, spermatids and spermatozoa in the siminiferous tubule, especially, a lot of spermatozoa in the seminiferous tubule as a feature of gonadal precocity (Plate I-1). At the same time, Sertoli cells are seen to be located at the basal membrane and arranged alternately with germinal cells (Plate I-2), and most of them have already migrated from germinal epithelium to the center or near the central lumen. Another character of gonadally precocious testis is that Leydig cell is shuttle-shaped and distributed between two seminiferous tubules. The cell is well developed with large elliptical nucleus and faint staining cytoplasm. This cell is large in number (Plate I-3). Immature testis is at the stages 2-3. Spermatogonia, primary and secondary spermatocytes and spermatids, occasionally a few spermatozoa, are seen in the siminiferous tubule.

Leydig cell is rare in number, and has small ellipesis nucleus and unstaining cytoplasm (Plate I-4). While the distribution position of Sertoli cells in the immature fish is similar to that in the gonadally precocious fish, most Sertoli cells are still located in the basal part of germinal epithelium and do not migrate to the center.

2.2 Ultrastructural observation on Leydig cell and Sertoli cell in testis

The results of ultrastructure study on the testis of large yellow croaker indicate that the nucleus of Leydig cell in immature fish is characterized by abundant euchromatin and rare heterochromatin scattered in the nucleus inner membrane. A few oval or irregular mitochondria exist in the cytoplasm. The cristae of mitochondria are tubulose and the electronic density of matrix is also low. At the base part of the nuclear or around the nuclear, the developing smooth endoplasmic reticules, which are vesicle in the morphological structure, are scattered in the cytoplasm. Golgi complex is very difficult to be seen (Plate I-5). Another kind of somatic cell, Sertoli cell or support cell, is located at the base part of germinal epithelium and arranged alternately with germinal cells. Sertoli cell is long colum or shuttle in shape, and has a large kidney-shape nucleus with abundant euchromatin but rare heterochromatin close to the nuclear inner membrane. Developing cell organelles are seen in the cytoplasm. For example, a few smooth endoplasmic reticules are found surrounding the nucleus, the develping Golgi complex is composed of two-three layers of plate cisternae with Golgi vesicle on the mature face, and a few oval mitochondria are found with poor-developed mitochondria cristae (Plate I-6).

The ultrastructure of Leydig cell in the testis of gonadal precocity differs from that in the immature Leydig cell in that various cell organells have been well developed in the cytoplasm. Many large-type mitochondria with tubular cristae are seen on one side of the nucleus, the mitochondria are ellipsis or irregular in shape, and the maximum diameter is about 1.2 μ m. The vesicular smooth endoplasmic reticular cisternae are distributed around the nucleus and in the center of cytoplasm, showing a multi-layer arrangement. The nucleus is irregular in shape with very abundant euchromatin but rare heterochromatin along the nuclear inner membrane. Sertoli cell in testis migrates from the base region of germinal epithelium to the top part of seminiferous tubule, near tubular cavity. The Sertoli cell is long columnshaped with several cytoplasmic processes attached with spermatids. The nucleus of Sertoli cell is a long ellipsis in shape with lumpy heterochromatins closed to nuclear inner membrane and abundant euchromatin. Various cell organelles in the cytoplasm of Sertoli cell in precocious testis develop better than that in immature tistis in that the mitochondria are well developed and have increased in number, and the electronic density of matrix is high. The smooth endoplasmic reticular cisterna in the cytoplasm on the top region of nucleus is more developed (Plate I-8).

3 Discusion

The present results have indicated that the development of Leyding cells and Sertoli cells in precocious fish testis is obviously better than that in immature fishes testis, which provides new clue for further analysing the mechanism of gonadal precocity of large yellow croaker. Previous study demonstrated that gonadotropic secretory cells in the pituitary gland of precocity fishes matured earlier than immature fish. The full proof was that vacuoles occurred in the cytoplasm of majority of GtH cells in the proximal pars distalis of adenohypophysis in precocious fish, which can be a mark of the GtH cells entering the stage of secretory activity. However, the mechnism of inducing gonadal precocity in male

large yellow croaker by GtH after its entry into secretory activity, has not been clarified. According to fish reproduction endocretory regulation mechanism[4,5], we have considered that GtH from fish pituitary might alert on the target cells in testis, *i.e.* Leydig cell and Sertoli cell. As everyone knows, Leydig cell and Sertoli cell are both body cells and endocretory cells in large yellow croaker testis, the former secreting androgen, for example testosterone and 5a-dihydrotestosterone[6], and the latter secreting androgen binding protein and a kind of Sertoli cell factor which can induce the localization of spermatid[6,7]. Both these body cells participate in the spermatogenesis and developmental maturation of spermatids, in that the number of Leydig cells in the gonadally precocious fish is more than that in immature fish and nuclear volume also is larger than that in immature fish. At the same time, the ultrastructure study has further demonstrated that in the gonadally precocious large yellow croaker, the smooth endoplasmic reticules in the cytoplasm of Leydig cell in the testis are well developed and large mitochondria with tubular cristae occur. In addition, the well-developed smooth endoplasmic reticular pool and mitochondria with tubular cristae are observed in the cytoplasm on the top region of nucleus of Sertoli cell. These facts have illustrated that the two kinds of endocrine cell have already entered the stage of secretory activity and directly participated in regulating the spermatogenesis of large yellow croaker.

The above change of body cells in large yellow croaker corresponds to the entry into maturation and secretory activity of Leydig cell in testis when earlier spermatogenesis presents in the male fish induced by exogenous androgen via positive feedback[8,9]. Therefore, it is suggested that the mechanism of gonadal precocity in large yellow croaker is that the gonadotropin secreted from pituitary gland binds with the receptors of Leydig cell and Sertoli cell in testis, and then stimulates the synthesis and secretion of androgen, which directly initiates the proliferation of spermatogonia and meiotic division of primary spermatocyte. At the same time, androgen can cause the GnRH neuron system in the hypothalamus to enter secretory activity via positive feedback mechanism, and further stimulate the secretory activity of GtH cell in the pituitary gland. These actions of androgen have already been proved[10,11] by many evidences. This article only reveales the internal factors of gonadal precocity in large yellow croaker, and how the environmental factors induce gonadal precocity via internal factors remains to be further studied.

Acknowledgements

This work is supported by the National 863 Project (819-02-012).

References

[1] Fang Yongqiang, Weng Youzhu, Zhou Jing, *et al.* (2000) Study on earlier gonadal maturation in cultured large yellow croaker, Pseudosciaena crocea I. Status of gonadal development in culture of net cages. *J. Oceanography in Taiwan Strait*, 19:354~359.

[2] Weng Youzhu, Fang Yongqiang, Zhou Jing, *et al.* (2001) The mechanism of inhibitory gonadal precocity of GnRH-A and Ziqi in cultured Pseudosciaena crocea. *J. Fisheries of China*, 25:518~521.

[3] Lin Danjun, Zhang Jian, Luo Jia (1992) Study of the gonadal development and reproductive cycle in cultured large yellow croaker, Pseudosciaena crocea. *Acta Fujian Normal University (Natural Science Edition)*, 7:81~87.

[4] Donaldson E. M. (1973) Reproductive endocrinology of fishes. *Amer. Zool*, 13: 909~927.

[5] Dobson S., Dodd J. M. (1977) Endocrine control of the testis in the dogfish Scyliorhinus canicula L. II. Histological and ultrastructural changes in the testis after partial hypophysectomy (ventral lobectomy). *Gen. Comp. Endocrinol*, 32: 53~71.

[6] Pierantoni R., Fasano S., Minucci S., *et al.* (1990) Regulation of the testicular activity in the marine teleost fish, Gobius paganellus. *Gen. Comp. Endocrinol*, 80:1~8.

[7] Fang Yongqiang (1978) Spermatogenesis and control. *Advance of Biological Science*, (5):15~22.

[8] Fang Yongqiang, Lee Chengsheng (1989) The preliminary study on the mechanism of the action of 17a-methyltestosterone stimulatory spermatogenesis in the grey mullet (Mugil cephalus L). *Oceanologia Limnologia Sinica*, 20: 10~14.

[9] Borg B. (1986) Stimulatory effects of methyltestosterone on pituitary gonadotropic cells and testes Leydig cells of the three-spined stickleback, Gasterosteus aculeatus in winter. *Gen. Comp. Endocrinol*, 62: 54~61.

[10] Crim L. W. (1981) Onset of gonadotropic hormone accumulation in the immature trout pituitary gland in response to estrogen or aromatizable androgen steroid hormones. *Gen. Comp. Endocrinol*, 44: 374~381.

[11] Lo A., Chang J. P. (1998) In vitro application of testosterone potentiates gonadotropin-releasing hormone-stimulated gonadotropin-II secretion from cultured goldfish pituitary cells. *Gen. Comp. Endocrinol*, 111:329~338.

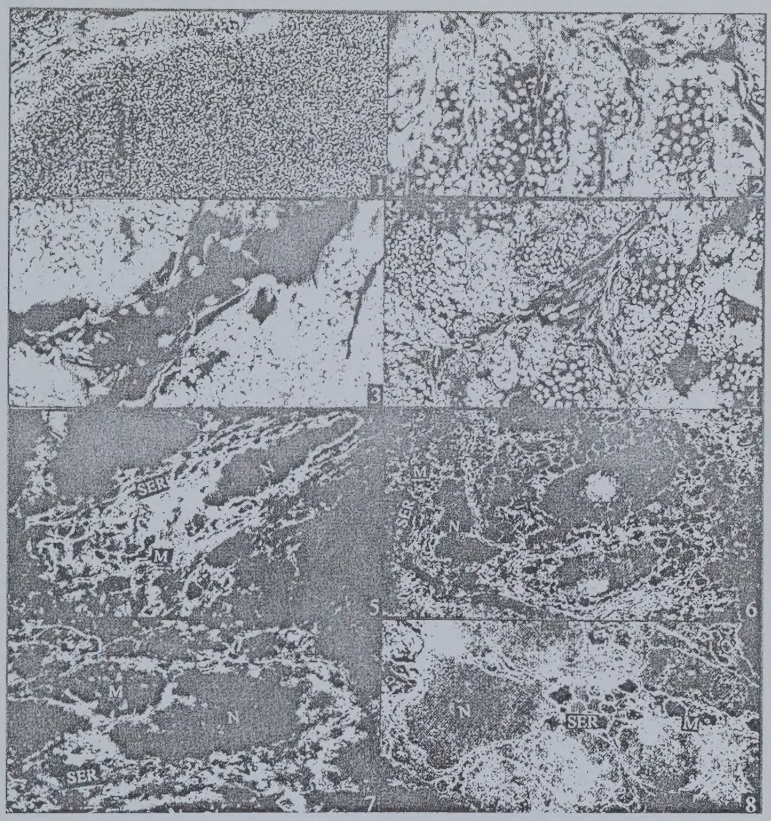

Plate I Ultrastructure of Leydig cell and Sertoli cell in testis of large yellow croaker

1. Well-developed spermatogenic cells of different stages and a lot of spermatozoa existing in tubular lumin can been found in the testis of gonadal precocious large yellow croaker. ×120

2. Sertoli cell (arrow) in the seminiferous tubule of testis of gonadal precocious large yellow croaker. ×240

3. Leydig cell or interstitial cell (arrow) in the seminiferous tubule of testis of gonadal precocious large yellow croaker. ×240

4. Leydig cell (thick arrow) and Sertoli cell (thin arrow) in the seminiferous tubule of testis of gonadal immature large yellow croaker. ×240

5. Ultrastructure of Leydig cell in the immature testis. SER: smooth endoplasmic reticular pool; M: mitochondria; N: nucleus. ×10 000

6. Ultrastructure of Sertoli cell in the immature testis. ×15 000

7. Ultrastructure of Leydig cell in the precocious testis. ×9 000

8. Ultrastructure of Sertoli cell in the precocious testis, showing well-developed mitochondria (M), smooth endoplasmic reticular pool (SER) and spermatids attached to Sertoli cell. ×6 400

Marine Science Bulletin

Marine Science Bulletin publishes papers on marine science and technology including physical oceanography, chemical oceanography, marine biology, marine geology, environmental oceanography, estuarine & coastal sciences, marine technology, digital ocean, coastal zone management, ocean engineering, marine economics, etc., and aims to promote international academic exchange.

Editor-in-Chief: Wang Hong（王　宏）
Deputy Editor-in-Chief: Lin Baofa（林宝法） He Guangshun（何广顺）
Yang Ying（杨　鹰）
Executive Editor: Xu Jie（徐　杰） Zhang Deshan（张德山）
Zhang Xiaoxian（张潇娴） Wang Zhankun（王占坤）
Computer typist: Cheng Xiuchun（程秀春）

Marine Science Bulletin （Vol.4 No.2 Oct. 2002）

Responsible Institution:
State Oceanic Administration of China
Edited and Published Semi-annually by:
National Marine Data and Information Service
Address: 93 Liuwei Road, Hedong District, Tianjin 300171, China
E-mail: msb@mail.nmdis.gov.cn

ISSN1000-9620
CN12-1271/N

Price: $ 30.00 Per year